# Evaluating & Informing Elk Habitat Management

## Relationships of NDVI with Elk Nutritional Resources, Elk Nutritional Condition, & Landscape Disturbance

Jesse DeVoe | *Montana Cooperative Wildlife Research Unit*

Kelly Proffitt, Justin Gude | *Montana Fish, Wildlife & Parks*

Steve Brown | *USDA Forest Service, Northern Region*

August 29, 2018



*Dinner with a view: elk in the Sapphire herd foraging above the Bitterroot Valley*

## Table of Contents

## Funding

# Acknowledgments

# Executive Summary



The distribution and availability of nutritional resources strongly influence elk movements and behaviors and are particularly important for female elk (*Cervus canadensis*) to meet nutritional requirements of lactation, mass gain, and pregnancy. Recent studies of elk resource selection during the summer have demonstrated that elk select strongly for areas associated with high values of the Normalized Difference Vegetation Index (NDVI), a remotely-sensed indicator of net primary productivity of canopy that has been used extensively as a surrogate for nutritional resources in a variety of species. In particular, two NDVI metrics that integrate phenological changes of vegetation into an annual measure of production, NDVI amplitude (AMP) and time-integrated NDVI (TIN), have been found to be important for elk selection in Montana. The studies that elucidated these relationships recommended that managers incorporate nutrition into elk habitat management plans; however, considerable uncertainty and lack of information exists regarding the relationship between the NDVI metrics and nutritional resources for elk. This study aims to fill these knowledge gaps and provide recommendations for the management of elk habitat in western Montana. We evaluated 3 relationships: 1) NDVI and nutritional resources across the landscape, 2) NDVI and female elk nutritional condition, and 3) NDVI and landscape disturbances.

We used extensive ground-sampled vegetation data and elk nutritional condition measurements from 2 study areas and 4 elk populations: the Elkhorn Mountains comprising the Elkhorn population and the Bitterroot Valley comprising the West Fork, East Fork, and North Sapphire populations. Both study areas generally consist of lower-elevation grass- and shrub-dominated foothills adjacent to privately-owned residential and agricultural lands and higher-elevation dry coniferous forests. The Bitterroot Valley additionally supports extensive valley bottom riparian areas and higher-elevation mesic mixed conifer forests. From 510 vegetation plots sampled during peak growing season 2012-2017, we estimated elk forage abundance and quality. We determined best-supported models predicting forage abundance and quality from the NDVI metrics and

landscape attributes. From 172 nutritional condition measurements of individual elk sampled during fall and winter 2011-2015, we estimated ingesta-free body fat and pregnancy status. We determined best-supported models predicting body fat and pregnancy from individual elk exposure to NDVI metrics on their summer-fall ranges. We additionally obtained U.S. Forest Service disturbance data on wildfire, prescribed fire, and timber harvest for the study areas to examine the correlation between NDVI values and landscape disturbances. We determined best-supported models predicting the NDVI metrics from disturbance type, the amount of time since the disturbance, and forest vegetation type.

We found evidence for associations of AMP with forage quality and forage abundance and of TIN with forage abundance, fall and winter body fat, and landscape disturbances. We found TIN to be more consistently supported across our analyses than AMP, suggesting that TIN may be a more biologically relevant metric. Although the NDVI metrics were positively or optimally related to nutritional resources, the associations were weak, suggesting that NDVI does explain some variance but is insufficient to fully characterize summer forage for elk. We did find a strong positive relationship between levels of TIN experienced by elk on their summer ranges and body fat levels during the fall. We also found a weaker positive relationship between TIN that elk experience on their summer range and body fat levels during the winter. Elk selection of TIN during the summer may therefore be beneficial to the nutritional status of elk following the growing season. We did not find a significant relationship between elk exposure to NDVI and pregnancy status. Lastly, our results indicated that TIN is correlated with several landscape disturbances. TIN was significantly reduced in areas burned by wildfires all years post-disturbance, burned by prescribed fires ≤ 5 years post-disturbance, and clearcut 6-10 years post-disturbance. Areas treated by thinning (≥ 11 years post-disturbance) and clearcutting (≥ 21 years post-disturbance) significantly increased TIN. We additionally found some evidence that TIN increased within 10 years in areas treated by thinning and combination thinning-prescribed burning and after 10 years in areas treated by prescribed burning alone. Within 10 years after disturbance, the greatest increase in TIN occurred in areas treated by thinning (3.3-5.9% increase) and combination thinning-prescribed burning (1.4-4.7%), however, these relationships were weak. Between 11-20 years after disturbance, the greatest increase in TIN occurred in areas treated by thinning (5.5% increase) and prescribed burning (3.9%), but only the relationship with the thinning treatment was significant. After 21 years, the greatest increase in TIN occurred in areas treated by prescribed burning (10.1% increase), thinning (7.5%), and clearcutting (6.7%), but the relationship with prescribed burning was weak.

Together these results indicate that managing areas for greater levels of TIN may increase the availability of summer nutritional resources and improve the ability of elk to gain body fat. Forage abundance may be enhanced through forest treatments designed to increase TIN. While we found uncertainty in the short term relationships between TIN and disturbance, forest treatments that include thinning or combination thinning-prescribed burning may improve TIN within 10 years of disturbance. In the long term (> 10 years), forest treatments that improve TIN may include thinning or prescribed burning. Reductions in TIN across all years post-wildfire disturbance may be due to higher severity

fires constraining plant revegetation and the limited spatial scale at which minimal plant growth can be detected by satellite sensors. Forage abundance and forage quality may also be enhanced through timber harvest treatments that reduce overstory canopy cover. We suggest that focusing management treatments on public lands and in forest vegetation types that are common within a region but with lower nutritional value may be one tool available to attract more elk onto public lands during the summer and reducing the redistribution of elk to private lands prior to and during the fall hunting seasons. Managers could also consider forest treatments in areas identified as important seasonal travel corridors for elk. Combining forest treatments with other strategies, such as reducing availability of high quality nutritional resources on private lands to elk, increasing hunter access on private lands, or altering harvest regulations to more evenly distribute harvest risk across public and private lands, may provide a more holistic approach to encouraging elk to remain on public lands.

# Section 1 - Background



Craig Jourdonnais

During 2011-2014, biologists from the United States Forest Service (USFS) and Montana Fish, Wildlife and Parks (MFWP) partnered to develop a set of recommendations for elk habitat management on the Custer, Gallatin, Helena, and Lewis and Clark National Forests. The purpose of these recommendations were to describe the habitat needs for maintaining elk on public lands throughout the year and the habitat management guidelines for USFS lands appropriate to meet this goal. The document identified knowledge gaps and uncertainties in our collective understanding of elk and elk habitat management. Building from that work, during 2015-2016, Montana State University, USFS, and MFWP conducted a regional elk habitat selection modeling effort and provided detailed information regarding the influence of various factors such as nutrition and travel management on elk summer and fall habitat selection and distributions (Ranglack et al. 2016, 2017).

A key result of the habitat selection analyses was that nutritional resources, as indexed by NDVI metrics, are the primary factor affecting summer-fall elk distributions and maintain importance in determining elk distributions during the fall archery hunting season (Ranglack et al. 2016, 2017). In a subsequent study evaluating tradeoffs of risk and forage during the fall archery season in Montana, elk selection for nutritional resources, as estimated from measuring vegetation, increased during the archery season (DeVoe et al. in review). These results highlight the importance of nutrition in influencing elk distributions and the need to incorporate nutritional resource considerations in elk habitat management, particularly if habitat management is being used as a tool for maintaining a distribution of elk that includes elk using public lands during the fall season. The importance of summer nutritional resources on ungulate population dynamics is well documented (Cook et al. 2013, Monteith et al. 2014). In southwest Montana, most studies indicate that nutrition is not commonly limiting elk pregnancy rate or overwinter survival (Cook et al. 2004b, Evans et al. 2006, White et al. 2011, MFWP unpublished data), however some populations do experience nutritional limitations that limit elk pregnancy rates (Proffitt et al. 2016a).

The habitat selection study completed by Ranglack et al. (2016, 2017) resulted in a recommendation that managers incorporate nutrition into elk habitat management strategies as part of the effort to accommodate elk habitat requirements and maintain a distribution of elk across public and private lands during the fall hunting seasons. Although these studies suggest that NDVI amplitude and time integrated NDVI may be useful indices of ungulate nutritional resources, additional information is required to clarify the relationship between NDVI, vegetation communities, and ungulate nutritional resources, as well as the consequences of variability in nutritional resources on elk vital rates. NDVI is a metric of greenness based on satellite imagery and has become one of the most widely used vegetation indices in ecology (Pettorelli et al. 2005). Ranglack et al. (2016, 2017) showed that elk selected for areas that have the highest NDVI during the summer growing season, but did not provide insights for managers regarding the relationships between NDVI and vegetation communities or how to manage vegetation in order to increase elk nutritional resources in a way that matters for elk population dynamics. Particularly for forested landscapes that experience disturbances, such as wildfire, timber harvest, or insect-damage, understanding how NDVI relates to elk nutritional resources can help resources agencies to develop and improve elk habitat management standards.

This project was initiated to provide specific recommendations for vegetation management to benefit elk and that may help maintain a distribution of elk on public lands during the fall hunting season. The objectives of the project were to: 1) evaluate the relationship between ground-based vegetation data and NDVI; 2) evaluate the effect of NDVI on elk nutritional condition, including body condition and pregnancy rate; and 3) evaluate the effect of variable forest disturbances and time since disturbance on NDVI.
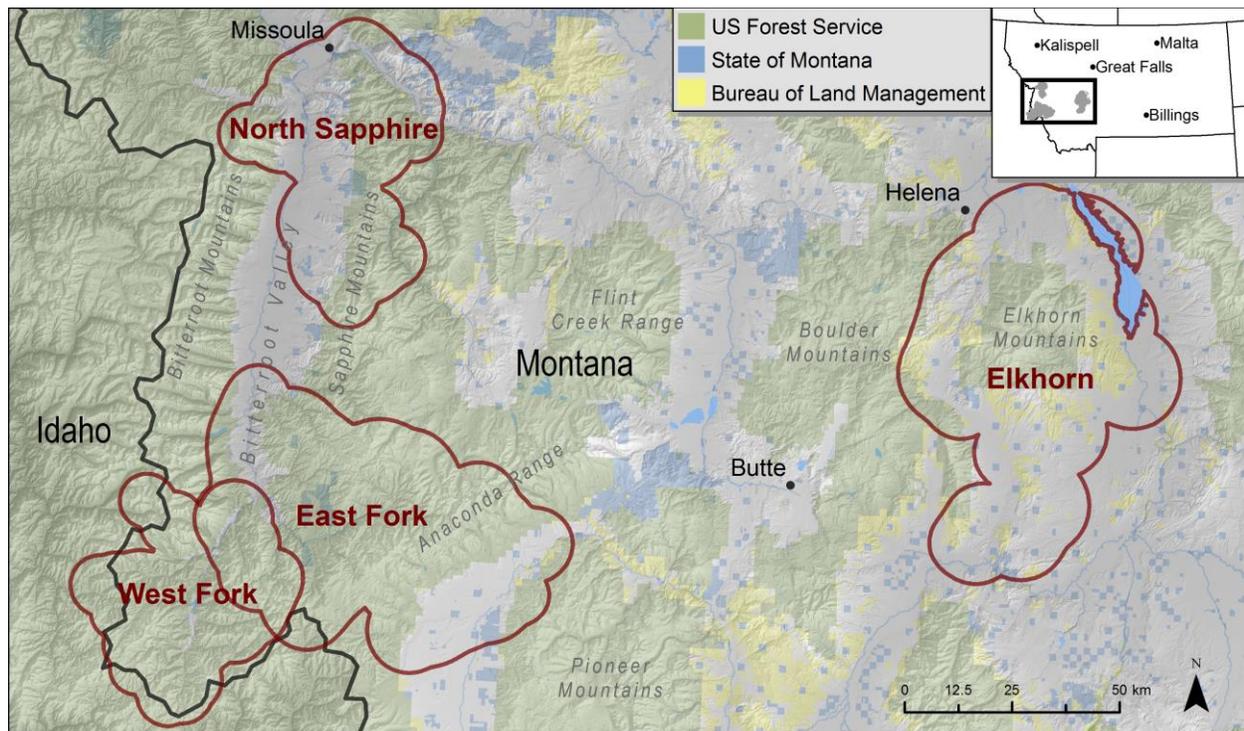
**Figure 1 – The North Sapphire, West Fork, East Fork, and Elkhorn elk population annual ranges in west-central Montana, USA, 2012-2017.**

We conducted the study in west-central Montana, USA within the annual ranges of 4 elk populations: 1 population in the Elkhorn Mountains and 3 populations in the Bitterroot Valley: the North Sapphire, East Fork, and West Fork (Fig. 1). The Elkhorn Mountains (1,120-2,866 m elevation) are a relatively isolated mountain chain with lower elevations dominated by open sage-grassland (e.g., big sagebrush [*Artemisia tridentata*], bluebunch wheatgrass [*Pseudoroegnaria spicata*], Idaho fescue [*Festuca idahoensis*], rough fescue [*Festuca scabrella*], bluegrasses [*Poa* spp.]) and upper elevations dominated by dry coniferous forests (e.g. lodgepole pine [*Pinus contorta*], Douglas fir [*Pseudotsuga menziesii*], ponderosa pine [*Pinus ponderosa*]) with small interspersed meadows. Cultivated crops (pasture grasses and leguminous forbs) border the northern and southwestern portions of the range. The climate is characterized by short, cool summers (17.8°C mean July temperature) and long, cold winters (-4.7°C mean January temperature), with mean annual precipitation ranging 269-811 mm (PRISM Climate Group 2016). The Elkhorn population annual range (3,787 km$^2$) included a mix of private lands and public lands that were primarily managed by the Helena and Beaverhead-Deerlodge National Forests, Bureau of Land Management, and state of Montana. Elk are counted annually from a fixed-wing aircraft. The long-term population average (1994-2014) is 1,861 elk, with a peak in 1996 of 2,893 elk. The current population is estimated at 2,100 animals. Elk are sympatric with moose (*Alces alces*), mule deer (*Odocoileus hemionus*), white-tailed deer (*O. virginianus*), and a small population of bighorn sheep (*Ovis canadensis*). Resident carnivores included

mountain lion (*Puma concolor*), bobcat (*Lynx rufus*), coyote (*C. latrans*), and American black bear (*Ursus americanus*).

The Bitterroot Valley (950-3,300 m elevation) gradates from flat bottomland and gentle foothills to steep slopes of the surrounding Sapphire and Bitterroot Mountains. Lower elevations support similar vegetation communities to the Elkhorn Mountains, however, higher elevations are primarily mesic mixed coniferous forests of lodgepole pine (*Pinus contorta*), grand fir (*Abies grandis*), and subalpine fir (*Abies lasiocarpa*). Cultivated crops (pasture grasses, corn, and leguminous forbs) can also be found at lower elevations and primarily in the northern portion of the valley. The climate is characterized by more moderate temperatures (-4.4°C mean January and 17.1°C mean July temperatures) and higher mean annual precipitation (ranging 284-963 mm) compared to the Elkhorn Mountains (PRISM Climate Group 2016). Sympatric species were similar to the Elkhorn Mountains and additionally included gray wolf (*Canis lupus*).

The 3 elk ranges in the Bitterroot Valley included varying proportions of private and public lands. The Sapphire range (2,482 km²) was comprised of nearly equal portions of private lands and public lands managed by the Bitterroot and Lolo National Forests and the state of Montana. The East Fork (3,971 km²) and West Fork (1,990 km²) ranges were comprised primarily (~78-97%) of public lands managed by the Bitterroot, Beaverhead-Deerlodge, and Salmon-Challis National Forests, and the state of Montana. From the mid-2000s to the mid-2010s, the North Sapphire population steadily increased from 750 to 1,051 elk due to a combination of moderate calf recruitment and limited female harvest. During this same time, the East Fork and West Fork populations declined from 4,135 to 3,332 elk and 1,900 to 722 elk, respectively, due to a combination of antlerless elk harvest and increasing predation pressure (Eacker et al. 2016).

Timber harvest, wildfire, and insect-caused damage have resulted in heterogeneous forests of varying successional stages across the study areas. Timber harvest peaked in the 1980s on the Bitterroot, Lolo, and Helena National Forests, averaging 32.5, 67.4, and 20.8 million board feet cut per year, respectively, but had declined 69-76% across all forests by the 2000s (U.S. Forest Service 2016). In contrast, wildfire activity and insect-caused damage have more recently become widespread disturbances throughout the study areas. In the Bitterroot Valley, the annual area burned increased from an average of 16 km² during 1950-1999 to 159 km² during 2000-2015. Forest damage caused by insects, primarily the mountain pine beetle (*Dendroctonus ponderosae*), peaked in 2009 in the Elkhorn Mountains and 2012 in the Bitterroot Valley, affecting approximately 746 and 920 km² of coniferous forest within the elk annual ranges, respectively.

Craig Jourdonnais
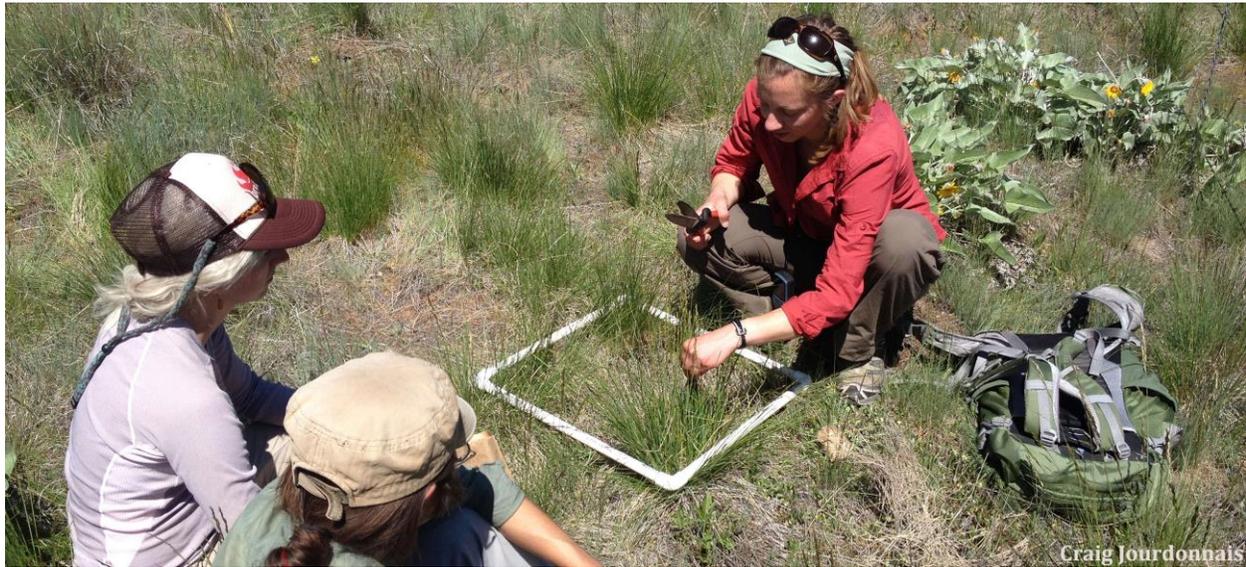
## Introduction

The distribution and availability of nutritional resources are important driving mechanisms of ungulate resource selection and migration (Fryxell et al. 1988, Sawyer and Kauffman 2011, Bischof et al. 2012, Merkle et al. 2016) and strongly influence ungulate survival and reproduction (Cook et al. 2004a, 2013, 2016, Monteith et al. 2014, Proffitt et al. 2016a). For ungulates living at northern latitudes with strong seasonality, summer and autumn (henceforth, summer-fall) nutritional resources allow individuals to replenish winter-depleted body fat reserves and accrue sufficient fat to survive the nutrient-limited winter months (Cook et al. 2004a). Summer-fall nutrition is particularly important for supporting the energetic demands of female lactation and pregnancy and for increasing winter survival of calves which can have important implications to population performance. In elk (*Cervus canadensis*), females with higher body fat at the end of summer are more likely to become pregnant in the fall, and calves exposed to higher nutrition during the summer-fall exhibit faster growth rates and higher winter survival (Cook et al. 1996, 2004a). In western North America, the effects of limited summer-fall nutritional resources to free-ranging elk have been correlated to reduced population performance (Cook et al. 2013, Proffitt et al. 2016a).

Ranglack et al. (2017) highlighted the important influence of summer-fall nutrition on elk distributions and the need to incorporate elk forage considerations in elk habitat management plans. An understanding of the distribution and availability of summer-fall forage for elk may be a useful tool for resource managers to maintain distributions of elk on public lands during the fall hunting seasons, a current challenge across many western states (Burcham et al. 1999, Conner et al. 2001, Haggerty and Travis 2006, Proffitt et al. 2010, 2013, 2016b). This understanding may also provide managers with insight into the potential nutritional condition, productivity, and, ultimately, the performance of elk populations.

Characterizing the distribution and availability of nutritional resources for elk provides resource managers with valuable information to manage elk distributions and populations but remains a challenge even on small landscapes. Accurate measurements to capture the heterogeneous spatial and temporal distribution of forage requires extensive annual ground-sampling of vegetation across broad areas and habitat types, an option that is largely not feasible for managers. The satellite-derived Normalized Difference Vegetation Index (NDVI) may provide a simple and efficient alternative to ground-sampling (Pettorelli et al. 2011). NDVI, the ratio of red and near-infrared radiation absorbed and/or reflected by vegetation, is directly related to vegetation productivity and photosynthetic activity in a defined area (Pettorelli et al. 2005). In studies of ungulates, NDVI has often been used as a proxy for nutritional resources representing forage quantity or quality (Pettorelli et al. 2006, Ryan et al. 2006, Wiegand et al. 2008, Bischof et al. 2012, DeVoe et al. 2015, Merkle et al. 2016, Rivrud et al. 2016, Lowrey et al. 2017, Mysterud et al. 2017, e.g., Aikens et al. 2017, Marshal et al. n.d.). Recent studies of elk in western Montana found that elk selected for areas with higher NDVI values during the summer and fall (Ranglack et al. 2016, 2017), in addition to other seasons (Proffitt et al. 2011), indicating that NDVI may be a relevant indicator of nutritional resources.

Several studies have evaluated the validity of using NDVI to represent nutritional resources for ungulates and have found correlations of NDVI with measurements of fecal crude protein (Hamel et al. 2009, Ryan et al. 2012) and ground vegetation biomass, digestibility, and crude protein (Borowik et al. 2013, Garroutte et al. 2016). Studies focusing on nutritional resources for elk in particular are limited, however. Garroutte et al. (2016) assessed the relationship of NDVI and ground-based vegetation measurements of vegetation abundance and quality within elk summer migratory ranges. However, this study focused only on grassland and irrigated agricultural areas, which represent small portions of landscapes occupied by elk during the summer-fall and administered by public land resource managers.

In the present study, our objective was twofold: 1) use extensive ground-based vegetation measurements across a landscape of diverse vegetation cover types and within the annual ranges of 4 elk populations to evaluate the relationship between NDVI metrics and summer-fall nutritional resources that are important for elk (i.e., forage quality and abundance), and 2) provide resource managers in western Montana with insight for using NDVI to represent the availability and distribution of nutritional resources for elk across large landscapes. We expected that NDVI metrics would be correlated with forage abundance given the correlation of NDVI with above-ground productivity of vegetation in other studies (Pettorelli et al. 2005, 2011, Borowik et al. 2013, Garroutte et al. 2016). NDVI metrics may also or alternatively be related to forage quality, a relationship that has not yet been investigated.

## Methods

## Nutritional resources

We collected 2 measures of elk nutritional resources estimated from ground-based vegetation sampling: forage abundance (g of forage species biomass per m$^2$) and forage

quality (kcal of digestible energy per g of forage species). The availability of data to estimate each measure varied by study area due to different ground-sampling objectives across studies. Forage abundance data were collected at all study areas, while forage quality data were only collected within the Bitterroot Valley. Sampling methodology was standardized across study areas. Vegetation cover type, species composition, percent cover, and biomass were recorded at all sampling sites. In estimates of forage abundance and forage quality, we screened these data to only include elk summer forage species (identified from elk fecal samples). In estimates of forage quality, we accounted for the nutritional availability of species in different phenological stages by collecting samples of forage species in several phenological stages and analyzing for the digestibility of the samples (Appendix A).

We sampled vegetation during peak growing season (7 July-31 August) at random sites proportionally allocated within vegetation cover types for each population annual range (Krebs 1989). We sampled sites (n = 1,023) within the East Fork and West Fork ranges during 2012-2013 (Proffitt et al. 2016a), the North Sapphire range during 2014-2015 (Proffitt et al. 2017), and the Elkhorn range during 2016-2017. To focus our analysis on areas and habitats managed by the U.S. Forest Service, we constrained the data to the spatial extent and vegetation cover types of the Region 1 Vegetation Mapping Program (VMap) database (see *Landscape covariates* section). We therefore excluded sites occurring off U.S. Forest Service lands (n = 110; 10.7% of the sites) and excluded sites occurring in disturbed or transitional (i.e., burned < 15 years prior or insect-infested < 10 years prior) areas (n = 371; 36.3% of the sites). At each sampling site, we placed a 40 m transect along the contour of the slope. We recorded species composition and percent cover of forb, shrub, graminoid, and tree (< 2 m tall) lifeforms at five 1 $m^2$ quadrats placed every 10 m along the transect. We estimated cover of lifeforms independently, allowing total cover per quadrat to exceed 100%. Within the 0, 20, and 40 m quadrats, we established a nested 0.25 $m^2$ clip plot and collected all graminoid and forb biomass >1 cm above ground. On shrubs, we clipped all leaves and non-woody stems (however, see changes to sampling methods below). We dried samples at 50°C in a drying oven for 48 hours and measured dry weight to the nearest gram. In 2012-2013 and 2016-2017, we apportioned the dry weight to plant lifeform (e.g., forb, graminoid, and shrub) based on the percent cover of each lifeform. In 2014-2015, we made 2 minor changes to sampling. First, because clipping shrubs was time-intensive and shrubs comprised only a small percentage of the diet, we did not clip shrub biomass but instead estimated shrub biomass from shrub basal diameters. Second, we measured the weight of forbs and graminoids separately to more precisely estimate biomass by lifeform.

To identify the forage species that are important for elk, we collected 12-21 pellet samples within each elk population summer-fall range over 2 summer-fall seasons (May-September). Each composite pellet sample included 10-20 individual pellets randomly selected from 10 pellet groups within a 2-5 ha area. We collected only moist samples to ensure pellets were fresh and from the season of interest. We estimated diet composition using Level B fecal plant fragment analyses (Wildlife Habitat and Nutrition Laboratory, Pullman, WA, USA) and identified elk forage species for each elk population as the set of species that constituted 95% of the total diet. We combined the top forage species for the 3

elk populations in the Bitterroot Valley due to their close proximity and identified the Elkhorn forage species separately.

To estimate forage abundance at each sampling site, we first apportioned clipped, dry biomass (g per 0.25 m$^2$) for each lifeform to each species based on rescaled percent cover (species cover proportional to cover within the appropriate lifeform). Second, we filtered out forage species and summed biomass across lifeform. Finally, we averaged biomass per lifeform across clip plots, scaled up to square meters (0.25 m$^2$ x 4 = 1 m$^2$), and summed graminoid and forb biomass. We did not include shrub biomass in the estimate of forage abundance because modeled estimates of shrub biomass were considered to be imprecise and because shrubs comprised only a small portion of the elk diets.

To estimate forage quality at each sampling site in the Bitterroot Valley, we first estimated the proportion of each forage species in each phenological stage (see Appendix A for details). Second, we estimated the digestible energy (kcal/g) of each forage species in each phenological stage. Finally, we estimated forage quality as the weighted mean of values of digestible energy, where the proportion of each species in each phenological stage was used to weight the estimate.

## NDVI metrics

We used NDVI metrics developed from 30-m resolution Landsat satellite products. We chose to use the Landsat NDVI data because the higher spatial resolution better matches the scale at which ground-vegetation was collected and better represents understory forage where canopy cover was greater, as compared to other NDVI sources. We first obtained pre-processed and smoothed 16-day composite images of NDVI from the dynamic web application (https://ndvi.ntsg.umt.edu/) developed by Robinson et al. (2017). For the years 2012-2017 corresponding to the ground-based vegetation sampling, we downloaded images with Landsat 7 ETM+ SLC-off and climatology gap-filling of 10 years. We calculated 2 annual-summarized NDVI metrics related to vegetation productivity and phenology during the growing season: time integrated NDVI (TIN) and NDVI amplitude (AMP; Pettorelli et al. 2005, 2006). We calculated TIN as the accumulation of NDVI values for each pixel between the beginning of the growing season, April 14 (the mean growing season identified for the North Sapphire elk population in Ranglack et al. 2016), and the end of the ground-sampling period, August 31, to index net primary production. This included Landsat images from Julian days 113 to 241. We calculated AMP as the increase in NDVI during this period (i.e., the difference between the maximum NDVI during the growing season and the NDVI at the start of the growing season). These annual NDVI metrics have been found to be important in resource selection studies of elk in Montana (Ranglack et al. 2016, 2017).

## Landscape covariates

In addition to the NDVI metrics and to account for attributes of the landscape that may influence vegetation productivity and quality, we obtained the following covariates for inclusion in the analysis of forage quality and abundance (Table 1): vegetation cover type, canopy cover (CC), precipitation, elevation (ELEV), slope (SLP), solar radiation index (SRI),

and 2 indices of site moisture potential: compound topography index (CTI) and precipitation-, heat load-, and elevation-adjusted topographic index (PHEAT).

**Table 1 - NDVI and landscape covariates, functional forms (L = linear, Q = quadratic, PS = pseudothreshold), and hypothesized directions of relationships considered in models of elk forage in west-central Montana, USA, 2012-2017. Refer to text for covariate descriptions. *PHEAT = Precipitation-, Heat Load-, and Elevation-adjusted Topographic index.**

| Vegetation metric | Suite | Covariate | Acronym | L | Q | PS |
|---|---|---|---|---|---|---|
| Forage abundance | NDVI | Amplitude | AMP | + | | + |
| | | Time Integrated | TIN | + | | + |
| | Terrain | Elevation | ELEV | - | | - |
| | | Slope | SLP | - | | - |
| | | Solar Radiation Index | SRI | + | +/- | + |
| | | Compound Topography Index | CTI | + | +/- | + |
| | | PHEAT* | PHEAT | + | +/- | + |
| | Precipitation | Winter-Spring | WSp | + | | + |
| | | Winter-Spring-Summer | WSSp | + | | + |
| | Vegetation | Canopy cover | CC | - | | - |
| Forage quality | NDVI | Amplitude | AMP | + | +/- | + |
| | | Time Integrated | TIN | + | +/- | + |
| | Terrain | Elevation | ELEV | - | | - |
| | | Slope | SLP | - | | - |
| | | Solar Radiation Index | SRI | + | +/- | + |
| | | Compound Topography Index | CTI | + | +/- | + |
| | | PHEAT* | PHEAT | - | +/- | - |
| | Precipitation | Winter-Spring | WSp | + | | + |
| | | Winter-Spring-Summer | WSSp | + | | + |
| | Vegetation | Canopy cover | CC | - | | - |

We obtained vegetation cover types from the Region 1 Vegetation Mapping Program (VMap) databases maintained and used extensively by the Northern Region of the U.S. Forest Service (Barber et al. 2011). To classify vegetation cover types, we used the dominance 60% plurality classifications that included grass (dry and wet), shrub (xeric and mesic), and tree (species-specific or heterogeneous mixed species) lifeforms (Table 2). For tree lifeforms, the dominance 60% plurality classification represents the species comprising ≥ 60% of the abundance present within vegetation polygons or a heterogeneous mix of shade-tolerant or -intolerant species where no single species makes up ≥ 60% of the abundance present within vegetation polygons.

**Table 2 - Descriptions of vegetation cover types as defined by dominance 60% plurality classifications from the U.S. Forest Service Region 1 Vegetation Mapping Program (VMap) databases (Barber et al. 2011).**

| VMap classification | Species or description |
|---|---|
| GRASS-DRY | Dry grassland communities |
| GRASS-WET | Moist grassland communities |
| SHRUB-MESIC | Moist shrubland communities |
| SHRUB-XERIC | Dry shrubland communities |
| ABLA | *Abies lasiocarpa* |
| LAOC | *Larix occidentalis* |
| PIAL | *Pinus albicaulis* |
| PICO | *Pinus contorta* |
| PIPO | *Pinus ponderosa* |
| PSME | *Pseudotsuga menziesii* |
| IMIX | Mixed shade-intolerant conifer and hardwood species |
| TMIX | Mixed shade-tolerant conifer and hardwood species |
| POPUL | *Populus* spp. |

We obtained 30-m elevation data from The National Map (https://nationalmap.gov/) and calculated SLP, SRI (Fu and Rich 1999), and CTI variables. We obtained 30-m forest canopy cover data from Landfire (<https://www.landfire.gov/) to account for the influence of canopy cover on vegetation productivity. We also expected that the effect of the NDVI metrics on forage abundance and quality would depend on the effect of canopy cover (e.g., where canopy cover is lower, the effect of the NDVI metrics will be stronger). To account for annual variations in growing season conditions during the 6 years of vegetation sampling, we calculated 2 precipitation metrics for each year of sampling from 4-km PRISM data (PRISM Climate Group 2016). We calculated winter-spring precipitation (WSp) by accumulating precipitation from December 1 to May 31 to characterize the moisture available leading into the growing season. We calculated winter-spring-summer precipitation (WSSp) by accumulating precipitation from December 1 to the date of sampling to characterize the moisture available throughout the growing season.

The PHEAT variable is a 10-m resolution index of site moisture potential developed to characterize the biophysical properties of the landscape (S. Brown, U.S. Forest Service, unpublished data). PHEAT estimates the relative availability of moisture at a given site based on the integration of fine-scale, 30-year average precipitation, elevation-adjusted heat load (annual insolation), and the compound topographic index. Starting with a given amount of precipitation, moisture becomes either more or less available based on the topography downhill (i.e., a moisture shedding or collecting area) and by the evaporative demand as modeled by the radiative heat load (watts/m$^2$) impacting the site. The radiative heat load model is adjusted by elevation to attenuate the evaporative demand due to the altitude-related temperature that would be experienced at those sites (e.g., the evaporative demand at a low elevation southern exposure site would be greater than at a high elevation southern exposure site). The combined output is a unit-less index of site moisture potential, with values ranging from low to high representing low to high moisture potential.

## Analysis

To develop models that predict forage abundance and forage quality from NDVI metrics, we extracted the values of the NDVI metrics and landscape covariates to each sampling site that corresponded to the year of ground-sampling. We standardized all continuous covariates and excluded covariate pairs with Pearson correlation coefficients of $|r| > 0.6$ from consideration in the same model to avoid collinearity problems (Appendix B). Additionally, to allow flexibility in the relationships between nutritional resources and covariates, we evaluated linear, quadratic, and pseudothreshold (natural log transform; after Franklin et al. 2000) forms for each continuous covariate in an exploratory framework unless the most appropriate functional form could be identified *a priori* from existing literature (Table 1). For the NDVI metrics, we expected a positive association with forage abundance and therefore considered only linear and pseudothreshold functional forms of each NDVI metric in forage abundance models. We expected a positive association with or a peak at intermediate values of forage quality (Hebblewhite 2006) and therefore considered all functional forms of each NDVI metric in forage quality models. If necessary, variables considered for the pseudothreshold form were adjusted by addition of a small value to allow log transformation. We used log-linear and linear regression using Program R version 3.4.3 (R Development Core Team 2018) to predict forage abundance and quality, respectively, as a function of the NDVI metrics and landscape covariates. We log transformed forage abundance to meet assumptions of normality for linear modeling.

We used Akaike's Information Criterion (AIC) to rank and select best-supported ($\Delta$AIC < 4; Burnham and Anderson 2002) models in several model tiers for each forage abundance and forage quality response variable. We used model tiers to reduce the number of competing models considered in each subsequent tier (Franklin et al. 2000). We removed any uninformative covariates from models advancing to the next tier (Arnold 2010). We used 5 model tiers to determine the most-supported functional forms and combinations of an NDVI metric and landscape covariates and to select models that best represent the relationship between elk nutritional resources and NDVI.

In model tier 1, we competed univariate models of each hypothesized functional form of the NDVI metrics. We considered the most-supported functional forms of the NDVI metrics from this model tier in separate evaluations (i.e., for each NDVI metric functional form, we evaluated a second, third, and fourth model tier) excluding the fifth model tier that we used to compete the two NDVI metrics (described below). Within each respective evaluation, we included the NDVI metric functional form additively in all models of subsequent model tiers. In model tier 2, we competed hypothesized functional forms of each landscape covariate in independent sets for each covariate. We included in each set a "null" model with the NDVI metric functional form considered alone and, in the canopy cover set, models interacting canopy cover with the NDVI metric functional form. We did not evaluate canopy cover covariates in the TIN sets and WSp and WSSp covariates in the AMP sets due to collinearities with the respective NDVI metric. We advanced the most-supported covariate forms to model tier 3 in which we competed additive combinations of the most-supported functional forms in each of a terrain (ELEV, SLP, SRI, CTI, and PHEAT), and vegetation (VMap and canopy cover) model suite. We did not consider PHEAT with ELEV, SLP, SRI, or

CTI in the same models due to the similarity of landscape properties described by the covariates. In a precipitation suite, we compared WSp and WSSp in separate models (i.e., not considered additively).

In model tier 4, we evaluated all additive combinations of the most-supported models from each model suite in model tier 3. We used model tier 5, if necessary, to compete the top models from each NDVI metric functional form's respective fourth model tier. From model tier 5, we selected the most-supported model to make inference from; however, where substantial model selection uncertainty ($\Delta$AIC < 2; Burnham and Anderson 2002) existed between the NDVI metrics, we selected the model with the most-supported functional form for each NDVI metric (e.g., one model for each AMP and TIN metric). We assessed the fit of the models based on $R^2$ values and evaluated the magnitude and direction of covariate effects on forage abundance and quality based on standardized coefficient estimates and sign, as well as comparisons of predictions estimated by holding covariates at mean values.

## Results

## Nutritional resources

A total of 22 and 62 species comprised 95% of the summer-fall diets for the Elkhorn and Bitterroot Valley elk populations, respectively. Within the Elkhorn population, the most common graminoid forage species were *Poa* and *Festuca* spp., comprising 36.5% of the diet. The most common graminoid forage species within the Bitterroot Valley populations were *Poa* spp. and *Carex* spp., comprising 18.0-37.6% of the diets. *Agropyron* spp., *Bromus tectorum*, and *Stipa comata* were relatively common (16.1%) only to the North Sapphire diet. The most common forb forage species across all populations were *Lupinus* spp., comprising 6.2-12.1% of the diets. *Balsamorhiza sagitata* was common (2.6-5.5%) only to the Bitterroot Valley populations. *Verbascum* spp. and *Medicago sativa* were relatively common (7.1%) only to the North Sapphire diet. The most common shrub forage species in the Elkhorn population were *Vaccinium* spp., comprising 4.7% of the diet, and in the Bitterroot Valley populations were *Salix* spp. and *Vaccinium* spp., comprising 2.9-3.7% of the diets. *Shepherdia canadensis* and *Physocarpus malvaceus* were relatively common (3.1%) only to the North Sapphire diet.

We sampled vegetation at 110 and 460 sites in the Elkhorn Mountains and Bitterroot Valley, respectively. Within the Elkhorn Mountains, the most common forb forage species included *Lupinus SP* (n=29), *Astragalus SP* (n=25), *Lithospermum ruderale* (n=6), and *Equisetum arvense* (n=5). The most common graminoid forage species included *Pseudoroegneria spicata* (n=59), *Festuca idahoensis* (n=54), and *Carex geyeri* (n=51). The most common shrub forage species included *Vaccinium scoparium* (n=54), *Artemisia frigida* (n=38), and *Vaccinium membranaceum* (n=34). Within the Bitterroot Valley, the most common forb forage species included *Achillea millefolium* (n=170), *Balsamorhiza sagittata* (n=116), *Centaurea stoebe* (n=108), and *Xerophyllum tenax* (n=108). The most common graminoid forage species included *Carex geyeri* (n=165), *Pseudoroegneria spicata* (n=153), and *Festuca idahoensis* (n=147). The most common shrub forage species included *Symphoricarpos albus* (n=143), *Berberis repens* (n=67), and *Vaccinium membranaceum* (n=66).

Median forage abundance was 25 g/m$^2$ (ranging 0-419.7) and varied between the Elkhorn Mountains (9 g/m$^2$) and Bitterroot Valley (30.4 g/m$^2$) across vegetation cover types (Fig. 2). Across all sampling sites, median forage abundance varied by vegetation cover type (Fig. 3). Median forage abundance was highest in GRASS-DRY (40.2 g/m$^2$) and GRASS-WET (35.7 g/m$^2$) and lowest in PIAL (1.1 g/m$^2$) and LAOC (6 g/m$^2$). Forage abundance was least variable in SHRUB-MESIC (± 26.5 g/m$^2$) and PIPO (± 33.2 g/m$^2$) and most variable in ABLA (± 101.5 g/m$^2$) and LAOC (± 67.7 g/m$^2$).
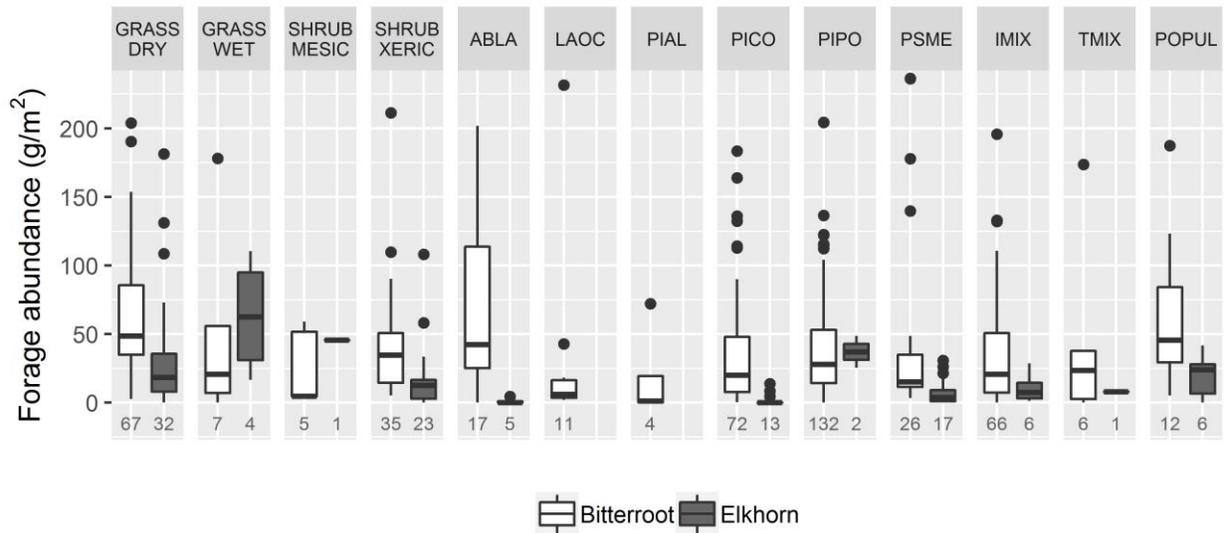


**Figure 2 - Herbaceous forage abundance (g/m$^2$) measured within each vegetation cover type for the Elkhorn Mountains and Bitterroot Valley study areas of west-central Montana, USA, 2012-2017. Box-and-whisker plots show the traditional 5-number summary (minimum, first quartile, median, third quartile, and maximum). Values along x-axis indicate the sample size within each vegetation cover type and study area. Refer to Table 2 for definitions of vegetation cover types.**
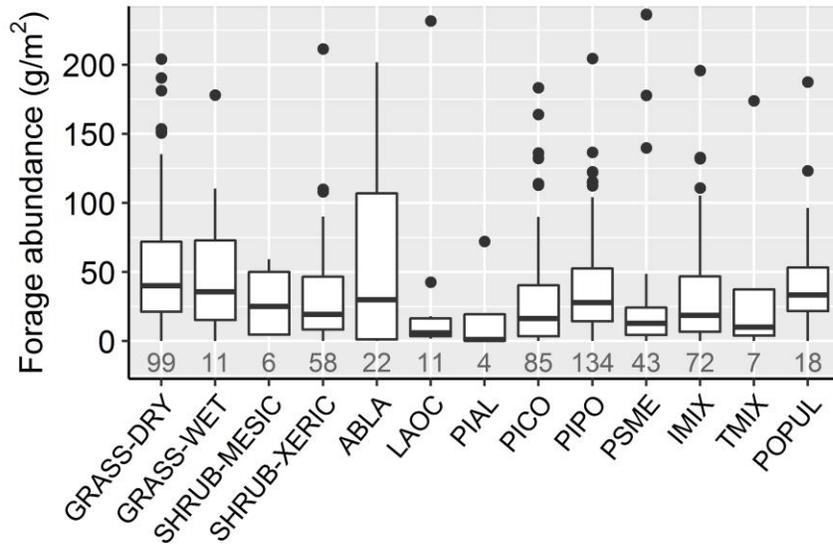
**Figure 3 - Herbaceous forage abundance (g/m²) measured within each vegetation cover type combined for the Elkhorn Mountains and Bitterroot Valley study areas of west-central Montana, USA, 2012-2017. Box-and-whisker plots show the traditional 5-number summary (minimum, first quartile, median, third quartile, and maximum). Values along x-axis indicate the sample size within each vegetation cover type. Refer to Table 2 for definitions of vegetation cover types.**

Forage quality across sampling sites in the Bitterroot Valley averaged 2.74 ± 0.38 kcal/g and varied by vegetation cover types (Fig. 4). Mean forage quality was highest in POPUL (2.96 kcal/g) and PIPO (2.95 kcal/g) and lowest in TMIX (2.18 kcal/g) and PIAL (2.21 kcal/g). Forage quality was least variable in POPUL (± 0.16 kcal/g) and PIPO (± 0.16 kcal/g) and most variable in GRASS-WET (± 1.52 kcal/g) and ABLA (± 0.39 kcal/g).
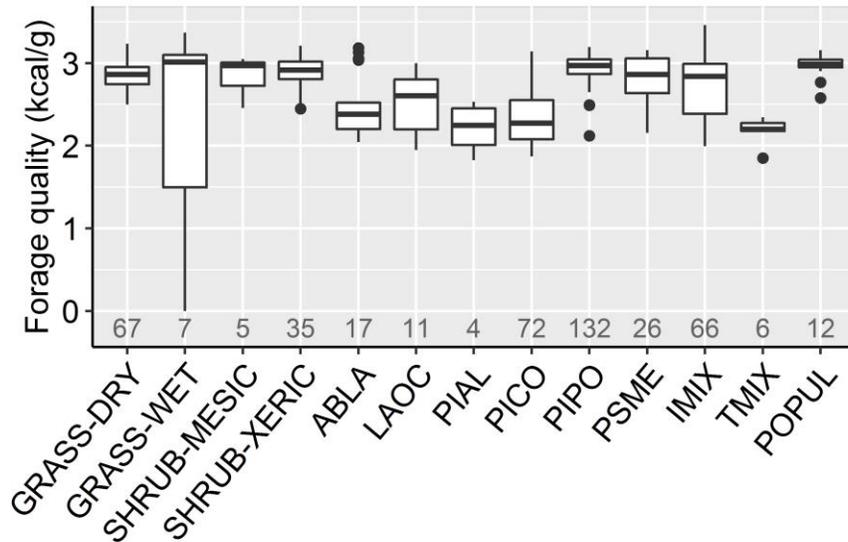
**Figure 4 - Forage quality (i.e., mean digestible energy; kcal/g) measured within each vegetation cover type for the Bitterroot Valley study area of west-central Montana, USA, 2012-2015. Box-and-whisker plots show the traditional 5-number summary (minimum, first quartile, median, third quartile, and maximum). Values along x-axis indicate the sample size within each vegetation cover type. Refer to Table 2 for definitions of vegetation cover types.**

## NDVI metrics

AMP values across all sampling sites averaged 0.21 ± 0.16 and varied between the Elkhorn Mountains (0.19 ± 0.19) and the Bitterroot Valley (0.22 ± 0.16). Across all sampling sites, AMP varied by vegetation cover types (Fig. 5). Mean AMP was highest in PIAL (0.60 g/m$^2$) and GRASS-WET (0.53) and lowest in SHRUB-XERIC (0.12) and GRASS-DRY (0.13). AMP was least variable in PIAL (± 0.04) and SHRUB-XERIC (± 0.1) and most variable in TMIX (± 0.22) and ABLA (± 0.2). TIN values across all sampling sites averaged 4.5 ± 1.3 and varied between the Elkhorn Mountains (3.8 ± 1.3) and the Bitterroot Valley (4.7 ± 1.2). Across all sampling sties, TIN varied by vegetation cover types (Fig. 5). Mean TIN was highest in LAOC (6.6 g/m$^2$) and SHRUB-MESIC (5.6) and lowest in SHRUB-XERIC (2.9) and GRASS-DRY (3.1). TIN was least variable in LAOC (± 0.4) and PIAL (± 0.4) and most variable in SHRUB-MESIC (± 1.1) and IMIX (± 1.0).
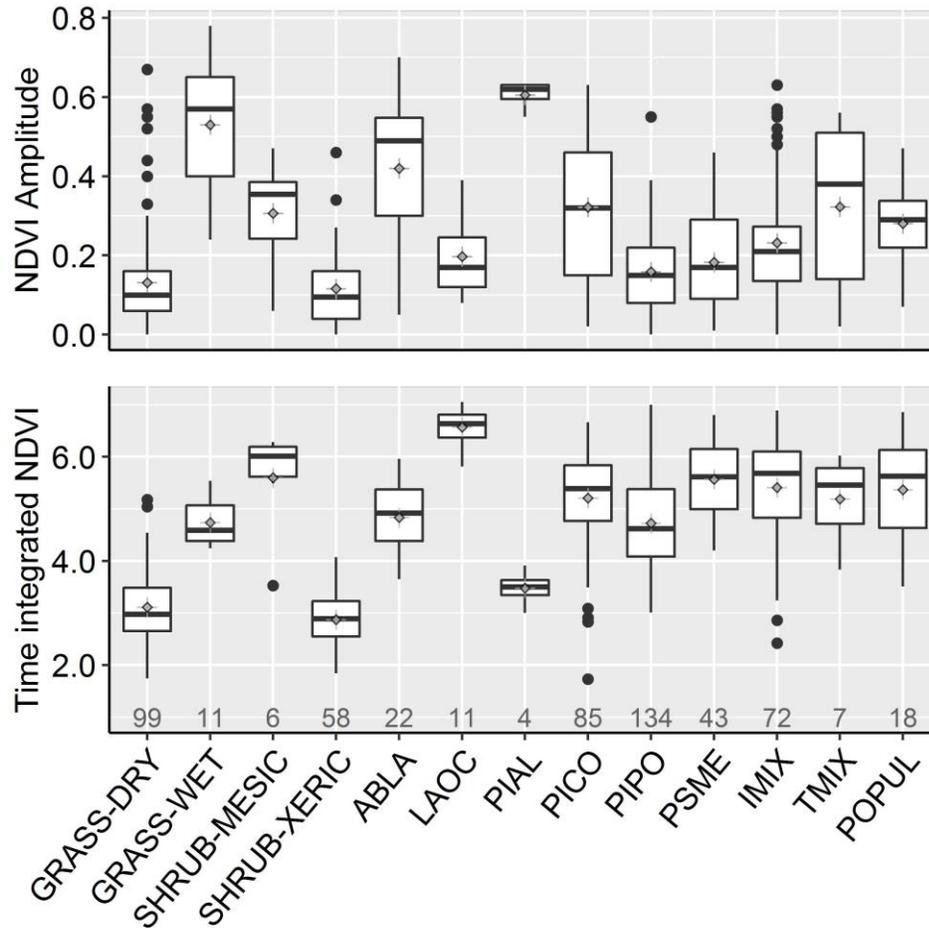
**Figure 5 - Landsat Time Integrated NDVI and NDVI amplitude values within each vegetation cover type in the Elkhorn Mountains and Bitterroot Valley of west-central Montana, USA, 2012-2017. Box-and-whisker plots show the traditional 5-number summary (minimum, first quartile, median, third quartile, and maximum). Mean values are indicated by cross-hair diamonds. Values along x-axis indicate the sample size within each vegetation cover type. Refer to Table 2 for definitions of vegetation cover types.**

## Forage Abundance Analysis

In model tier 1 for predicting forage abundance, the most-supported NDVI metric was linear AMP (Akaike weight [$w_i$] = 0.46); however, linear TIN ($w_i$ = 0.21), pseudothreshold AMP ($w_i$ = 0.18), and pseudothreshold TIN ($w_i$ = 0.15) were also supported ($\Delta$AIC < 2.30). We therefore considered all NDVI metrics in separate model sets for each metric. In model tier 2, the NDVI metric sets shared similar support for the following functional forms of covariates: linear ELEV, linear and pseudothreshold SRI, and linear, quadratic, and pseudothreshold CTI (Table 3). For all NDVI metric sets, the most-supported SLP model was the null model containing only the NDVI metric. In both TIN sets, quadratic PHEAT, linear WSp, and linear WSSp were additionally supported, with further support for pseudothreshold WSSp in the linear TIN set. In both linear and pseudothreshold AMP sets, linear canopy cover was most-supported.

**Table 3** - Tier 2 model selection results comparing forage abundance models within and across NDVI metric model sets for examining relationships of NDVI and elk nutritional resources in west-central Montana, USA, 2012-2017. The top models within 4 AIC units of the top-ranked model for each set are presented. Covariate superscripts indicate functional form (2 = quadratic, PS = pseudothreshold, [none] = linear). K = no. of parameters, $wt_i$ = AIC weight. Models with uninformative parameters are not presented. Null model AIC = 2519.87. Refer to text for covariate descriptions.

| NDVI metric | Covariate | Model | K | AIC | ΔAIC | $wt_i$ |
|---|---|---|---|---|---|---|
| AMP | ELEV | ELEV | 4 | 2493.30 | 0.00 | 0.97 |
| | SRI | SRI | 4 | 2506.33 | 0.00 | 0.44 |
| | | SRI$^{PS}$ | 4 | 2506.55 | 0.22 | 0.40 |
| | CTI | CTI$^2$ | 5 | 2512.88 | 0.00 | 0.53 |
| | | CTI | 4 | 2514.04 | 1.16 | 0.30 |
| | | CTI$^{PS}$ | 4 | 2515.72 | 2.85 | 0.13 |
| | CC | CC | 4 | 2489.84 | 0.00 | 0.69 |
| TIN | ELEV | ELEV | 4 | 2495.20 | 0.00 | 0.95 |
| | SRI | SRI | 4 | 2510.08 | 0.00 | 0.43 |
| | | SRI$^{PS}$ | 4 | 2510.17 | 0.09 | 0.41 |
| | CTI | CTI$^2$ | 5 | 2514.42 | 0.00 | 0.49 |
| | | CTI | 4 | 2515.20 | 0.78 | 0.33 |
| | | CTI$^{PS}$ | 4 | 2516.85 | 2.43 | 0.14 |
| | PHEAT | PHEAT$^2$ | 5 | 2519.09 | 0.00 | 0.42 |
| | WSp | WSp | 4 | 2516.66 | 0.00 | 0.71 |
| | WSSp | WSSp | 4 | 2514.33 | 0.00 | 0.87 |
| | | WSSp$^{PS}$ | 4 | 2518.19 | 3.86 | 0.13 |
| AMP$^{PS}$ | ELEV | ELEV | 4 | 2492.58 | 0.00 | 0.97 |
| | SRI | SRI | 4 | 2508.71 | 0.00 | 0.44 |
| | | SRI$^{PS}$ | 4 | 2508.88 | 0.17 | 0.40 |
| | CTI | CTI$^2$ | 5 | 2514.45 | 0.00 | 0.52 |
| | | CTI | 4 | 2515.50 | 1.05 | 0.31 |
| | | CTI$^{PS}$ | 4 | 2517.22 | 2.77 | 0.13 |
| | CC | CC | 4 | 2489.47 | 0.00 | 0.71 |
| TIN$^{PS}$ | ELEV | ELEV | 4 | 2494.99 | 0.00 | 0.95 |
| | SRI | SRI | 4 | 2510.05 | 0.00 | 0.42 |
| | | SRI$^{PS}$ | 4 | 2510.11 | 0.06 | 0.41 |
| | CTI | CTI$^2$ | 5 | 2514.74 | 0.00 | 0.52 |
| | | CTI | 4 | 2515.73 | 0.99 | 0.32 |
| | | CTI$^{PS}$ | 4 | 2517.45 | 2.71 | 0.13 |
| | PHEAT | PHEAT$^2$ | 5 | 2520.07 | 0.00 | 0.38 |
| | WSp | WSp | 4 | 2516.47 | 0.00 | 0.77 |
| | WSSp | WSSp | 4 | 2513.99 | 0.00 | 0.88 |

In the third model tiers, the NDVI metric model sets shared 3 most-supported models in the terrain model suite: (1) quadratic CTI, linear ELEV, and linear SRI; (2) quadratic CTI, linear ELEV, and pseudothreshold SRI; and (3) linear CTI, linear ELEV, and linear SRI (Table 4). The linear and pseudothreshold AMP sets had additional support for a model that included linear CTI, linear ELEV, and pseudothreshold SRI. The model with quadratic CTI, linear ELEV, and linear SRI was the top terrain model in each NDVI metric model set. In the linear and pseudothreshold TIN sets, the most-supported model in the vegetation suite included VMap. The most-supported models in the precipitation suite included linear WSSp and WSp; the linear TIN set additionally included pseudothreshold WSSp. In the linear and

pseudothreshold AMP sets, the most-supported models in the vegetation suite included: 1) canopy cover and VMap and 2) canopy cover alone.

**Table 4 - Tier 3 model selection results comparing forage abundance models within and across NDVI metric model sets for examining relationships of NDVI and elk nutritional resources in west-central Montana, USA, 2012-2017. The top models within 4 AIC of the top-ranked model for each set are presented. Covariate superscripts indicate functional form (2 = quadratic, PS = pseudothreshold, [none] = linear). K = no. of parameters, $wt_i$ = AIC weight. Models with uninformative parameters are not presented. Refer to text for covariate descriptions.**

| NDVI metric | Suite | Model | K | AIC | ΔAIC | $wt_i$ |
|---|---|---|---|---|---|---|
| AMP | Terrain | ELEV + SRI + CTI$^2$ | 7 | 2450.98 | 0.00 | 0.47 |
| | | ELEV + SRI + CTI | 6 | 2452.66 | 1.68 | 0.20 |
| | | ELEV + SRI$^{PS}$ + CTI$^2$ | 7 | 2452.85 | 1.87 | 0.19 |
| | | ELEV + SRI$^{PS}$ + CTI | 6 | 2454.37 | 3.40 | 0.09 |
| | Vegetation | CC + VMAP | 16 | 2487.36 | 0.00 | 0.78 |
| | | CC | 4 | 2489.91 | 2.55 | 0.22 |
| TIN | Terrain | ELEV + SRI + CTI$^2$ | 7 | 2453.27 | 0.00 | 0.53 |
| | | ELEV + SRI$^{PS}$ + CTI$^2$ | 7 | 2455.20 | 1.93 | 0.20 |
| | | ELEV + SRI + CTI | 6 | 2455.70 | 2.42 | 0.16 |
| | Vegetation | VMAP | 15 | 2496.78 | 0.00 | 1.00 |
| | Precipitation | WSSp | 4 | 2514.40 | 0.00 | 0.67 |
| | | WSp | 4 | 2516.73 | 2.33 | 0.31 |
| | | WSSp$^{PS}$ | 4 | 2518.26 | 3.86 | 0.15 |
| AMP$^{PS}$ | Terrain | ELEV + SRI + CTI$^2$ | 7 | 2451.44 | 0.00 | 0.49 |
| | | ELEV + SRI$^{PS}$ + CTI$^2$ | 7 | 2453.18 | 1.75 | 0.21 |
| | | ELEV + SRI + CTI | 6 | 2453.49 | 2.06 | 0.18 |
| | | ELEV + SRI$^{PS}$ + CTI | 6 | 2455.08 | 3.64 | 0.08 |
| | Vegetation | CC + VMAP | 16 | 2486.61 | 0.00 | 0.81 |
| | | CC | 4 | 2489.55 | 2.94 | 0.18 |
| TIN$^{PS}$ | Terrain | ELEV + SR+ CTI$^2$ | 7 | 2451.16 | 0.00 | 0.55 |
| | | ELEV + SRI$^{PS}$ + CTI$^2$ | 7 | 2453.08 | 1.92 | 0.21 |
| | | ELEV + SRI + CTI | 6 | 2453.88 | 2.72 | 0.14 |
| | Vegetation | VMAP | 15 | 2492.45 | 0.00 | 1.00 |
| | Precipitation | WSSp | 4 | 2514.06 | 0.00 | 0.78 |
| | | WSp | 4 | 2516.54 | 2.48 | 0.22 |

In the fourth model tiers, we ran 14 models in the linear AMP, pseudothreshold AMP, and linear TIN sets and 15 models in the pseudothreshold TIN set. Top models in each NDVI metric set included quadratic or linear CTI, linear ELEV, and linear or pseudothreshold SRI (Table 5). Three models were most-supported for both pseudothreshold and linear TIN sets and models included only terrain covariates. Seven and six models were most-supported for linear and pseudothreshold AMP, respectively, and models varied whether linear canopy cover was included. No models in any NDVI metric set supported the inclusion of WSp, WSSp, or VMap.

We ran 19 models in model tier 5 comparing across NDVI metric functional form model sets (Table 5). Model selection uncertainty indicated support for all linear and pseudothreshold AMP models, 2 pseudothreshold TIN models, and 1 linear TIN model. The

most-supported AMP model included pseudothreshold AMP, quadratic CTI, linear ELEV, linear SRI, and canopy cover. The second most-supported AMP model included linear AMP and shared the same landscape covariates. There was substantial model selection uncertainty between the top AMP and TIN metric models, with the most-supported ($\Delta$AIC = 1.83) TIN model including pseudothreshold TIN, quadratic CTI, linear ELEV, and linear SRI. We therefore selected both the top AMP and TIN models for inference. The coefficient estimates from the top AMP model followed expected predictions, indicating that forage abundance increased: (1) as AMP and SRI increased, (2) to a maximum at moderate levels of CTI, and (3) as ELEV and CC decreased (Table 6; Fig. 6). The coefficient estimates from the top TIN model indicated similar relationships but with no effect of CC (Table 6; Fig. 7). Based on the standardized coefficient estimates of terrain covariates, ELEV and SRI had the largest effect size in both AMP and TIN models, followed by CC in the AMP model and CTI in the TIN model. The proportion of the variation (adjusted $R^2$) in forage abundance explained by the covariates in both the top AMP and TIN models was 0.12. The proportion of the variation explained by pseudothreshold AMP alone and pseudothreshold TIN alone were both 0.01.

**Table 5 - Model selection results comparing forage abundance models within (model tier 4) and across (model tier 5) NDVI metric model sets for examining relationships of NDVI and elk nutritional resources in west-central Montana, USA, 2012-2017. The top models within 4 AIC of the top-ranked model for each set are presented. Covariate superscripts indicate functional form (2 = quadratic, PS = pseudothreshold, [none] = linear). K = no. of parameters, $wt_i$ = AIC weight. Models with uninformative parameters are not presented. Refer to text for covariate descriptions.**

| NDVI metric | Model | K | AIC | Within $\Delta$AIC | Within $wt_i$ | Across $\Delta$AIC | Across $wt_i$ |
|---|---|---|---|---|---|---|---|
| AMP$^{PS}$ | CC + CTI$^2$ + ELEV + SRI | 8 | 2449.53 | 0.00 | 0.37 | 0.00 | 0.16 |
| | CC + CTI$^2$ + ELEV + SRI$^{PS}$ | 8 | 2450.89 | 1.36 | 0.19 | 1.36 | 0.08 |
| | CC + CTI + ELEV + SRI | 7 | 2451.01 | 1.48 | 0.17 | 1.48 | 0.08 |
| | CTI$^2$ + ELEV + SRI | 7 | 2451.64 | 2.10 | 0.13 | 2.10 | 0.06 |
| | CC + CTI + ELEV + SRI$^{PS}$ | 7 | 2452.24 | 2.70 | 0.09 | 2.70 | 0.04 |
| | CTI$^2$ + ELEV + SRI$^{PS}$ | 7 | 2453.38 | 3.85 | 0.05 | 3.85 | 0.02 |
| AMP | CC + CTI$^2$ + ELEV + SRI | 8 | 2450.08 | 0.00 | 0.30 | 0.55 | 0.12 |
| | CTI$^2$ + ELEV + SRI | 7 | 2451.17 | 1.09 | 0.17 | 1.64 | 0.07 |
| | CC + CTI + ELEV + SRI | 7 | 2451.21 | 1.14 | 0.17 | 1.68 | 0.07 |
| | CC + CTI$^2$ + ELEV + SRI$^{PS}$ | 8 | 2451.60 | 1.52 | 0.14 | 2.06 | 0.06 |
| | CC + CTI + ELEV + SRI$^{PS}$ | 7 | 2452.60 | 2.52 | 0.08 | 3.06 | 0.03 |
| | CTI + ELEV + SRI | 6 | 2452.80 | 2.72 | 0.08 | 3.27 | 0.03 |
| | CTI$^2$ + ELEV + SRI$^{PS}$ | 7 | 2453.05 | 2.97 | 0.07 | 3.51 | 0.03 |
| TIN$^{PS}$ | CTI$^2$ + ELEV + SRI | 7 | 2451.36 | 0.00 | 0.61 | 1.83 | 0.06 |
| | CTI$^2$ + ELEV + SRI$^{PS}$ | 7 | 2453.28 | 1.92 | 0.23 | 3.74 | 0.02 |
| | CTI + ELEV + SRI | 6 | 2454.02 | 2.67 | 0.16 | 4.49 | 0.02 |
| TIN | CTI$^2$ + ELEV + SRI | 7 | 2453.47 | 0.00 | 0.59 | 3.94 | 0.02 |
| | CTI$^2$ + ELEV + SRI$^{PS}$ | 7 | 2455.40 | 1.93 | 0.23 | 5.87 | 0.01 |
| | CTI + ELEV + SRI | 6 | 2455.84 | 2.37 | 0.18 | 6.31 | 0.01 |

**Table 6 - Estimated coefficients and 95% confidence intervals for the top NDVI amplitude (AMP) and time-integrated NDVI (TIN) models examining relationships of NDVI and elk forage abundance in west-central Montana, USA, 2012-2017. Covariate superscripts indicate functional form (2 = quadratic, PS = pseudothreshold, [none] = linear). Bolded estimates indicate p < 0.05. Refer to text for covariate descriptions.**

| Covariate | AMP Model | | TIN Model | |
|---|---|---|---|---|
| | Estimate | C.I. | Estimate | C.I. |
| Intercept | **3.34** | (2.88, 3.80) | **1.62** | (0.75, 2.49) |
| $AMP^{PS}$ | **0.32** | (0.09, 0.54) | – | (–, –) |
| $TIN^{PS}$ | – | (–, –) | **0.79** | (0.21, 1.38) |
| $CTI^2$ | -0.11 | (-0.23, 0.00) | **-0.13** | (-0.25, -0.01) |
| CTI | -0.17 | (-0.42, 0.07) | -0.14 | (-0.39, 0.11) |
| ELEV | **-0.68** | (-0.90, -0.46) | **-0.72** | (-0.91, -0.54) |
| SRI | **0.38** | (0.18, 0.57) | **0.52** | (0.34, 0.70) |
| CC | **-0.21** | (-0.41, -0.01) | – | (–, –) |



**Figure 6 - Predicted forage abundance (black line), 95% confidence intervals (shaded), and observed forage abundance (gray dots) across levels of canopy cover (CC) and solar radiation (SRI) estimated from the inferential NDVI amplitude (AMP) model for evaluating the relationship of NDVI and elk nutritional resources in west-central Montana, USA, 2012-2017.**
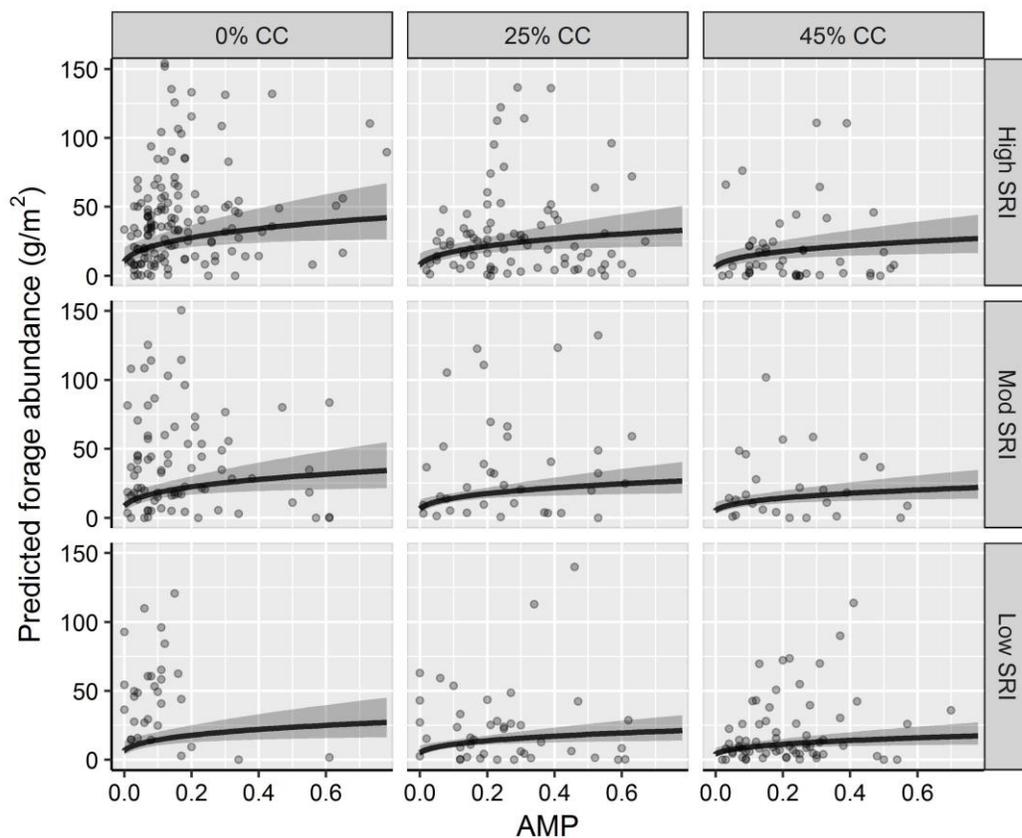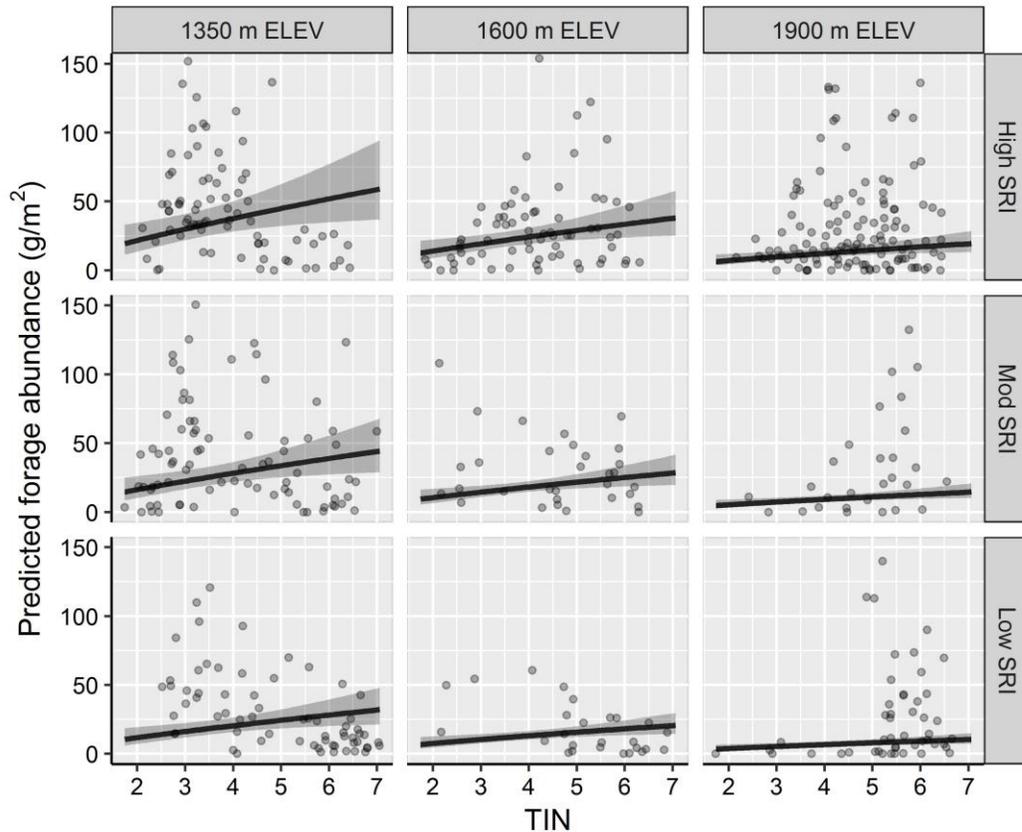
**Figure 7 - Predicted forage abundance (black line), 95% confidence intervals (shaded), and observed forage abundance (gray dots) across levels of elevation (ELEV) and solar radiation (SRI) estimated from the inferential time-integrated NDVI (TIN) model for evaluating the relationship of NDVI and elk nutritional resources in west-central Montana, USA, 2012-2017.**

## Forage Quality Analysis

In model tier 1 for predicting forage quality, the most-supported NDVI metric included quadratic AMP ($w_i$ = 1.0). The remaining NDVI metrics were $\Delta$AIC > 17.2 and were therefore not considered in subsequent model tiers. In model tier 2, the most-supported functional forms included linear ELEV, linear and pseudothreshold SRI, linear and pseudothreshold PHEAT, and linear canopy cover (Table 7). The most-supported SLP model was the null model containing only quadratic AMP. In model tier 3, the most-supported models in the terrain suite included: 1) linear ELEV and linear SRI and 2) linear ELEV and pseudothreshold SRI (Table 8). The most-supported model in the vegetation suite included: 1) linear canopy cover and VMap and 2) VMap alone.

**Table 7 - Tier 2 model selection results comparing forage abundance models within and across NDVI metric model sets for examining relationships of NDVI and elk nutritional resources in west-central Montana, USA, 2012-2017. The top models within 4 AIC units of the top-ranked model for each set are presented. Covariate superscripts indicate functional form (2 = quadratic, PS = pseudothreshold, [none] = linear). K = no. of parameters, wti = AIC weight. Models with uninformative parameters are not presented. Refer to text for covariate descriptions.**

| NDVI metric | Covariate | Model | K | AIC | ΔAIC | $wt_i$ |
|---|---|---|---|---|---|---|
| AMP | ELEV | ELEV | 4 | 321.29 | 0.00 | 0.92 |
| | SRI | SRI | 4 | 343.99 | 0.00 | 0.35 |
| | | SRI$^{PS}$ | 4 | 344.20 | 0.20 | 0.32 |
| | PHEAT | PHEAT | 4 | 328.45 | 0.00 | 0.42 |
| | | PHEAT$^{PS}$ | 4 | 328.78 | 0.33 | 0.36 |
| | CC | CC | 4 | 316.80 | 0.00 | 0.96 |

**Table 8 - Tier 3 model selection results comparing forage abundance models within and across NDVI metric model sets for examining relationships of NDVI and elk nutritional resources in west-central Montana, USA, 2012-2017. The top models within 4 AIC of the top-ranked model for each set are presented. Covariate superscripts indicate functional form (2 = quadratic, PS = pseudothreshold, [none] = linear). K = no. of parameters, wti = AIC weight. Models with uninformative parameters are not presented. Refer to text for covariate descriptions.**

| NDVI metric | Suite | Model | K | AIC | ΔAIC | $wt_i$ |
|---|---|---|---|---|---|---|
| AMP | Terrain | ELEV + SRI | 5 | 312.63 | 0.00 | 0.67 |
| | | ELEV + SRI$^{PS}$ | 5 | 314.14 | 1.50 | 0.32 |
| | Vegetation | CC + VMAP | 16 | 214.96 | 0.00 | 0.66 |
| | | VMAP | 15 | 216.28 | 1.32 | 0.34 |

We ran 8 models in model tier 4 (Table 9), of which 6 had $\Delta$AIC $\leq$ 1.17. The most-supported model included linear canopy cover and VMap. All top models included VMap with the next nearest-ranking model without VMap having $\Delta$AIC > 91.93. We selected the most-supported model for inference. In the top model, the coefficient estimates followed expected predictions, indicating that forage quality increased: (1) to a maximum at moderate levels of AMP and (2) as CC decreased (Table 10, Fig. 8). Coefficient estimates indicated that forage quality varied by VMap cover type with highest and lowest predicted forage quality in POPUL and TMIX, respectively. Based on the standardized coefficient estimates, the quadratic term of AMP had the largest effect size, followed by canopy cover. The proportion of the variation in forage quality explained by the covariates in the top model and by AMP alone was 0.39 and 0.03 (adjusted $R^2$), respectively.

**Table 9 - Tier 4 model selection results comparing forage quality models for examining relationships of NDVI and elk nutritional resources in west-central Montana, USA, 2012-2015. The top models within 4 AIC units of the top-ranked model for each set are presented. Covariate superscripts indicate functional form (2 = quadratic, PS = pseudothreshold, [none] = linear). K = no. of parameters, wti = AIC weight. Models with uninformative parameters are not presented. Refer to text for covariate descriptions.**

| NDVI metric | Model | K | AIC | ΔAIC | $wt_i$ |
|---|---|---|---|---|---|
| $AMP^2$ | CC + VMAP | 17 | 216.16 | 0.00 | 0.21 |
| | ELEV + SRI + CC + VMAP | 19 | 216.43 | 0.26 | 0.18 |
| | ELEV + SRI + VMAP | 18 | 216.50 | 0.33 | 0.18 |
| | ELEV + SRI$^{PS}$ + CC + VMAP | 19 | 216.65 | 0.49 | 0.17 |
| | ELEV + SRI$^{PS}$ + VMAP | 18 | 216.93 | 0.77 | 0.14 |
| | VMAP | 16 | 217.33 | 1.17 | 0.12 |
| | ELEV + SRI | 6 | 308.10 | 91.93 | 0.00 |
| | ELEV + SRI$^{PS}$ | 6 | 309.53 | 93.37 | 0.00 |

**Table 10 - Estimated coefficients and 95% confidence intervals for the top model examining relationships of NDVI and elk forage quality in west-central Montana, USA, 2012-2015. Covariate superscripts indicate functional form (2 = quadratic, [none] = linear). Effects of VMap cover types are in relation to the reference (intercept) cover type GRASS-DRY. Bolded estimates indicate p < 0.05. Refer to text for covariate descriptions and Table 2 for definitions of VMap cover types.**

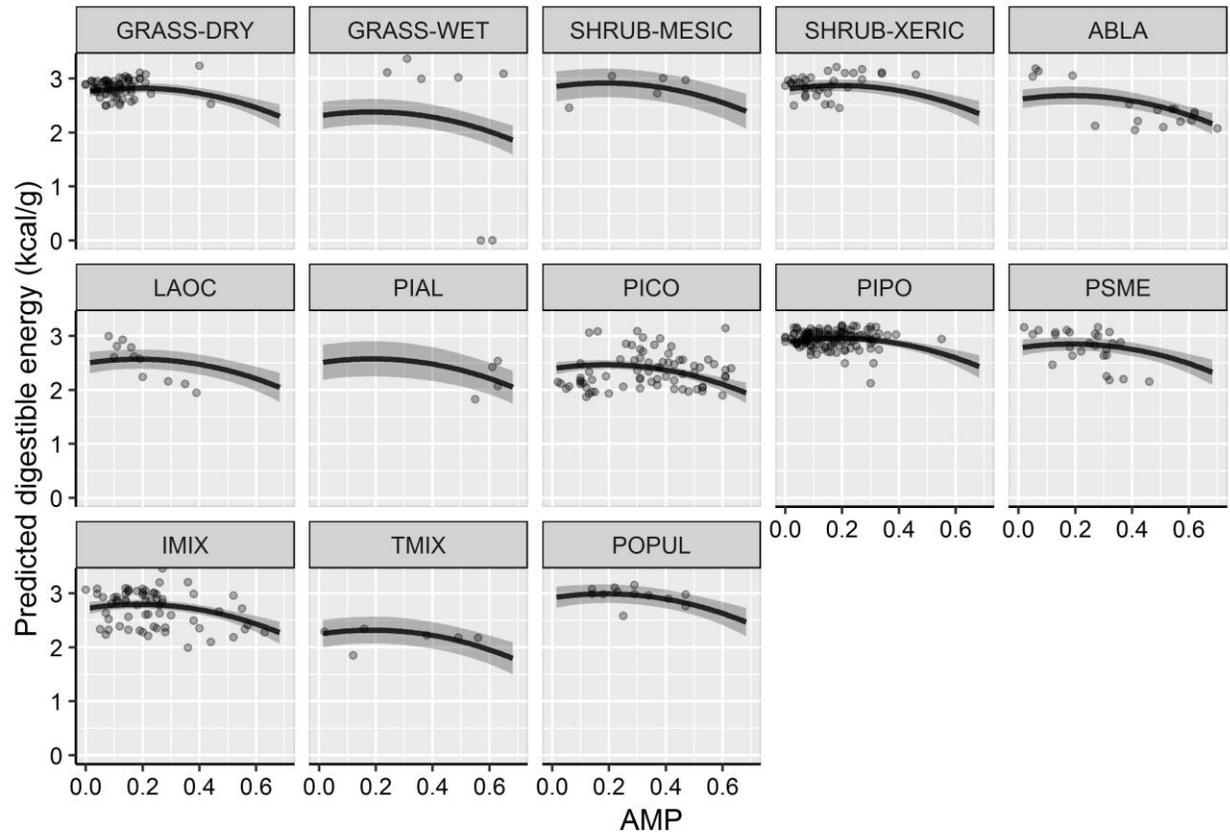| Covariate | Estimate | C.I. |
|---|---|---|
| Intercept | **2.82** | (2.73, 2.91) |
| AMP | -0.02 | (-0.06, 0.02) |
| $AMP^2$ | **-0.05** | (-0.08, -0.02) |
| CC | -0.04 | (-0.08, 0.01) |
| GRASS-WET | **-0.44** | (-0.69, -0.19) |
| SHRUB-MESIC | 0.10 | (-0.18, 0.37) |
| SHRUB-XERIC | 0.05 | (-0.07, 0.17) |
| ABLA | -0.14 | (-0.33, 0.05) |
| LAOC | **-0.25** | (-0.45, -0.05) |
| PIAL | -0.25 | (-0.58, 0.09) |
| PICO | **-0.35** | (-0.48, -0.23) |
| PIPO | **0.14** | (0.04, 0.23) |
| PSME | 0.03 | (-0.13, 0.18) |
| IMIX | -0.03 | (-0.15, 0.10) |
| TMIX | **-0.50** | (-0.77, -0.24) |
| POPUL | 0.17 | (-0.02, 0.36) |

**Figure 8 - Predicted forage quality (black line), 95% confidence intervals (shaded), and observed forage quality (gray dots) for each VMap cover type in the inferential model for the relationship of NDVI and elk nutritional resources in west-central Montana, USA, 2012-2015. Refer to Table 2 for definitions of VMap cover types.**

## Discussion

We found some evidence for a relationship between NDVI and summer-fall nutritional resources for elk, and that NDVI, in association with other landscape attributes, may be useful for representing elk forage during the summer-fall on west-central Montana landscapes. In our models predicting both forage abundance and quality, NDVI amplitude was the most-supported NDVI metric. We additionally found time-integrated NDVI to share substantial support in our models predicting forage abundance. Time-integrated NDVI may better represent summer-fall resources for elk because it accounts for changes in vegetation beyond maximum productivity and extending throughout the late-summer and fall (unlike NDVI amplitude), the period when acquiring adequate nutrition is particularly important for female elk (Cook et al. 2004a, 2013, 2016).

NDVI amplitude and time-integrated NDVI were predicted to be have a non-linear, positive association with forage abundance, and NDVI amplitude was predicted to have a quadratic association with forage quality, following our expectations based on previous studies of NDVI and its correlation with "greenness" (i.e., net primary productivity; Garroutte et al. 2016) and quality (i.e., fecal nutrients; Ryan et al. 2012, Christianson and Creel 2009,

Hamel et al. 2009). The forage abundance model with NDVI amplitude predicted a threshold in forage abundance of approximately 42 g/m² at sites with high solar radiation and open canopy and 27 g/m² at similar sites with high canopy closure (Fig. 6). The forage abundance model with time-integrated NDVI model predicted a near-linear relationship that was most positive at low elevation sites with high solar radiation (ranging 19.5 - 59.1 kcal/g) and less positive with increasing elevation or decreasing solar radiation (Fig. 7). The forage quality model indicated that forage quality peaked at intermediate levels of NDVI amplitude (approximately 0.18) and that the peak (ranging 2.32-2.99 kcal/g) varied by vegetation cover type (Fig. 8). This pattern likely reflects the association of intermediate levels of biomass with the highest levels of forage quality (Mueller et al. 2008, Hebblewhite et al. 2008, Pettorelli et al. 2011).

The NDVI metrics, however, explained only a small amount of the variation in both forage abundance and quality ($R^2$ = 0.01-0.03). The majority of the explained variation was accounted for by other landscape attributes, including terrain features, canopy cover, and vegetation cover type. Although uncertainty exists across the range of NDVI amplitude values, particularly at lower values (<0.2) where observed values of forage abundance ranged 0-305.6 g/m², our results suggest that NDVI metrics should not be interpreted alone and without consideration of the effects of terrain, canopy, and vegetation cover type attributes. Our study, therefore, provides some evidence that NDVI metrics can be used as an index or to predict nutritional resources for elk on landscapes in west-central Montana; however, managers using NDVI as a proxy for elk forage should keep in mind that using NDVI alone may be insufficient to fully characterize habitat quality and that uncertainty exists in the relationship between NDVI and forage. Further investigation is needed to understand the specific relationship between elk selection patterns and NDVI, why elk select for areas of higher NDVI, what benefits elk receive from the vegetation associated with elevated NDVI (also see Section 4), and how managers can manipulate vegetation to increase NDVI response to benefit or redistribute elk on the landscape (also see Section 5).

Several factors may have existed that limited our ability to detect a stronger relationship between NDVI and nutritional resources for elk. First, we considered only herbaceous plant species that were important in the summer-fall diets of elk and therefore excluded shrubs and non-forage herbaceous plants from estimates of forage abundance and quality. These excluded plants may influence the level of greenness measured by satellites and serve as the basis for a relationship between NDVI and biomass (Borowik et al. 2013, Garroutte et al. 2016). Elk are known to be intermediate foragers with the ability to consume and digest moderate volumes of food with relatively high cell wall concentrations (Cook 2002); nevertheless, elk demonstrate strong selectivity for high quality forage, particularly where abundance is high (Cook et al. 2016). Shrubs may also provide microclimates favorable to herbaceous species foraged by elk. Elk selection for areas of higher NDVI may reflect this foraging behavior if elk select for broad patches of higher total herbaceous and shrub abundance, which was not measured in our data, and for high quality forage at a finer scale within those broad patches. The resolution of NDVI, as measured by satellite, likely does not capture this fine-scale foraging behavior of elk.

Second, while we attempted to account for the effect of tree canopy cover in the NDVI amplitude models (we could not do so for the time-integrated NDVI models due to

correlation), over-story tree canopy cover may have limited our ability to detect a relationship. We expected that the effect of the canopy on NDVI amplitude, for example, would be mediated given that the NDVI values we considered are a function of the total increase in NDVI from the start of the growing season to the maximum NDVI; any change in NDVI, therefore, should be related to changes in the understory vegetation due to the relatively constant greenness of coniferous canopies through the growing season. At high levels of canopy cover, however, signals from understory vegetation may have been effectively swamped out or blocked given that only a fraction of the radiation reflected originates from the ground layer in dense canopy forests (Wessels et al. 2006, Borowik et al. 2013).

Third, NDVI may saturate for high abundance values given that it represents a two-dimensional greenness measurement of vegetation cover (Hobbs 1995, Santin-Janin et al. 2009). Saturated values of NDVI would result in lower values of NDVI amplitude and time-integrated NDVI than might be expected and may explain why many higher estimates of forage abundance occur at lower values of NDVI amplitude or time-integrated NDVI (Fig. 6 & 7). This may be particularly evident in areas with more open canopy cover where we might expect to find larger values of NDVI amplitude (Fig. 6).

Lastly, forage abundance and quality are likely influenced strongly by micro-site conditions (e.g., soil mineral content, soil type, moisture retention, etc.) that cannot be measured by the satellite-derived NDVI products we used, given their spatial scale, and were not accounted for in our models. This disjunct between the spatial scale of our vegetation sampling and NDVI products may help explain the low proportion of variance explained by the models (forage abundance $R^2 = 0.12$; forage quality $R^2 = 0.39$), which were slightly below or at the low end of the range of reported $R^2$ from other studies predicting measures of forage abundance (0.18-0.76; Borowik et al. 2013, Garroutte et al. 2016) and quality (0.37-0.9; Ryan et al. 2012, Garroutte et al. 2016, Hamel et al. 2009) with NDVI.

Craig Jourdonnais

## Introduction

Variation in nutrition strongly influences many aspects of ungulate ecology, including body mass dynamics, body fat levels, pregnancy rate, over-winter survival, timing of parturition, juvenile growth rates and survival, and neonatal birth mass and survival (Cook et al. 2004a, 2013, 2016, Herfindal et al. 2006, Parker et al. 2009, Monteith et al. 2014, Proffitt et al. 2016a). The spatial and temporal distribution and availability of nutritional resources across large landscapes can vary considerably, which may have important effects to ungulate nutritional condition and potentially demographic performance. Given the strong association of NDVI with the greenness of vegetation cover, NDVI has been used as a proxy for the availability of nutritional resources and may indicate nutritional benefit to ungulates (Pettorelli et al. 2005). NDVI has been positively associated with fecal nitrogen in mountain goats, bighorn sheep, and African buffalo (Hamel et al. 2009, Ryan et al. 2012), suggesting it is a good indicator of forage quality that may be imparting nutritional benefits (Pettorelli et al. 2011). Evidence for a direct relationship between NDVI and nutritional condition of ungulates is limited, however. Whereas studies have shown positive correlations of NDVI with body condition (Pettorelli et al. 2005, 2006, Martínez-jauregui et al. 2009, Ryan et al. 2012) and reproduction (Ryan et al. 2007, Wittemyer et al. 2007, Trimble et al. 2009) in a variety of ungulate species, a lack of a correlation has been found in some populations in these same studies (Pettorelli et al. 2006, Martínez-jauregui et al. 2009) and other studies (Mysterud et al. 2007).

For elk, the relationship between NDVI and summer-fall nutritional resources (Section 3), combined with strong selection by elk for areas with higher NDVI during the late summer (Ranglack et al. 2016, 2017) provides some evidence that differences in NDVI across a large landscape can be interpreted as differences in elk forage abundance and quality. However, data are lacking to understand if differences in elk exposure to NDVI are related to differences in elk nutritional condition. This information may benefit managers by allowing

use of an easily obtainable metric (NDVI) for large-scale monitoring and managing of nutritional condition in populations of elk and to identify populations that may have nutritional limitations affecting pregnancy and productivity. To address this, we used elk location and nutritional condition data, measured by body fat and pregnancy status, to evaluate if variation in individual elk exposure to NDVI is correlated with biologically meaningful variation in nutritional condition.

## Methods

We used location and nutritional condition data collected from collared elk to determine if differences in individual elk exposure to NDVI were associated with differences in body fat and pregnancy rates. We captured > 30 female adult ($\geq$ 1.5 years old) elk per population using helicopter net-gunning or chemical immobilization in compliance with the Montana Fish, Wildlife and Parks (FWP19-2013) and University of Montana (027-11MHWB-042611) animal handling protocols.

Captures occurred in the late fall (November-December) and winter (January-March). We sampled elk body condition and pregnancy status and fitted elk with Global Positioning System radiocollars. Each elk was sampled only one time. Fall sampling occurred in the East Fork and West Fork populations during 2012 and 2013, and winter sampling occurred in the East Fork and West Fork populations during 2011, 2012, and 2013, the North Sapphire population in 2014, and the Elkhorn population in 2015. We sampled different individuals within each population during each season and year. We collected a blood sample from each elk to estimate pregnancy status based on pregnancy-specific protein-B levels (Noyes et al. 1997) and assessed lactation status during fall sampling based on the presence of milk in the udder, presence of saliva on the udder, and overall udder size. During winter sampling, we were unable to determine if elk had lactated the previous summer and fall. We estimated body fat by calculating ingest-free body fat (IFBF) from measurements of chest girth and allometrically-scaled estimates of maximum thickness of the rump-fat layer obtained using a portable ultrasound machine (Cook et al. 2010). We aged elk based on tooth eruption patterns and classified elk into three age classes: yearling (1), prime (2-9) and older (10+). We screened blood samples for exposure to a suite of common diseases previously known to occur in Montana and removed elk with brucellosis seropositive results to reduce confounding of nutritional condition with disease effects.

We programmed radiocollars to collect 1-48 locations per day and drop off after 2 years. We collected elk location data across 2 years (2014-2015) in the North Sapphire population, 3 years (2011-2013) in the East Fork and West Fork populations, and 2 years (2015-2016) in the Elkhorn population. From each individual's associated radiocollar locations, we retained only the first year of locations after sampling of nutritional condition. We used these locations to estimate individual elk exposure to NDVI during the summer-fall (July 1-August 31) prior to sampling of nutritional condition based on evidence that most individual elk selected summer-fall home ranges within the same areas each year (Appendix C). We removed individuals that had no recorded locations due to collar malfunctions or mortality. We estimated exposure to NDVI for each individual elk by first estimating a summer-fall home range based on a 95% kernel utilization distribution (using the adehabitatHR package in Program R version 3.4.3; R Development Core Team

2018), and, second, calculating the mean NDVI value within the summer-fall home range during the summer-fall prior to body condition and pregnancy sampling. We evaluated both NDVI amplitude (AMP) and time-integrated NDVI (TIN) that we found to be supported in our evaluation of the association of NDVI with elk forage abundance and quality (Section 3).

We used linear and logistic regression models in Program R version 3.4.3 (R Development Core Team 2018) to investigate the effect of elk exposure to NDVI metrics on IFBF and pregnancy status, respectively. We estimated relationships for IFBF separately for fall and winter sampling events given the expected decline in body fat levels during winter. For fitting models of pregnancy rate, we combined data from fall and winter sampling events for each population and year (e.g., fall 2011 and winter 2012 data from the West Fork combined as 2012 data). We competed several hypothesized models for each response (fall IFBF, winter IFBF, and pregnancy rate) that included additive combinations of age class, population, and year variables (Tables 13 and 14). We used a population variable to account for unmeasured factors (e.g., harvest management or predators) specific to each population that may be influencing the nutritional condition of elk. We evaluated AMP and TIN metrics separately for each IFBF and pregnancy model suite. We competed the two estimates of elk exposure to NDVI (mean NDVI and proportion NDVI) by additively including each estimate separately in each hypothesized model. We fit and compared models using Akaike's Information Criterion corrected for small sample sizes (AICc; Burnham and Anderson 2002).

In fall IFBF models, we controlled for lactation status in all models because of its importance in predicting fall IFBF (Proffitt et al. 2016a) and we expected that the relationship between elk exposure to NDVI and fall IFBF might vary due to increased energetic demands for supporting lactation (Cook et al. 2004a). In winter IFBF models, we evaluated a year variable to account for differences in weather conditions experienced during the winter each year that may be influencing body fat levels. We additionally evaluated a population-year (e.g., "Sapphire-2014") variable in winter IFBF models to account for the effect of population and year because winter sampling events occurred in study areas during different years. In pregnancy models, we included the effect of IFBF in all models given its important influence on pregnancy rate (Proffitt et al. 2016a).

We expected that elk exposed to greater levels of NDVI would have higher levels of IFBF and rates of pregnancy based on the positive relationship of forage abundance with AMP and TIN (Section 3) and the evidence that elk select for areas with higher NDVI (Ranglack et al. 2016, 2017). Alternatively, the quadratic relationship between forage quality and AMP (Section 3) and the evidence for the importance of high quality forage for female elk (Cook et al. 2004a, 2013, 2016) may indicate that intermediate levels of NDVI enhance elk nutritional condition. In our evaluations, therefore, we lastly compared top models within each model suite with models including a pseudothreshold and quadratic functional form of the NDVI metric. We tested for the effect of the NDVI metric by including a model identical to the top model but excluding the NDVI metric.

Post hoc, after selecting a final inferential model for the relationship between fall IFBF and mean TIN, we evaluated whether the availability of higher quality areas within summer-fall

home ranges was an important predictor of IFBF. We estimated the availability of higher quality areas by calculating the proportion of the summer-fall home ranges greater than or equal to a TIN threshold value. We used the 75th percentile of TIN values from within all elk summer-fall home ranges as a threshold value. We then compared the top model with models including a linear and a pseudothreshold effect of the proportion TIN variable in place of the mean TIN variable.

## Results

We captured, sampled nutritional condition, and collected radiocollar locations from a total of 172 female elk. In the fall, we sampled IFBF and pregnancy status from a total of 33 elk. Age of elk sampled in the fall averaged 5.2 ± 2.3 (SD). Thirty-one and 2 elk were prime- and older-age, respectively. Fall IFBF averaged 8.66 ± 2.78% , 76% were pregnant, and 44% were lactating. In the winter, we sampled IFBF from a total of 136 elk and pregnancy status from a total of 137 elk. Age of elk sampled in the winter averaged 6.4 ± 2.8. One hundred-twelve, 21, and 6 elk were prime-, older-, and unknown age, respectively. Winter IFBF averaged 7.09 ± 1.85% and 88% were pregnant. Fall IFBF varied by population, year, and lactation status (Table 11; panel A in Figure 9). Winter IFBF varied by population and year (Table 11; panel A in Figure 10). Across both fall and winter sampling events, pregnancy rates averaged 87.7, 75.0, 90.5, and 88.9% for the East Fork, West Fork, Sapphire, and Elkhorn populations, respectively, and varied by year for the East Fork and West Fork (panel A in Figure 11).

**Table 11 - Summary of ingesta-free body fat (IFBF; %), pregnancy rate, and lactation rate from fall (Nov.-Dec.) and winter (Jan.-Mar.) capture events in 4 populations of west-central Montana, USA, 2011-2015. Lactation could not be assessed during winter captures.**

| Sampling event | Population | Year | n | IFBF Mean | SD | Min | Max | % Pregnant | Lactating |
|---|---|---|---|---|---|---|---|---|---|
| Fall | East Fork | 2011 | 9 | 8.16 | 2.47 | 6.73 | 14.15 | 67 | 44 |
| Fall | East Fork | 2012 | 10 | 8.30 | 1.85 | 6.73 | 12.66 | 90 | 70 |
| Fall | West Fork | 2011 | 7 | 6.82 | 1.99 | 3.87 | 10.11 | 71 | 29 |
| Fall | West Fork | 2012 | 7 | 11.66 | 2.98 | 6.22 | 15.34 | 71 | 17 |
| Winter | East Fork | 2011 | 25 | 7.21 | 1.79 | 2.70 | 12.13 | 96 | – |
| Winter | East Fork | 2012 | 9 | 6.15 | 2.72 | 2.70 | 10.44 | 89 | – |
| Winter | East Fork | 2013 | 6 | 7.83 | 1.74 | 6.33 | 11.04 | 83 | – |
| Winter | West Fork | 2011 | 10 | 6.11 | 1.43 | 3.87 | 7.84 | 70 | – |
| Winter | West Fork | 2012 | 9 | 5.95 | 2.82 | 1.52 | 9.45 | 78 | – |
| Winter | West Fork | 2013 | 11 | 7.53 | 1.29 | 6.12 | 10.80 | 82 | – |
| Winter | Sapphire | 2014 | 42 | 7.83 | 1.44 | 6.14 | 13.29 | 90 | – |
| Winter | Elkhorn | 2015 | 27 | 6.55 | 1.68 | 2.70 | 9.23 | 89 | – |

**Figure 9 - Ingesta-free body fat (IFBF; A), mean NDVI amplitude (AMP; B), and time-integrated NDVI (TIN; C) values within individual summer-fall ranges for elk sampled during fall (Nov.-Dec.) captures in the West Fork and East Fork populations of west-central Montana, USA, 2011-2012.**
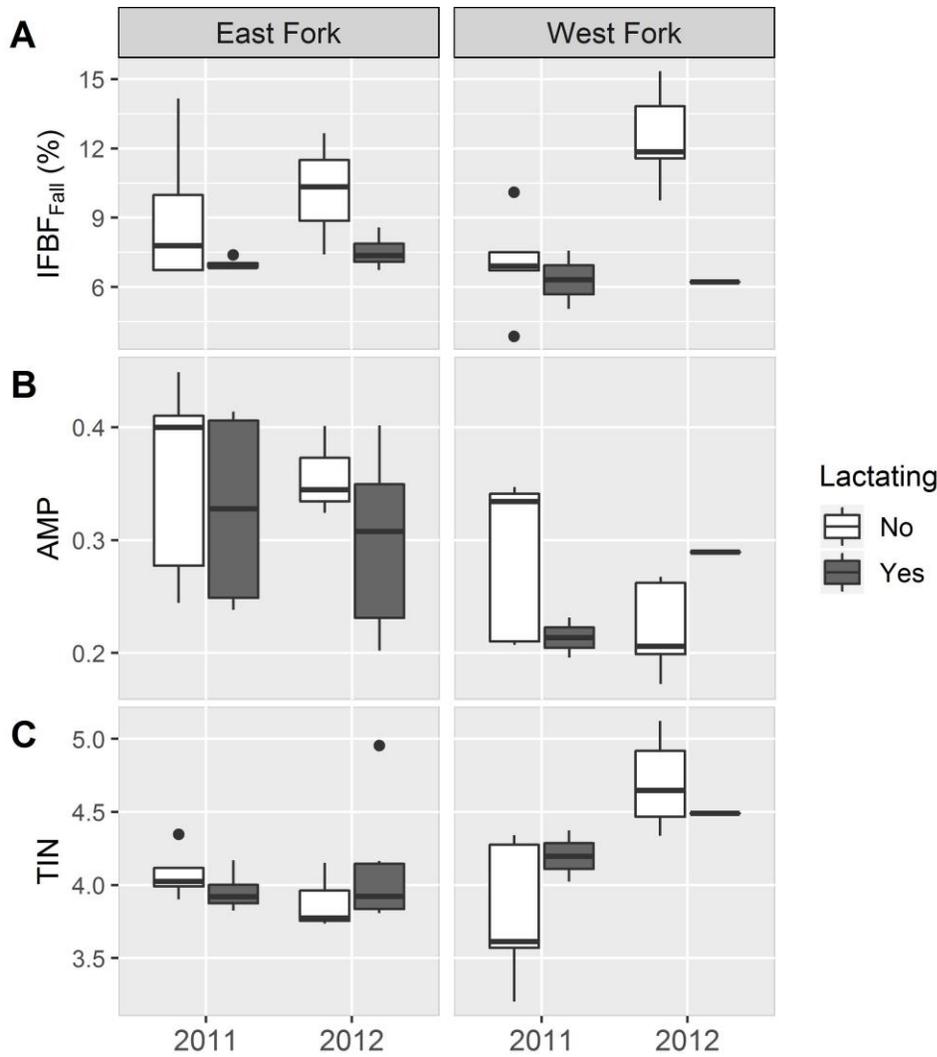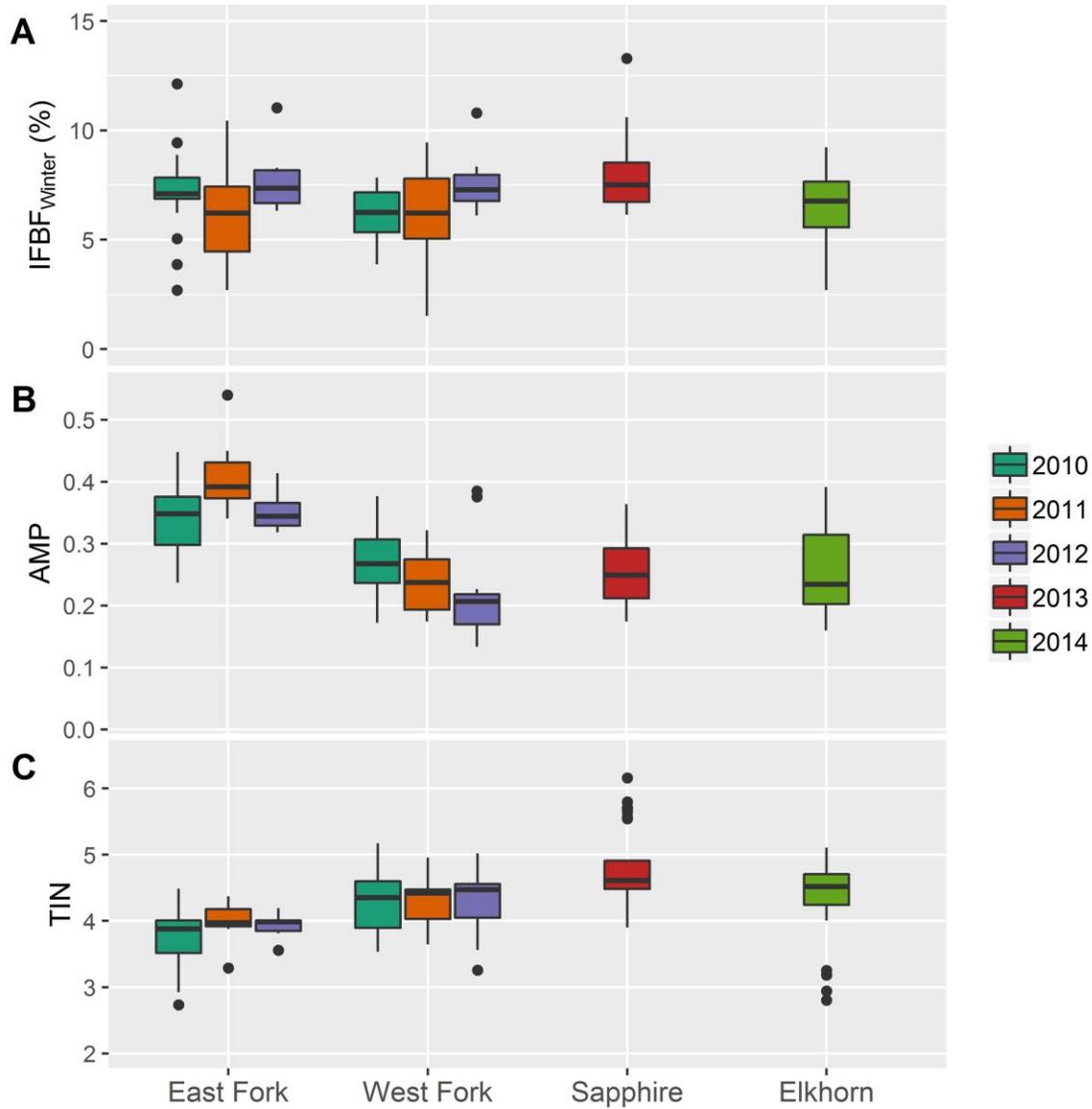
**Figure 10 - Ingesta-free body fat (IFBF; A), mean NDVI amplitude (AMP; B), and time-integrated NDVI (TIN; C) values within individual summer-fall ranges for elk sampled during winter (Jan.-Mar.) captures in 4 populations of west-central Montana, USA, 2011-2015.**
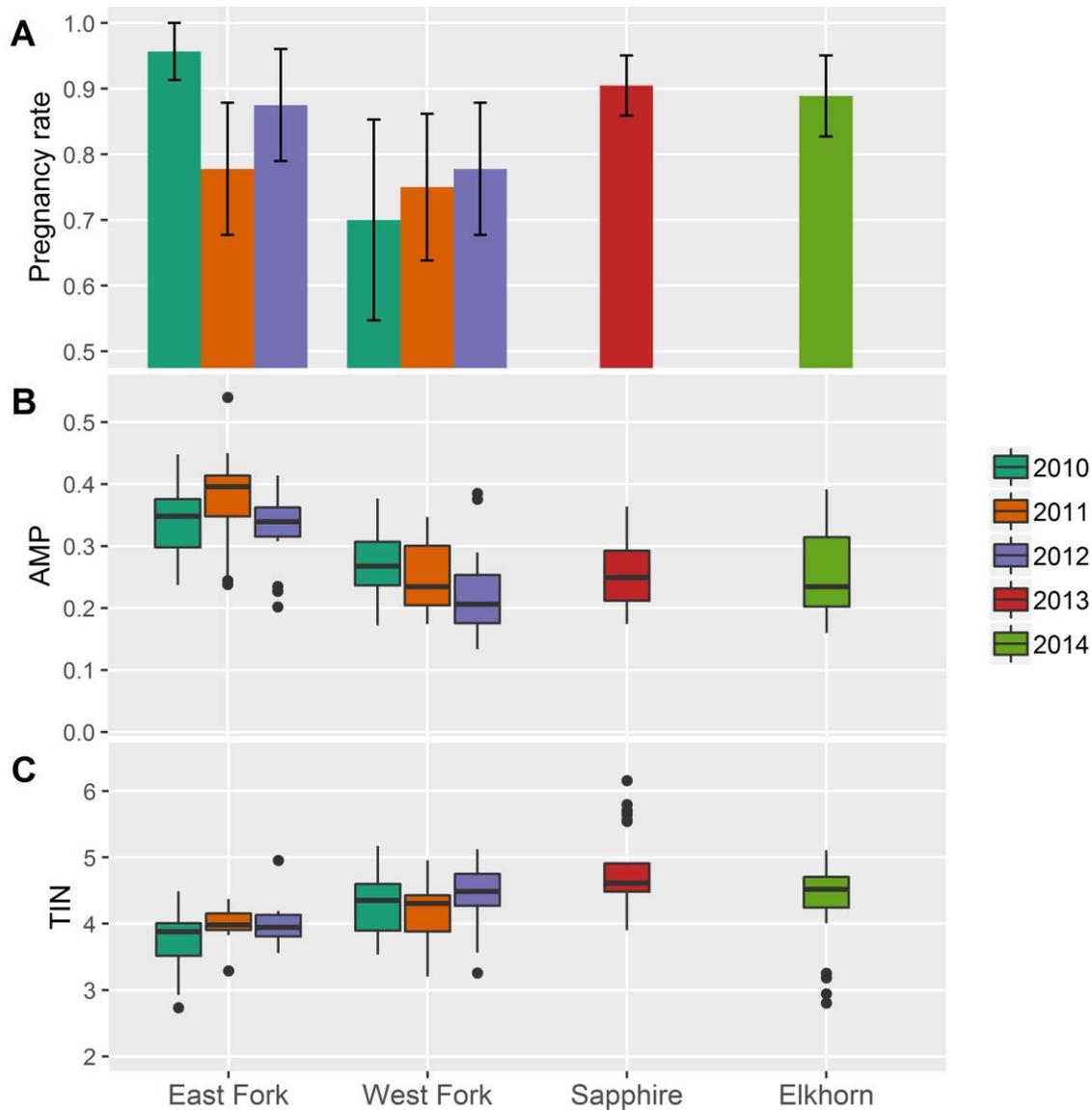
**Figure 11 - Pregnancy rate (A), average mean NDVI amplitude (AMP; B), and time-integrated NDVI (TIN; C) within individual summer-fall ranges for elk sampled during fall (Nov.-Dec.) and winter (Jan.-Mar.) captures in 4 populations of west-central Montana, USA, 2011-2015.**

We collected an average of 727.6 (± 77.6), 2249.2 (± 1034), 1944.8 (± 1123.8), and 48.6 (± 10.7) summer-fall locations per elk in the Sapphire, West Fork, East Fork, and Elkhorn populations, respectively. Summer-fall home ranges of elk averaged 46.5 (± 22.1), 36.1 (± 23.3), 44.6 (± 26.9), and 36.2 (± 26.1) km² in the Sapphire, West Fork, East Fork, and Elkhorn populations, respectively.

Mean AMP and TIN values of summer-fall home ranges of the summer-fall previous to capture and sampling averaged 0.284 ± 0.078 and 4.3 ± 0.61, respectively, and varied by sampling event, population, year, and lactation status (Table 12; panels B and C in Figures 9, 10, and 11). We assumed summer-fall home ranges were similar between the year elk were radiocollared and the previous year prior to sampling.

**Table 12 - Summary of average NDVI amplitude (AMP) and time-integrated NDVI (TIN) values of summer-fall home ranges from the summer-fall previous to capture and sampling of nutritional condition of elk in 4 populations of west-central Montana, USA, 2011-2015.**

| Sampling event | Population | Capture Year | Summary Year | AMP Mean | AMP SD | TIN Mean | TIN SD |
|---|---|---|---|---|---|---|---|
| Fall | East Fork | 2011 | 2011 | 0.343 | 0.087 | 4.02 | 0.16 |
| Fall | East Fork | 2012 | 2012 | 0.314 | 0.071 | 4.03 | 0.36 |
| Fall | West Fork | 2011 | 2011 | 0.267 | 0.070 | 3.91 | 0.46 |
| Fall | West Fork | 2012 | 2012 | 0.229 | 0.044 | 4.70 | 0.29 |
| Winter | East Fork | 2011 | 2010 | 0.338 | 0.054 | 3.74 | 0.50 |
| Winter | East Fork | 2012 | 2011 | 0.410 | 0.059 | 3.98 | 0.31 |
| Winter | East Fork | 2013 | 2012 | 0.353 | 0.035 | 3.92 | 0.22 |
| Winter | West Fork | 2011 | 2010 | 0.266 | 0.064 | 4.30 | 0.50 |
| Winter | West Fork | 2012 | 2011 | 0.239 | 0.051 | 4.33 | 0.39 |
| Winter | West Fork | 2013 | 2012 | 0.221 | 0.083 | 4.28 | 0.52 |
| Winter | Sapphire | 2014 | 2013 | 0.251 | 0.049 | 4.83 | 0.54 |
| Winter | Elkhorn | 2015 | 2014 | 0.260 | 0.073 | 4.36 | 0.63 |

## Fall Ingesta-free Body Fat Analysis

We evaluated 4 AMP and 4 TIN models predicting fall IFBF (Table 13). In both the AMP and TIN model comparisons, the most-supported model included the respective NDVI metric and lactation status ($R^2$ = 0.18 and 0.43, respectively). Model selection uncertainty in both model comparisons indicated potential importance for the additional effect of age class or population. The most-supported AMP model predicted 2.6% higher IFBF for non-lactating elk than for lactating elk (p < 0.01) and a 0.36% decrease in IFBF for every 0.1-unit increase in AMP (p = 0.51; Table 14; panel A in Fig. 12). However, 95% confidence intervals overlapped 0 and there was substantial support for the same model that lacked the effect of mean AMP ($\Delta$AICc = -2.02; $R^2$ = 0.19). The model including a pseudothreshold effect of mean AMP was only marginally more supported ($\Delta$AICc = -0.12; $R^2$ = 0.18) than the top model; however, models including the pseudothreshold and quadratic ($\Delta$AICc = 2.35; $R^2$ = 0.16) effect of mean AMP were less supported than the model lacking mean AMP.

The most-supported TIN model predicted 2.4% higher IFBF for non-lactating elk than for lactating elk (p < 0.01) and a 2.8% increase in IFBF for every 1-unit increase in mean TIN (p < 0.01). The model including a pseudothreshold effect of mean TIN was marginally more supported ($\Delta$AICc = -0.04; $R^2$ = 0.37) than the top model and identified a near-identical relationship (Table 14; panel B in Fig. 12). The models including the quadratic effect of mean TIN ($\Delta$AICc = 2.80; $R^2$ = 0.34) and lacking TIN ($\Delta$AICc = 6.09; $R^2$ = 0.19) were less supported than the top model. In the post hoc evaluation of the availability of high quality areas in summer-fall home ranges, the TIN threshold value was calculated to be 5.14. The proportion of summer-fall ranges equal to or greater than the threshold value averaged 0.25 ± 0.2. The models including a pseudothreshold and linear effect of the proportion of the summer-fall ranges equal to or greater than the threshold value were 0.44 and 0.16 AICc more supported than the model including the pseudothreshold effect of mean TIN, respectively. The pseudothreshold model predicted a positive curvilinear relationship with a decreasing effect on fall IFBF as mean TIN increases (Table 15; panel C in Fig. 12).

**Table 13 - Model selection results for models examining relationships of NDVI amplitude (AMP) and time-integrated NDVI (TIN) with ingesta-free body fat (IFBF) and pregnancy rate of elk from 4 populations sampled in fall (Nov.-Dec.) and winter (Jan.-Mar.) in west-central Montana, USA, 2011-2015. K = no. of parameters, $wt_i$ = AICc weight.**

| Response | NDVI Metric | Model | K | AICc | ΔAICc | $wt_i$ |
|---|---|---|---|---|---|---|
| IFBF (Fall) | AMP | Lactation | 4 | 154.60 | 0.00 | 0.62 |
| | | Lactation + Population | 5 | 156.96 | 2.37 | 0.19 |
| | | Lactation + Age | 5 | 157.42 | 2.82 | 0.15 |
| | | Lactation + Population + Age | 6 | 159.98 | 5.39 | 0.04 |
| | TIN | Lactation | 4 | 146.36 | 0.00 | 0.54 |
| | | Lactation + Population | 5 | 147.80 | 1.43 | 0.27 |
| | | Lactation + Age | 5 | 149.18 | 2.82 | 0.13 |
| | | Lactation + Population + Age | 6 | 150.85 | 4.49 | 0.06 |
| IFBF (Winter) | AMP | Population + Age | 7 | 517.18 | 0.00 | 0.62 |
| | | Age + PopulationYear | 11 | 518.44 | 1.27 | 0.33 |
| | | Age | 4 | 522.42 | 5.24 | 0.05 |
| | | Year | 7 | 548.81 | 31.63 | 0.00 |
| | | Population | 6 | 552.13 | 34.95 | 0.00 |
| | | PopulationYear | 10 | 552.90 | 35.73 | 0.00 |
| | | (AMP alone) | 3 | 557.72 | 40.54 | 0.00 |
| | TIN | Population + Age | 7 | 516.62 | 0.00 | 0.46 |
| | | Age + PopulationYear | 11 | 517.12 | 0.50 | 0.36 |
| | | Age | 4 | 518.48 | 1.86 | 0.18 |
| | | Year | 7 | 548.41 | 31.79 | 0.00 |
| | | PopulationYear | 10 | 550.98 | 34.36 | 0.00 |
| | | Population | 6 | 551.12 | 34.50 | 0.00 |
| | | (TIN alone) | 3 | 553.64 | 37.02 | 0.00 |
| Pregnancy rate | AMP | IFBF | 3 | 137.96 | 0.00 | 0.44 |
| | | IFBF + Age | 4 | 138.75 | 0.78 | 0.30 |
| | | IFBF + Population | 6 | 139.87 | 1.91 | 0.17 |
| | | IFBF + Population + Age | 7 | 141.03 | 3.07 | 0.09 |
| | TIN | IFBF | 3 | 137.98 | 0 | 0.46 |
| | | IFBF + Age | 4 | 138.79 | 0.81 | 0.31 |
| | | IFBF + Population | 6 | 140.16 | 2.18 | 0.15 |
| | | IFBF + Population + Age | 7 | 141.38 | 3.4 | 0.08 |

**Table 14 - Estimated coefficients and 95% confidence intervals for the top model examining relationships of NDVI amplitude (AMP) and time-integrated NDVI (TIN) with ingesta-free body fat (IFBF) of elk from the East Fork and West Fork populations sampled in fall (Nov.-Dec.) and winter (Jan.-Mar.) in west-central Montana, USA, 2011-2015. For the fall IFBF model, effects of lactation are in relation to the reference (intercept) of non-lactating elk. For the winter IFBF model, effects of age and population are in relation to the reference of old-age class elk in the East Fork population. Covariate subscript of PS indicates pseudotheshold functional form. Bolded estimates indicate p < 0.05.**

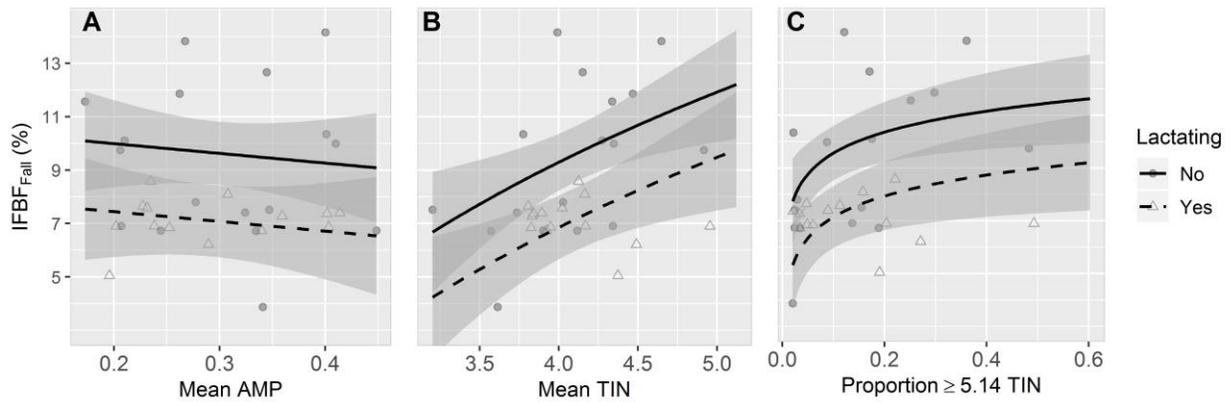| | IFBF (Fall) | | | | IFBF (Winter) | | | |
| | AMP | | TIN | | AMP | | TIN | |
| Covariate | Est. | C.I. | Est. | C.I. | Est. | C.I. | Est. | C.I. |
|---|---|---|---|---|---|---|---|---|
| Intercept | **10.72** | (7.15, 14.29) | -7.01 | (-18.32, 4.30) | **6.62** | (4.66, 8.59) | **4.99** | (2.63, 7.35) |
| Mean AMP | -3.64 | (-14.88, 7.60) | – | – | -1.60 | (-6.59, 3.38) | – | – |
| Mean TIN | – | – | – | – | – | – | 0.28 | (-0.29, 0.85) |
| TIN$^{PS}$ | – | – | **11.76** | (3.80, 19.72) | – | – | – | – |
| Lactating | **-2.55** | (-4.34, -0.76) | **-2.44** | (-4.01, -0.87) | – | – | – | – |
| Prime-age | – | – | – | – | **1.02** | (0.18, 1.85) | **1.01** | (0.18, 1.84) |
| Elkhorn | – | – | – | – | -0.62 | (-1.65, 0.40) | -0.61 | (-1.54, 0.32) |
| Sapphire | – | – | – | – | 0.69 | (-0.27, 1.65) | 0.56 | (-0.44, 1.57) |
| West Fork | – | – | – | – | -0.47 | (-1.50, 0.57) | -0.42 | (-1.30, 0.47) |



**Figure 12 - Predicted fall ingesta-free body fat (IFBF) for non-lactating (solid line) and lactating (dashed line) elk, 95% confidence intervals (shaded), and observed IFBF levels (gray dots) estimated from the top model evaluating the relationship of mean NDVI amplitude (AMP; A), mean time-integrated NDVI (TIN; B), and proportion of summer-fall range equal to or greater than 5.14 TIN (C) with fall IFBF of elk from the East Fork and West Fork populations in west-central Montana, USA, 2011-2012.**

**Table 15 - Estimated coefficients and 95% confidence intervals for the post hoc inferential model examining relationships of proportion of summer-fall range equal to or greater than 5.14 TIN with fall ingesta-free body fat (IFBF) of elk from the East Fork and West Fork populations in west-central Montana, USA, 2011-2012. Effects of lactation are in relation to the reference (intercept) of non-lactating elk. Covariate superscript of PS indicates pseudotheshold functional form. Bolded estimates indicate p < 0.05.**

| Covariate | Estimate | C.I. |
|---|---|---|
| Intercept | 12.21 | (10.22, 14.20) |
| Proportion TIN$^{PS}$ | 1.15 | (0.39, 1.91) |
| Lactating | -2.42 | (-3.98, -0.86) |

## Winter Ingesta-free Body Fat Analysis

We evaluated 7 AMP and 7 TIN models predicting winter IFBF (Table 13). In both the AMP and TIN model comparisons, the most-supported model included the respective NDVI metric, population, and age class ($R^2$ = 0.11 for each). Model selection uncertainty indicated potential importance for the effect of population-year instead of population in both model comparisons and of age alone in the TIN model comparison. The most-supported AMP model predicted 1.0% higher IFBF for prime-age elk than for old-age elk (p = 0.02; Table 14; panel A in Fig. 13). Elk in the Sapphire population were predicted to have 0.7% higher IFBF (p = 0.16) and elk in the West Fork and Elkhorn populations were predicted to have 0.5 (p = 0.37) and 0.6% (p = 0.23) lower IFBF, respectively, than elk in the East Fork population. Confidence intervals for the effects of population overlapped zero, however. The model predicted a 0.16% decrease in IFBF for every 0.1-unit increase in mean AMP (p = 0.5); however, confidence intervals overlapped 0 and there was more support for the same model that lacked the effect of mean AMP ($\Delta$AICc = -1.47; $R^2$ = 0.11). The model including a pseudothreshold effect of mean AMP was marginally more supported ($\Delta$AICc = -0.34; $R^2$ = 0.11) than the top model; however, models including the pseudothreshold and quadratic ($\Delta$AICc = 0.03; $R^2$ = 0.11) effect of mean AMP were less supported than the model lacking mean AMP.

The most-supported TIN model predicted 1.0% higher IFBF for prime-age elk than for old-age elk (p = 0.02; Table 14; panel A in Fig. 13). Elk in the Sapphire population were predicted to have 0.6% higher IFBF (p = 0.27) and elk in the West Fork and Elkhorn populations were predicted to have 0.4 (p = 0.36) and 0.6% (p = 0.20) lower IFBF, respectively, than elk in the East Fork population. Confidence intervals for the effects of population overlapped zero, however. The model predicted a 0.28% increase in IFBF for every 1-unit increase in mean TIN (p = 0.3); however, confidence intervals overlapped 0 and there was more support for the same model that lacked the effect of mean TIN ($\Delta$AICc = -1.04; $R^2$ = 0.11). The model including a pseudothreshold effect of mean TIN was marginally more supported ($\Delta$AICc = -0.21; $R^2$ = 0.11) than the top model; however, models including the pseudothreshold and quadratic ($\Delta$AICc = 1.46; $R^2$ = 0.11) effect of mean TIN were less supported than the model lacking mean TIN.
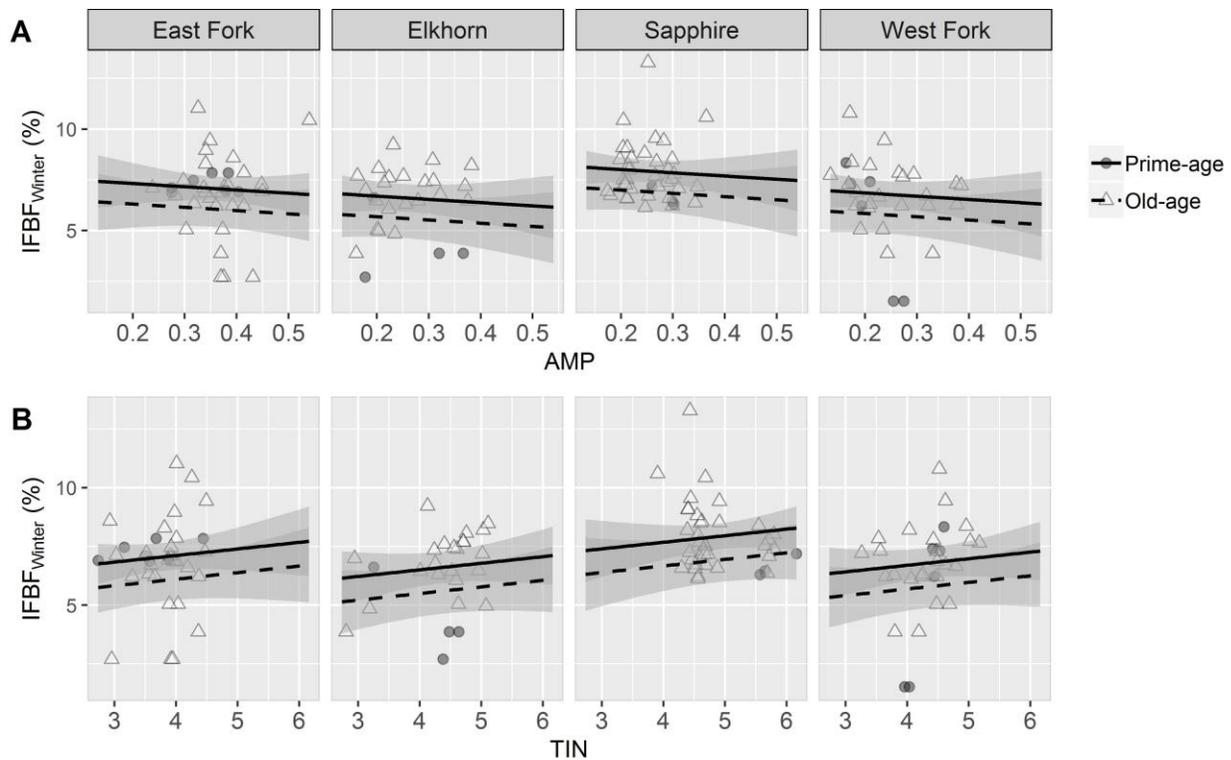
**Figure 13 - Predicted winter ingesta-free body fat (IFBF) for prime- (solid line) and old-age (dashed line) elk, 95% confidence intervals (shaded), and observed IFBF levels (gray dots) across 4 populations estimated from the top model evaluating the relationship of mean NDVI amplitude (AMP; A) and mean time-integrated NDVI (TIN; B) with winter IFBF of elk in west-central Montana, USA, 2011-2015.**

## Pregnancy Analysis

We evaluated 4 AMP and 4 TIN models predicting pregnancy rate (Table 13). In both the AMP and TIN model comparisons, the most-supported model included the respective NDVI metric and IFBF. Model selection uncertainty indicated potential importance for the additional effect of age class and population. The most-supported AMP model predicted that for every 1% increase in IFBF and 0.1 increase in mean AMP, the odds of pregnancy increased by a factor of 1.4 ($p < 0.01$) and decreased by a factor of 1.1 ($p = 0.81$), respectively (Table 16; panel A in Fig. 14). Confidence intervals overlapped 0 for the effect of mean AMP, however, and there was substantial support for the same model that lacked the effect of mean AMP ($\Delta$AICc = -2.02). The model including a pseudothreshold effect of mean AMP was similarly supported as the top model ($\Delta$AICc = 0.00) and the model including quadratic effect of mean AMP was least supported ($\Delta$AICc = 2.09).

The most-supported TIN model predicted that for every 1% increase in IFBF and 1-unit increase in mean TIN, the odds of pregnancy increased by a factor of 1.4 ($p < 0.01$) and decreased by a factor of 1.1 ($p = 0.81$), respectively (Table 16; panel B in Fig. 14). Confidence intervals overlapped 0 for the effect of mean TIN, however, and there was substantial support for the same model that lacked the effect of mean TIN ($\Delta$AICc = -2.03). The model including a pseudothreshold effect of mean TIN was similarly supported as the

top model (ΔAICc = 0.00) and the model including quadratic effect of mean TIN was least supported (ΔAICc = 2.02).

**Table 16 - Estimated coefficients, standard errors, and 95% confidence intervals for the top model examining relationships of mean NDVI amplitude (AMP) and mean time-integrated NDVI (TIN) with pregnancy rate of elk from 4 populations sampled in fall (Nov.-Dec.) and winter (Jan.-Mar.) in west-central Montana, USA, 2011-2015. Bolded estimates indicate p < 0.05.**

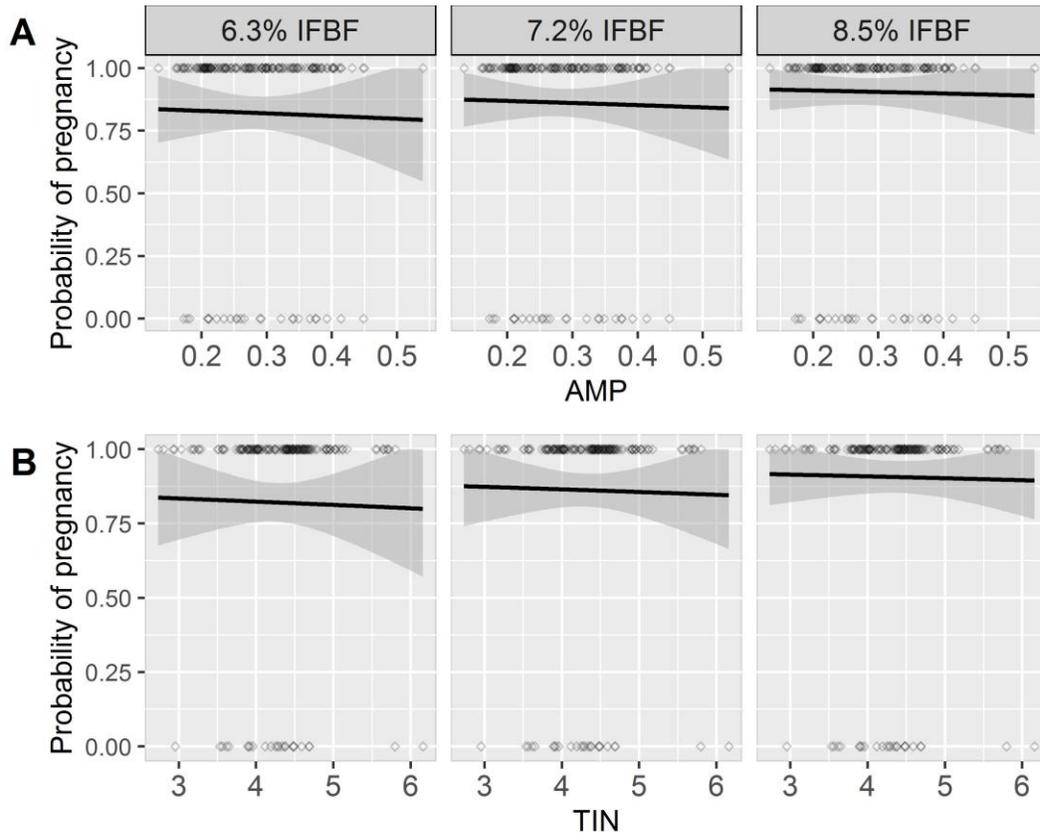| | AMP | | TIN | |
|---|---|---|---|---|
| Covariate | Estimate | C.I. | Estimate | C.I. |
| Intercept | -0.39 | (-2.76, 1.92) | -0.32 | (-3.49, 2.84) |
| Mean AMP | -0.70 | (-6.35, 5.10) | – | – |
| Mean TIN | – | – | -0.07 | (-0.79, 0.65) |
| IFBF | **0.34** | (0.11, 0.58) | **0.34** | (0.11, 0.59) |



**Figure 14 - Predicted probability of pregnancy (black line), 95% confidence intervals (shaded), and observed pregnancy status (gray dots) for elk across levels of ingesta-free body fat (IFBF) estimated from the top model evaluating the relationship of NDVI amplitude (AMP; A) and time-integrated NDVI (TIN; B) with pregnancy rate of elk sampled in fall (Nov.-Dec.) and winter (Jan.-Mar.) in west-central Montana, USA, 2011-2015.**

## Discussion

We found strong support for a relationship between the amount of elk exposure to time-integrated NDVI during the summer-fall and fall body fat levels, and only minimal evidence for other relationships of NDVI metrics with measures of elk body fat. The most-supported model with the strongest relationship indicated that elk with summer-fall ranges containing higher average levels of time-integrated NDVI had significantly greater IFBF levels during the fall. This model was substantially more supported than the same model with NDVI amplitude ($\Delta$AICc = 8.2) and explained 24% more variation than the same model lacking an NDVI metric. We also found some evidence for a positive relationship between time-integrated NDVI and winter IFBF levels across all elk populations, indicating that the nutritional benefits from greater exposure to areas with higher time-integrated NDVI during the summer-fall may be sustained through the winter season; however, there was uncertainty in this relationship, and a model lacking the NDVI metric was more supported.

The remaining models that considered the effect of time-integrated NDVI on pregnancy rates and of NDVI amplitude on body fat levels and pregnancy rates predicted negative relationships with uncertainty in the estimates and were less supported than models lacking NDVI metrics. These results suggest a lack of association between NDVI metrics and pregnancy rates. This may be because reproduction is more strongly linked to elk access to nutrition across multiple years (Cook 2002) and pregnancy rates across most populations were generally high in our populations, likely associated with the body fat levels exceeding thresholds that would otherwise limit pregnancy (Cook et al. 2004a, 2013).

Our findings that time-integrated NDVI correlates with fall body fat levels corroborates the relationship between pseudothreshold time-integrated NDVI and summer-fall nutritional resources (Section 3) given that fall body fat levels are strongly associated with the intake of nutritional resources during the previous summer and fall (Cook 2002, Cook et al. 2004a, 2013) and that the time-integrated NDVI metric incorporates greenness signals that accrue throughout the growing season (unlike NDVI amplitude). Although models including NDVI amplitude were more supported in our previous analysis of NDVI and nutritional resources, there was also substantial support for a model with pseudothreshold TIN. The model with pseudothreshold TIN performed only marginally better than the linear form and identified a near-identical relationship (results not shown). These correlations between time-integrated NDVI, nutritional resources, and body fat levels of elk also follow previous resource selection studies where elk were found to select for areas with higher time-integrated NDVI during the summer and fall (Ranglack et al. 2016, 2017).

The importance of the effect of time-integrated NDVI on fall body condition may not apply to all other elk populations in Montana, however, because our results were based only on two populations in near-proximity to each other in the Bitterroot Valley. Previous studies of elk and other ungulate species have found both positive correlations (Pettorelli et al. 2005, 2006, Martínez-jauregui et al. 2009, Ryan et al. 2012) and no correlations (Pettorelli et al. 2006, Mysterud et al. 2007, Martínez-jauregui et al. 2009) of NDVI with body condition, even in populations within the same study (Pettorelli et al. 2006, Martínez-jauregui et al. 2009). This may be due to different populations with dissimilar environmental conditions and being influenced by environmental drivers in different ways

(Martínez-jauregui et al. 2009). For example, harvest management, predators, limited resources, or parasites, which may have differing effects on the nutritional condition of elk, may vary across populations. Additional data regarding fall body fat, pregnancy, and nutritional resources across a broader geographical area are needed to further refine our understanding of NDVI, body fat, and pregnancy relationships.

Craig Jourdonnais

## Introduction

Forest management practices, such as timber harvest and prescribed fire, and natural disturbances, such as wildfire, have the potential to influence the distribution and availability of nutritional resources for elk (Jourdonnais and Bedunah 1990, Pearson et al. 1995, Sachro et al. 2005, Long et al. 2008, Proffitt et al. 2016a, Cook et al. 2016). These changes may in turn influence the productivity and distribution of elk populations (Turner et al. 1994, Van Dyke and Darragh 2007, Romme et al. 2011, Sittler et al. 2015). In addition, the effect of disturbances changes over time and likely varies by the type and severity of the disturbance, as well as site-specific environmental conditions (Canon et al. 1987, Long et al. 2008, Jain et al. 2012, Proffitt et al. 2016a, Cook et al. 2016). These disturbances can be common and widespread across landscapes, making ground-investigation and monitoring of changes to nutritional resources for elk challenging. Additionally, landscape-scale information on the effect of disturbances on nutritional resources is often unavailable to managers interested in understanding how disturbances, or in using disturbances to, influence or benefit elk populations.

Given its availability and spatial resolution, NDVI has been posited as a potential index for monitoring changes in vegetation in grasslands and forests due to landscape disturbances (Goodin and Henebry 1997, Hicke et al. 2003, Goetz et al. 2006, Spruce et al. 2011, Olsson et al. 2016), sometimes with varying results (Beurs and Townsend 2008, Eklundh et al. 2009, Buma 2012). In boreal forests disturbed by wildfires, NDVI has been found to dramatically decrease following burning, with a gradual increase to pre-fire levels within 5-10 years (Hicke et al. 2003, Goetz et al. 2006). In other studies of boreal forests, NDVI increased to a peak 20-50 years after wildfire which was followed by gradual decreases to pre-fire levels (Kasischke and French 1997). In subalpine forests, NDVI was not associated with post-wildfire vegetation recovery (Buma 2012). Limited studies exist for the effect of forest treatments on NDVI, but indicate that NDVI is poorly correlated with thinning or

prescribed burn treatments (Arnett et al. 2015, Su et al. 2016). For forested landscapes in the Rocky Mountains, very limited information exists for understanding the relationship between NDVI and disturbances, particularly across multiple forest community types. This information may be useful for understanding how disturbances affect nutritional resources for elk given evidence from this study that NDVI is correlated with elk forage (Section 3) and body condition (Section 4).

The forested landscapes within our study areas have a varied history of disturbances due to forest management activities and natural events (i.e., timber harvest, prescribed burning, and wildfire; see Section 2). Our objective for this study was to evaluate the relationship between NDVI and these forest disturbances in several time-since-disturbance classes to: 1) understand how different types of disturbances may influence elk forage (and, therefore, nutritional condition), and 2) provide land and wildlife managers with information on how to use or manage disturbances to influence or benefit elk nutritional resources

## Methods

We obtained data for each type of forest disturbance (wildfire, thinning, prescribed burning, thinning followed by prescribed burning [henceforth, thinning-prescribed burning], and clearcutting) from multiple sources. We obtained wildfire polygons for 1985-2015 from the U.S. Forest Service's Fire History for Region 1 database (https://www.fs.usda.gov/detailfull/r1/landmanagement/gis) and additional polygons from the Bitterroot National Forest Fire History database (https://www.fs.usda.gov/detailfull/bitterroot/landmanagement/gis/). We obtained prescribed burn polygons for 1996-2016 from the U.S. Forest Service's Hazardous Fuel Treatment Reduction database (https://data.fs.usda.gov/geodata/edw/datasets.php) and additional polygons from the Lolo National Forest (personal communication). We considered the prescribed burning disturbance type to be any treatment activity indicated as a prescribed or broadcast burn, and we excluded burning of piled materials. For thinning and clearcutting data, we obtained timber harvest activity polygons for 1980-2017 from both the U.S. Forest Service's Hazardous Fuel Treatment Reduction database and the Timber Harvest database (https://data.fs.usda.gov/geodata/edw/datasets.php). We obtained additional timber harvest polygons from the Bitterroot National Forest Hazardous Fuel Reductions Treatment database (https://www.fs.usda.gov/detailfull/bitterroot/landmanagement/gis/). We considered the thinning disturbance type to be any treatment activity indicated as thinning and that reduced the density of understory trees through the removal of selected trees and shrub. We considered the clearcut disturbance type to be treatment activities indicated as biomass removal. For the thinning-prescribed burning disturbance, we considered only polygons that had prescribed burning occur within 3 years after thinning.

We considered only disturbances that fell within the extent of our study areas and the U.S. Forest Service's Region 1 Vegetation Mapping Program (VMap) data. For each disturbance type and based on the available disturbance data, we considered 5 years (1999, 2003, 2007, 2011, and 2015) of NDVI data to capture annual variation in NDVI values associated with vegetation cover types and amount of time since disturbance. From the annual

disturbance information in the database(s) for each disturbance type, we classified the landscape into 5 classes of time-since-disturbance: undisturbed, 1-5, 6-10, 11-20, and $\geq$ 21 years post-disturbance. The undisturbed class included areas that were not disturbed by any of the treatments we considered. The $\geq$ 21 years post-disturbance class represents areas where a disturbance occurred between 21 and the oldest recorded year available within the time-span of the disturbance data (i.e., a maximum of 30, 25, 65, and 109 years post-disturbance for wildfire, prescribed burning, thinning, and clearcutting datasets, respectively). For the thinning-prescribed burning type, we calculated time-since-disturbance based on the year of the prescribed burning treatment.

For each year of NDVI data, we first created spatial polygons that included each combination (i.e., strata) of disturbance type and time-since-disturbance class, such that only the most recent disturbance type was used and no disturbance type was overlapping spatially. This allowed us to eliminate areas with multiple disturbance types from comparison. We used stratified random sampling to select 4,000 point locations proportionally allocated across strata based on area for sampling of the attributes of points and NDVI. Due to low sample sizes within some strata, we ensured a minimum of 100 points were selected in each strata and accounted for the disproportionate sampling in our analysis using weighted regression (see below). To the sampling points, we extracted the strata, vegetation cover types, terrain covariates, and NDVI values and combined all points from each year into one dataset. We delineated vegetation cover types from VMap classes, using only the forested cover types identified in Section 3 (Table 2; i.e., including only PSME [*Pseudotsuga menziesii*], PICO [*Pinus contorta*], PIPO [*Pinus ponderosa*], PIAL [*Pinus albicaulis*], LAOC [*Larix occidentalis*], IMIX [mixed shade-intolerant species], TMIX [mixed shade-tolerant species], and POPUL [*Populus* spp.]). We included terrain covariates to account for environmental factors that may influence vegetation and vegetation response to disturbance. Terrain covariates included elevation (ELEV), slope (SLP), solar radiation (SRI), compound topography index (CTI), and the precipitation-, heat load-, and elevation adjusted topographic index (PHEAT; described in Section 3). We used time-integrated NDVI (TIN) because we found it to be consistently associated with elk forage (Section 3) and body condition (Section 4).

Prior to analysis, we assessed Pearson correlation coefficients of covariate pairs and found no collinearity ($|r| > 0.6$; Appendix B). We did not consider PHEAT with ELEV, SLP, SRI, or CTI in the same models due to the similarity of landscape properties described by the covariates. We standardized all continuous covariates.

We first fit a two-way analysis of variance (ANOVA) with an interaction between disturbance type and time-since-disturbance class using Program R version 3.4.3 (R Development Core Team 2018) to evaluate: 1) how TIN varies by disturbance type and by time-since-disturbance, and 2) how the effect of disturbance type depends on time-since-disturbance. We used Tukey's honestly significant difference (HSD) to test all pairwise differences in disturbance types and time-since-disturbance classes. Tukey's HSD difference values represent the difference in mean TIN values between the two groups being compared. We then analyzed each disturbance type separately using weighted linear regression to model TIN as a function of time-since-disturbance and other spatial covariates. To account for the disproportionate sampling of point locations, we weighted

the points based on the proportion of the total area of each strata, where the smaller strata received less weight. We fit the same model for each disturbance type and used the same data for the undisturbed class as the reference level to allow for comparisons among disturbance types to be made. We selected this model prior to splitting the data into separate datasets for each disturbance type by using backwards-stepwise model selection based on a global model that included: 1) disturbance type, 2) time-since-disturbance, 3) vegetation cover type, 4) an interaction of disturbance type and time-since-disturbance, 5) an interaction of disturbance type and vegetation cover type, and 6) terrain covariates excluding PHEAT. We used $P = 0.05$ as the threshold for inclusion or exclusion of predictor variables. To evaluate the importance of PHEAT, we used AIC to compare the resulting model with the same model where we replaced the supported terrain covariates with PHEAT.

We then fit the most-supported model to each disturbance type dataset, excluding the terms containing disturbance type. For each disturbance type analyses, we assessed the fit of the model based on $R^2$ values. We interpreted the effects of disturbance on TIN based on the direction and magnitude of coefficient estimates and sign and on predictions made by holding continuous covariates at their mean value. To account for error due to multiple comparisons, we evaluated significance of estimates based on a Bonferonni-corrected alpha-level of 0.01. We compared the effects of disturbance on TIN across disturbance types.

## Results

We sampled a total of 89,011 point locations across the 5 disturbance types, 5 time-since-disturbance classes, and 5 years (Table 17; Fig. 15). Of these points, 18,919, 17,281, 17,659, 17,158, and 17,994 fell in areas disturbed by wildfire, prescribed burning, thinning, thinning-prescribed burning, and clearcutting, respectively. The number of points falling in VMap classes varied for each disturbance type and time-since-disturbance class (Fig. 16). Across all disturbance types, TIN averaged 4.74 ± 0.9 (SD). TIN averaged 4.66 ± 0.93, 4.76 ± 0.9, 4.78 ± 0.88, 4.74 ± 0.89, and 4.77 ± 0.89 in areas disturbed by wildfire, prescribed burning, thinning, thinning-prescribed burning, and clearcutting, respectively. TIN varied across time-since-disturbance classes (Fig. 15).

**Table 17 - Area (km$^2$) and number (n) of point locations sampled within each disturbance type and time-since-disturbance (TSD) class. The same undisturbed data were used for each disturbance type dataset and included 15,679 points sampled from 20,597.1 km^2.**

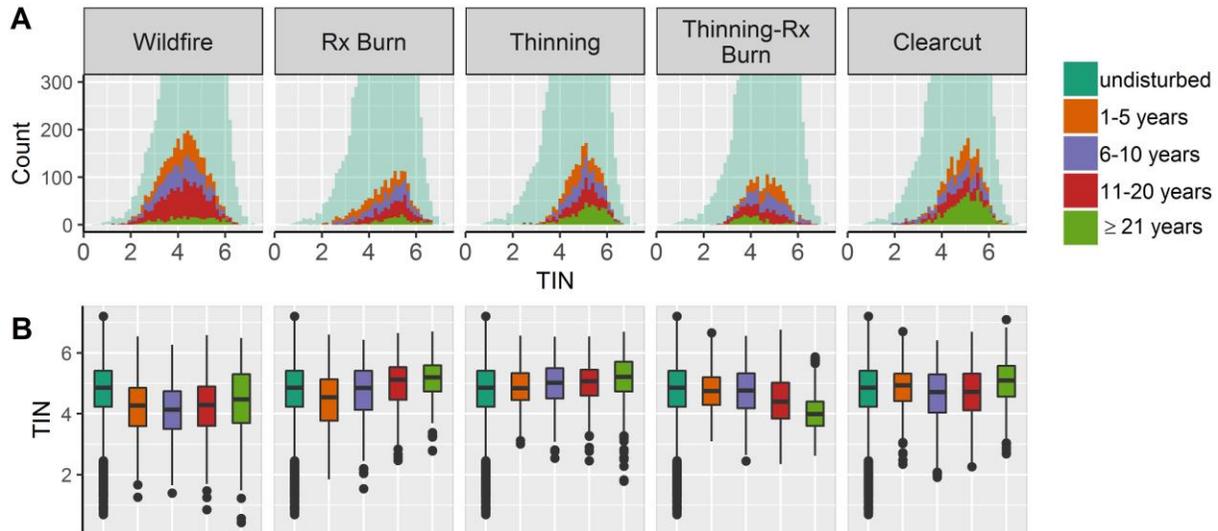| Disturbance type | 1-5 years | | 6-10 years | | 11-20 years | | >21 years | |
|---|---|---|---|---|---|---|---|---|
| | Area | n | Area | n | Area | n | Area | n |
| Wildfire | 931.5 | 838 | 791.1 | 836 | 1660.9 | 1241 | 287.5 | 325 |
| Rx Burn | 121.2 | 470 | 113.1 | 482 | 67.8 | 445 | 10.5 | 205 |
| Thinning | 55.3 | 488 | 51.5 | 496 | 118.1 | 481 | 332.2 | 515 |
| Thinning-Rx Burn | 6.9 | 405 | 7.5 | 475 | 5.8 | 400 | 2.4 | 199 |
| Clearcut | 35.9 | 529 | 45.7 | 500 | 140.6 | 478 | 1094.8 | 808 |

**Figure 15 - Counts (A) and boxplots (B) of sampling points located in disturbance types across values of TIN for each time-since-disturbance class in west-central Montana, USA. The undisturbed disturbance type is faded and the y-axis is scaled to better display the remaining disturbance types.**

We found strong evidence (P < 0.001) for differences in mean TIN between disturbance types and time-since-disturbance classes and for an interaction between disturbance type and time-since-disturbance class based on the ANOVA. The Tukey HSD test of disturbance types, however, indicated that only the pairwise comparisons of wildfire with all other disturbance types were significantly different (P < 0.001; Table 18). The Tukey HSD test of time-since-disturbance classes indicated all pairwise comparisons were significantly different (P < 0.05).

The most-supported model from the backwards-stepwise model selection included: 1) disturbance type, 2) time-since-disturbance, 3) vegetation cover type, 4) an interaction of disturbance type and time-since-disturbance, 5) an interaction of disturbance type and vegetation cover type, 6) ELEV, 7) SLP, 8) SRI, and 9) CTI. This model was substantially more supported than the model replacing PHEAT with the terrain covariates ($\Delta$AIC = 4191.4). We therefore fit the model with the following covariates to each disturbance type dataset: time-since-disturbance, vegetation cover type, ELEV, SLP, SRI, and CTI.

The effect of the time-since-disturbance classes on TIN varied across the disturbance models (Table 19; Fig. 17). The wildfire model (adjusted $R^2$ = 0.24) predicted TIN to be lower for all post-fire years relative to the undisturbed class (P < 0.001). Following wildfire, TIN was predicted to decline 13.1% to lowest values in 6-10 years and then increase in subsequent years (i.e., a 3.2% decrease from the undisturbed state). The prescribed burn model (adjusted $R^2$ = 0.21) predicted TIN to decrease 6.3% to lowest values within the first 5 years (P < 0.001) and then increase beyond 6 years following burning. TIN was predicted to be higher than the undisturbed class beyond 11 years and at highest values ≥ 21 years after burning, increasing 3.9% and 10.1% from the undisturbed state for the 6-10 year and ≥ 21 year classes, respectively. All time-since-disturbance classes greater than 6 years were not significantly different than the undisturbed class (P > 0.01), however.
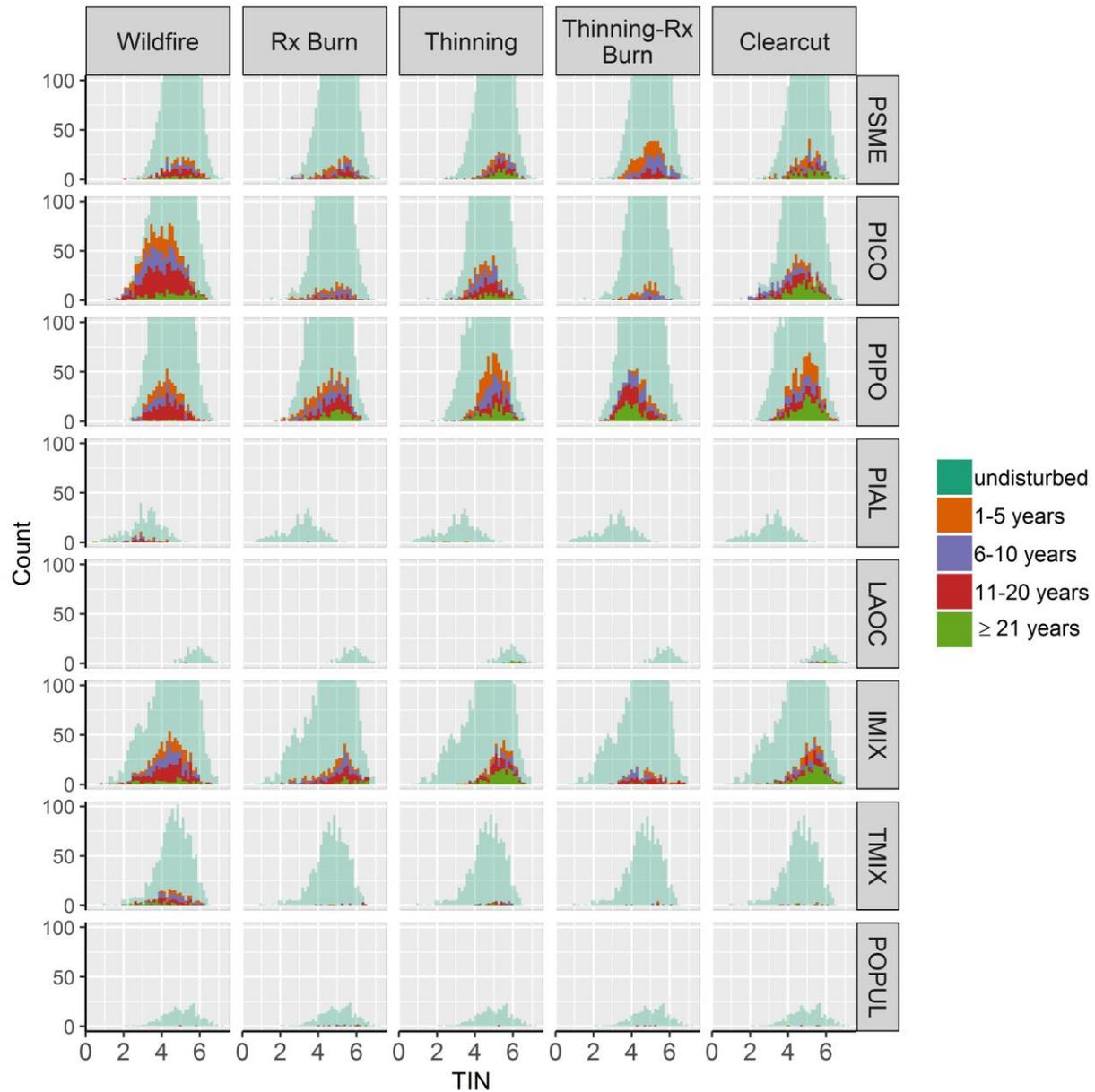
**Figure 16 - Counts of sampling points located in disturbance types across values of TIN for each VMap vegetation class and each time-since-disturbance class in west-central Montana, USA. The undisturbed disturbance type is faded and the y-axis is scaled to better display the remaining disturbance types. VMap vegetation classes include PSME (*Pseudotsuga menziesii*), PICO (*Pinus contorta*), PIPO (*Pinus ponderosa*), PIAL (*Pinus albicaulis*), LAOC (*Larix occidentalis*), IMIX (mixed shade-intolerant species), TMIX (mixed shade-tolerant species), and POPUL (*Populus* spp.).**

**Table 18 - Tukey Honestly Significantly Different pair-wise comparisons of differences in time-integrated NDVI for disturbance types and time-since-disturbance classes in west-central Montana, USA. Bolded estimates indicate p < 0.05.**

| Comparison category | Comparison | Difference | 95% C.I. Lower | 95% C.I. Upper |
|---|---|---|---|---|
| Disturbance type | Rx Burn – Wildfire | **0.08** | 0.06 | 0.11 |
| | Thinning – Wildfire | **0.09** | 0.07 | 0.12 |
| | Thinning-Rx Burn – Wildfire | **0.09** | 0.06 | 0.11 |
| | Clearcut – Wildfire | **0.10** | 0.07 | 0.12 |
| | Thinning – Rx Burn | 0.01 | -0.02 | 0.04 |
| | Thinning-Rx Burn – Rx Burn | 0.00 | -0.02 | 0.03 |
| | Clearcut – Rx Burn | 0.01 | -0.01 | 0.04 |
| | Thinning-Rx Burn – Thinning | -0.01 | -0.03 | 0.02 |
| | Clearcut – Thinning | 0.00 | -0.02 | 0.03 |
| | Clearcut – Thinning-Rx Burn | 0.01 | -0.01 | 0.04 |
| Time-since-disturbance class | 1-5 years – undisturbed | **-0.49** | -0.54 | -0.44 |
| | 6-10 years – undisturbed | **-0.56** | -0.60 | -0.51 |
| | 11-20 years – undisturbed | **-0.41** | -0.45 | -0.36 |
| | ≥21 years – undisturbed | **0.24** | 0.19 | 0.29 |
| | 6-10 years – 1-5 years | **-0.07** | -0.13 | -0.01 |
| | 11-20 years – 1-5 years | **0.08** | 0.02 | 0.14 |
| | ≥21 years – 1-5 years | **0.73** | 0.66 | 0.80 |
| | 11-20 years – 6-10 years | **0.15** | 0.09 | 0.21 |
| | ≥21 years – 6-10 years | **0.80** | 0.73 | 0.87 |
| | ≥21 years – 11-20 years | **0.65** | 0.58 | 0.72 |

The thinning model (adjusted $R^2$ = 0.22) predicted TIN to be 3.2-7.5% higher for all post-treatment years relative to the undisturbed class and to increase to highest values ≥ 21 years after treatment (P < 0.001). The time-since-disturbance classes between 1-10 years were not significantly different than the undisturbed class, however. The thinning-prescribed burn model (adjusted $R^2$ = 0.21) predicted TIN to increase 4.7% within the first 10 years, then decrease to lowest values 11-20 years (a 3.4% decrease from the undisturbed state), and finally increase ≥ 21 years after treatment (a 1.8% decrease from the undisturbed state). The highest TIN was predicted to occur 6-10 years after combined thinning-prescribed burning treatment; however, all time-since-disturbance classes were not significantly different than the undisturbed class. The clearcut model (adjusted $R^2$ = 0.22) predicted TIN to increase 0.4% within 5 years, then decrease to lowest values from 6-10 years (P < 0.001; a 7.9% decrease from the undisturbed state), and finally increase to highest values ≥ 21 years after treatment (a 6.7% increase from the undisturbed state). The time-since-disturbance classes spanning 1-5 and 11-20 years were not significantly different from the undisturbed class, however.

Across disturbance types, the highest predicted TIN values that were significantly different from the undisturbed class occurred in areas thinned ≥ 21 years prior (7.5% greater), followed by areas clearcut ≥ 21 years prior (6.7% greater) and areas thinned 11-20 years (5.5% greater) prior. The highest predicted TIN values occurring in areas treated 1-10 years prior had been thinned and thinned-prescribed burned, a 3.2-5.9% and 1.4-4.7% increase from the undisturbed state, respectively. Confidence intervals overlapped 0 for all

positive estimated coefficients in these time-since-disturbance classes across disturbance types, however. The lowest predicted TIN values that were significantly different from the undisturbed class occurred in areas burned by wildfire 6-10 years (13.1% less), 1-5 years (10.1% less), and 11-20 years (9.7% less) prior, followed by areas clearcut 6-10 years (7.9% less) and burned by prescribed fire 1-5 years (6.2% less) prior.

The effect of the forested VMap classes on TIN was generally consistent across disturbance types (Table 19; Fig. 17). TIN was predicted to be highest in LAOC (5.36) followed by PICO (5.05) and PSME (4.93) and lowest in PIAL (3.75) followed by PIPO (4.28) and POPUL (4.46). Confidence intervals excluded 0 for all VMap classes except TMIX across all disturbance models (P = 0.10-0.21) and PICO in the wildfire model (P = 0.32). Across disturbance types, TIN was predicted to decrease with increasing elevation (P < 0.001) and solar radiation (P < 0.001) and increase with increasing slope (P < 0.001) and compound topography index (P < 0.001).

**Table 19 - Estimated coefficients and 99% confidence intervals (Bonferonni-corrected) for models examining relationships of time-integrated NDVI (TIN) and disturbances in west-central Montana, USA. Effects of disturbances are in relation to the reference (intercept) time-since-disturbance (TSD) undisturbed class in PSME forested areas. Bolded estimates indicate p < 0.01. Continuous covariates are standardized. VMap vegetation classes include PSME (*Pseudotsuga menziesii*), PICO (*Pinus contorta*), PIPO (*Pinus ponderosa*), PIAL (*Pinus albicaulis*), LAOC (*Larix occidentalis*), IMIX (mixed shade-intolerant species), TMIX (mixed shade-tolerant species), and POPUL (*Populus* spp.).**

| Covariate | Wildfire Est. | Wildfire C.I. | Rx Burn Est. | Rx Burn C.I. | Thinned Est. | Thinned C.I. | Thinned-Rx Burn Est. | Thinned-Rx Burn C.I. | Clearcut Est. | Clearcut C.I. |
|---|---|---|---|---|---|---|---|---|---|---|
| Intercept | **4.96** | (4.92, 5.00) | **4.93** | (4.90, 4.97) | **4.93** | (4.90, 4.97) | **4.93** | (4.90, 4.97) | **4.93** | (4.89, 4.96) |
| TSD: 1-5 yrs | **-0.50** | (-0.58, -0.42) | **-0.31** | (-0.51, -0.10) | 0.16 | (-0.14, 0.46) | 0.07 | (-0.78, 0.93) | 0.02 | (-0.36, 0.39) |
| TSD: 6-10 yrs | **-0.65** | (-0.74, -0.57) | -0.09 | (-0.30, 0.13) | 0.29 | (-0.03, 0.60) | 0.23 | (-0.59, 1.06) | **-0.39** | (-0.72, -0.06) |
| TSD: 11-20 yrs | **-0.48** | (-0.54, -0.42) | 0.19 | (-0.08, 0.47) | **0.27** | (0.06, 0.47) | -0.17 | (-1.11, 0.77) | -0.10 | (-0.29, 0.09) |
| TSD: ≥21 yrs | **-0.16** | (-0.30, -0.02) | 0.50 | (-0.19, 1.20) | **0.37** | (0.24, 0.49) | -0.09 | (-1.54, 1.36) | **0.33** | (0.26, 0.40) |
| PICO | 0.02 | (-0.03, 0.07) | **0.12** | (0.07, 0.17) | **0.12** | (0.07, 0.17) | **0.12** | (0.07, 0.18) | **0.11** | (0.06, 0.16) |
| PIPO | **-0.66** | (-0.71, -0.60) | **-0.66** | (-0.72, -0.60) | **-0.65** | (-0.71, -0.60) | **-0.66** | (-0.72, -0.61) | **-0.63** | (-0.68, -0.57) |
| PIAL | **-1.17** | (-1.29, -1.06) | **-1.18** | (-1.31, -1.06) | **-1.19** | (-1.31, -1.07) | **-1.19** | (-1.31, -1.07) | **-1.18** | (-1.30, -1.06) |
| LAOC | **0.42** | (0.24, 0.59) | **0.43** | (0.26, 0.60) | **0.43** | (0.26, 0.60) | **0.43** | (0.25, 0.60) | **0.43** | (0.26, 0.59) |
| IMIX | **-0.26** | (-0.31, -0.21) | **-0.26** | (-0.31, -0.21) | **-0.26** | (-0.31, -0.21) | **-0.27** | (-0.32, -0.22) | **-0.25** | (-0.29, -0.20) |
| TMIX | -0.04 | (-0.11, 0.04) | -0.05 | (-0.12, 0.03) | -0.05 | (-0.12, 0.03) | -0.05 | (-0.12, 0.03) | -0.04 | (-0.11, 0.03) |
| POPUL | **-0.52** | (-0.65, -0.39) | **-0.48** | (-0.60, -0.35) | **-0.47** | (-0.60, -0.34) | **-0.47** | (-0.60, -0.35) | **-0.46** | (-0.59, -0.34) |
| ELEV | **-0.29** | (-0.32, -0.27) | **-0.28** | (-0.31, -0.26) | **-0.28** | (-0.31, -0.26) | **-0.29** | (-0.31, -0.26) | **-0.29** | (-0.31, -0.26) |
| SLP | **0.03** | (0.02, 0.05) | **0.04** | (0.02, 0.06) | **0.04** | (0.02, 0.06) | **0.04** | (0.03, 0.06) | **0.05** | (0.03, 0.06) |
| SRI | **-0.10** | (-0.12, -0.09) | **-0.12** | (-0.14, -0.10) | **-0.12** | (-0.14, -0.10) | **-0.12** | (-0.14, -0.10) | **-0.12** | (-0.14, -0.10) |
| CTI | **0.03** | (0.01, 0.04) | **0.03** | (0.01, 0.04) | **0.03** | (0.01, 0.04) | **0.03** | (0.01, 0.04) | **0.03** | (0.01, 0.04) |
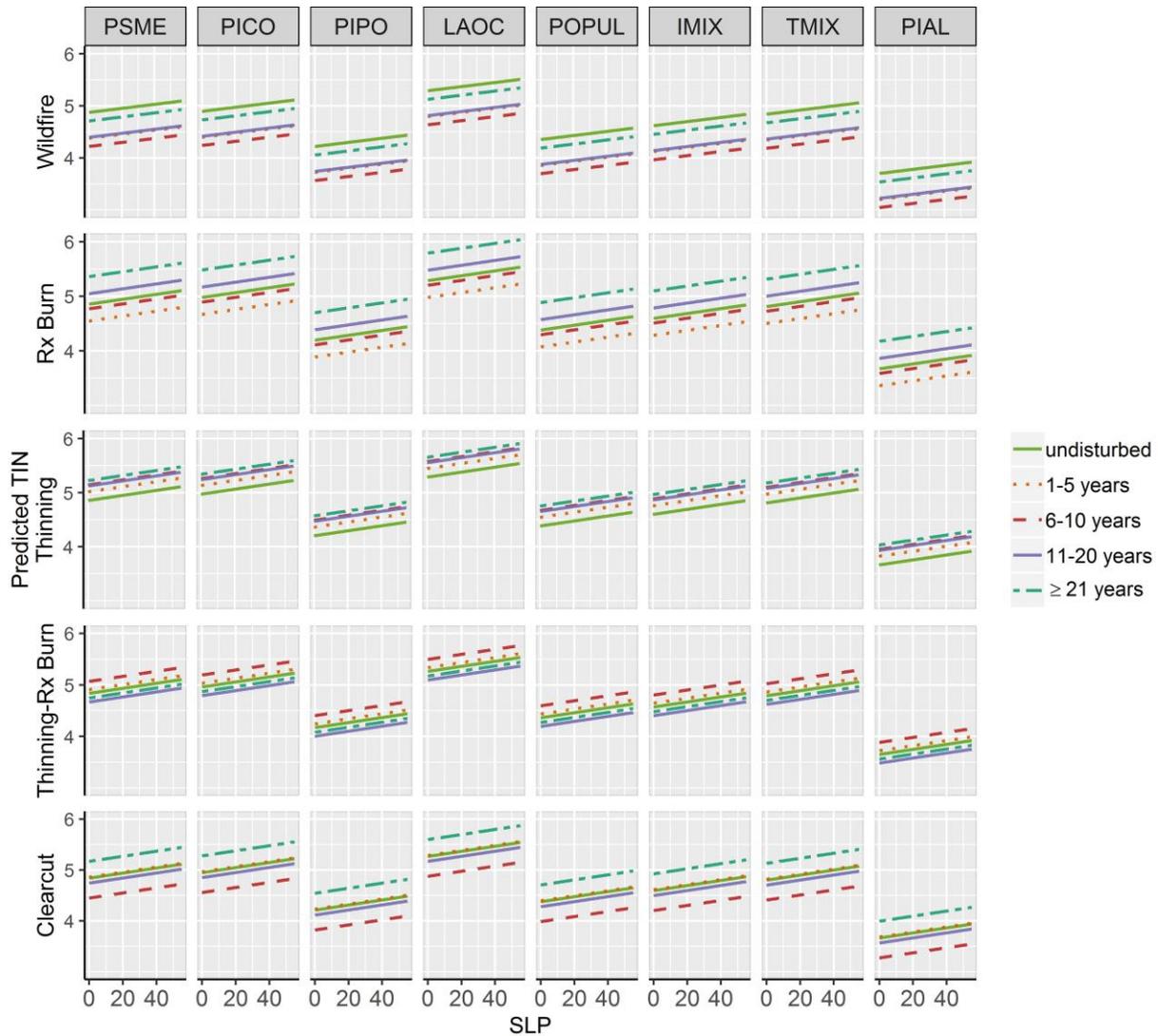
**Figure 17 - Predicted time-integrated NDVI (TIN) across disturbance types, VMAP vegetation classes, time-since-disturbance classes, and slope (SLP) in west-central Montana, USA. For differentiation of lines, 99% confidence intervals (Bonferonni-corrected) are not shown (refer to Table 19). VMap vegetation classes include PSME (*Pseudotsuga menziesii*), PICO (*Pinus contorta*), PIPO (*Pinus ponderosa*), PIAL (*Pinus albicaulis*), LAOC (*Larix occidentalis*), IMIX (mixed shade-intolerant species), TMIX (mixed shade-tolerant species), and POPUL (*Populus* spp.).**

## Discussion

We found strong support for associations of TIN with landscape disturbance, such as wildfire, prescribed burning, thinning, thinning-prescribed burning (i.e., prescribed burning within 3 years of thinning), and clearcutting, and number of years since disturbance (Table 19; Fig. 17). Our results indicate that the greatest positive effect on TIN occurred in areas thinned ≥ 11 years and clearcut ≥ 21 years prior. There was also marginal evidence that areas burned by prescribed fire ≥ 11 years, thinned 1-10 years, and thinned-prescribed burned 1-10 years prior had a positive effect on TIN. The greatest negative effect on TIN occurred in areas burned by wildfire. TIN was substantially reduced

within the first 10 years and appeared to be returning to undisturbed levels after 21 years following wildfire. There was also strong evidence that TIN decreased in areas burned by prescribed fires 1-5 years and clearcut 6-10 years prior decreased TIN and marginal evidence that TIN decreased in areas burned by prescribed fires 6-10 years, thinned-prescribed burned ≥ 21 years, and clearcut 11-20 years prior.

Overall, our results suggest that thinning and thinning-prescribed burning treatments are the most likely to yield the greatest short-term (1-10 years) increases in TIN; however, there was only weak evidence for this effect. There was no strong evidence that the additional effort of prescribed burning after thinning was different from thinning only; the effect of the additional effort on TIN was estimated to be less than thinning only. For longer time-frames (≥ 11 years), thinning may result in the greatest increases in TIN, however, there was strong evidence that clearcutting increased TIN after 21 years and weak evidence that prescribed burning increased TIN after 11 years. Thinning activities may create conditions most favorable to understory regrowth due to effects on microclimate, light, and soil nutrients and moisture (Moir 1966, Uresk and Severson 1989, Thomas et al. 1999, Naumburg and DeWald 1999, Ares et al. 2009). While the effects of thinning and prescribed burning on elk forage have varied across studies (Cook et al. 2016, Pilliod et al. 2006, Demarais and Krausman 2000, Peck and Peek 1991, Long et al. 2008, Proffitt et. al in review), the effect may depend on regional climates and environments. In Section 6, we further discuss these results in light of our previous evaluations of elk nutritional resources (Section 3) and fall nutritional condition (Section 4).

We found that differences in TIN were associated with forest vegetation cover types and were generally consistent across disturbance types (Table 19; Fig. 17). Overall, the highest TIN values were associated with LAOC; however, because of the deciduous nature of this species, these associations were likely more due to seasonal leaf-growth in the tree canopy than to understory vegetation available to elk. High TIN values were also associated with PICO and PSME. The lowest TIN values were associated with PIAL, PIPO, and POPUL. It is likely that the effect of time-since-disturbance on TIN also depends on vegetation cover type, however, we did not pursue this relationship and suggest that future evaluations consider this added complexity. Additionally, we could not account for any changes in forest vegetation types that may have occurred following disturbance due to the temporally invariant VMap classifications.

Our analysis provides a generalized evaluation of the relationships between TIN and forest disturbances; however, there are certain limitations to consider. First, these results suggest that certain treatments may increase TIN which may be associated with increases in elk forage (see Section 6). We did not know what plant species grow across time in response to these disturbances, however, and the relationship between TIN and forage for elk is therefore uncertain. Further research is needed to characterize the forage species that respond to various disturbances through time.

Second, we could not account for variation in the severity of wildfires or prescribed burns or the intensity or method of the different forest treatments. We found strong declines in TIN in all years following wildfires, a surprising result contrary to previous research in the same study area based on the same ground-based vegetation data used in this study

(Section 3) that indicated that wildfire generally increased forage quality and abundance for elk (Proffitt et al. 2017, Proffitt et al. in review). Our results may be related to the inclusion of different burn areas or a greater number of burns that burned at higher severities and consequently had limited revegetation. It is also plausible that wildfires decrease non-forage species while increasing forage species, but the increase in forage species is not substantial enough to be detectable by satellites. Alternatively, areas burned by natural fires may see strong responses from new growth of trees which may reduce the amount of understory vegetation due to shading or reduce the amount of greenness of the understory vegetation detectable by satellites. For areas affected by forest treatments, considerable variation in thinning or prescribed burning techniques (e.g., the number and size of trees removed or the time of year of a prescribed burn) likely existed in our data. Some techniques may affect TIN more strongly than others, however, we could not disentangle these associations. More detailed research would be required to understand the response of NDVI to wildfire and variable treatment techniques.

Third, we attempted to isolate the effect of each disturbance type by excluding areas that had experienced multiple types of disturbance within the span of available disturbance data. We recognize, however, that the composition and development of dry mixed-conifer forests are likely driven by multiple disturbance types which may respond to successive disturbances in different ways (Jain et al. 2012, Willms et al. 2017). Additionally, our disturbance data were limited by the amount of historical events available (i.e., the oldest recorded year of disturbance available was 30, 25, 65, and 109 years in the wildfire, prescribed burning, thinning, and clearcutting datasets). Because the majority of forests likely have historically experienced multiple disturbances, even of the same disturbance type, resulting in a diversity of vegetative compositions and structures (Willms et al. 2017), there is some limitation in the ability to generalize of our results to areas with multiple disturbance events. Lastly, additional research evaluating the effect of disturbances should consider areas affected by insect infestations that can strongly influence tree mortality and vegetation conditions.

Management strategies focused on altering the distribution and availability of summer nutritional resources for elk may provide an important means of manipulating distributions and health of elk populations. Here, we provide recommendations for forest treatments that may be valuable for improving the nutritional capacity of forested landscapes based on the results of the current study. We developed this study and the following recommendations in response to a need for integrating management of nutritional resources into forest management plans and to maintain elk nutritional resources and distributions on public lands during the summer and fall seasons. These recommendations are intended to be used holistically in conjunction with other management techniques for helping land and wildlife managers meet objectives for elk populations and habitat.

We found some evidence that NDVI amplitude (AMP) and time-integrated NDVI (TIN) are related to forage abundance and forage quality for elk (Section 3). While both NDVI metrics are strongly related to other landscape attributes (e.g., overstory canopy cover, vegetation community type, and terrain), management strategies focused on treatments for manipulating AMP and TIN may enhance nutritional resources for elk. Managers could direct treatments on sites that are predicted to have the lowest forage abundance and quality. The AMP and TIN relationships indicated that sites at high elevation (up to 2700 m [9000 ft]), with low solar radiation, and with high overstory canopy cover have the lowest forage abundance (Table 6; Fig. 6 and Fig. 18) and sites with high overstory canopy cover have the lowest forage quality (Table 10; Fig. 19). At sites where AMP levels are low (< 0.18), that generally may include dry grasslands, dry shrublands, and *Larix occidentalis*, *Pinus ponderosa*, *Pseudotsuga menziesii*, and shade-intolerant mixed forests (Fig. 5), treatments designed to increase AMP may enhance both forage abundance (Fig. 6) and forage quality (Fig. 8). At sites where AMP levels are higher (> 0.18), increases in AMP are predicted to have a diminishing positive response on forage abundance and a negative response on forage quality. Sites that are likely to have high AMP values that may benefit

from reductions in AMP for enhancing forage quality while only marginally reducing forage abundance include wet grasslands and shrublands and *Abies lasiocarpa*, *Pinus albicaulus*, *Pinus contorta*, *Pseudotsuga menziesii*, shade-intolerant mixed, shade-tolerant mixed, and *Populus* spp. forests (Fig. 5). Management efforts directed at increasing TIN are predicted to near-linearly enhance forage abundance regardless of community type, but the effect is stronger at sites at lower elevations and with higher solar radiation (Fig. 7).

Management efforts to improve the nutritional capacity of landscapes for elk may also consider reducing overstory canopy cover through thinning or logging, a recommendation that is further supported from our analysis of NDVI and landscape disturbances (see below; Section 5) and in a recent study in western Washington and Oregon forests (Cook et al. 2016). Our results provide some evidence that reducing canopy cover will increase forage abundance across all forest cover types, particularly at low elevation sites with high solar radiation and intermediate values of compound topographic index (Fig. 18), and increase forage quality, particularly in *Pinus contorta*, *Pinus ponderosa*, and shade-intolerant mixed forests (Fig. 19). Reductions in canopy cover increase forage abundance and quality across the entire range of canopy cover (0-75% in our data), similar to results from Cook et al. (2016), but the effect is stronger at lower canopy cover (approximately < 20% canopy cover). Eliminating canopy cover is predicted to maximize both forage abundance and quality across all sites; however, such treatments may not be effective for increasing forage abundance at high elevation and low solar radiation sites due to these sites demonstrating a negligible response to reductions in canopy cover, and may have other negative effects on elk including loss of thermal cover and/or security.
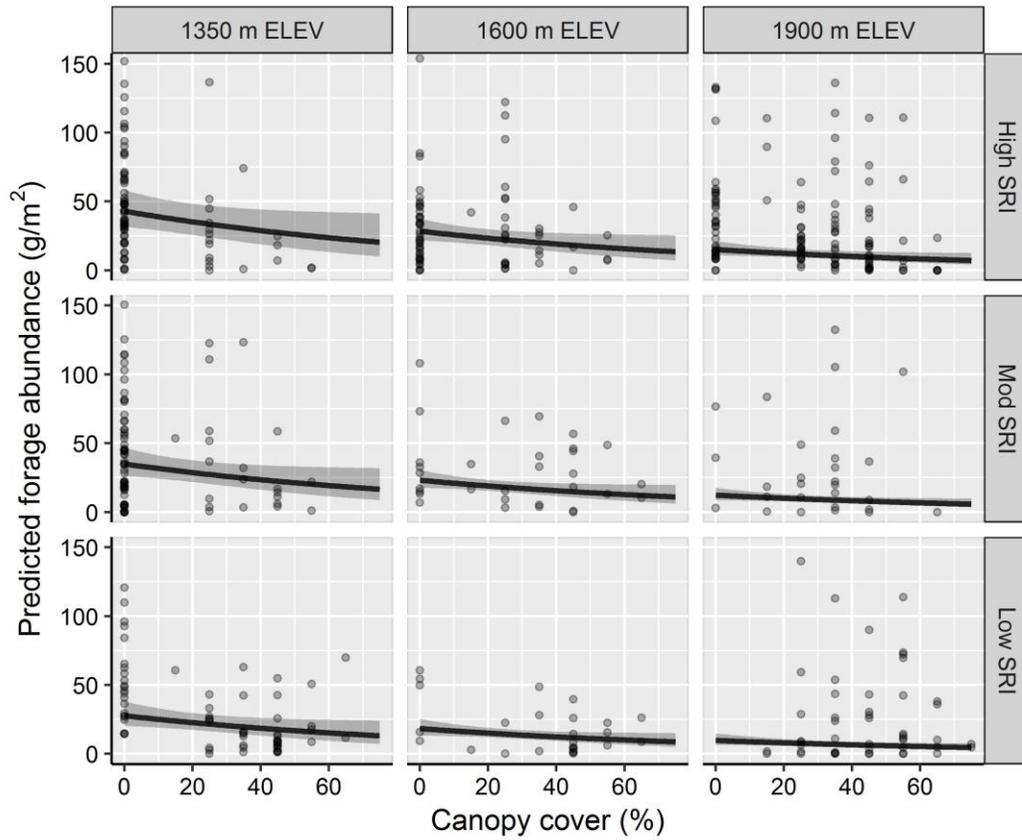
**Figure 18 - Predicted forage abundance with 95% confidence intervals across levels of canopy cover and solar radiation in the inferential model for the relationship of NDVI amplitude and elk forage abundance in west-central Montana, USA, 2012-2015.**
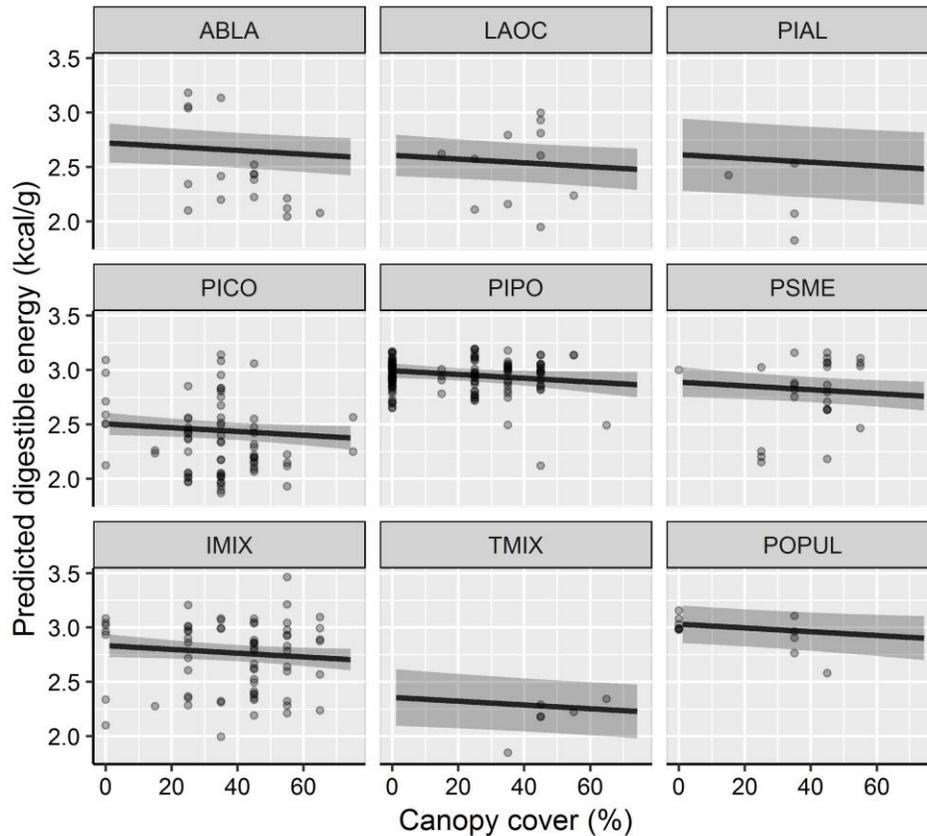
**Figure 19 - Predicted forage quality (digestible energy; kcal/g) with 95% confidence intervals across levels of canopy cover within each VMap forest cover type in the inferential model for the relationship of NDVI amplitude and elk forage quality in west-central Montana, USA, 2012-2015. Refer to Table 2 for definitions of VMap cover types.**

We found strong support for a relationship of TIN with both forage abundance (Section 3) and fall ingesta-free body fat of elk (Section 4), indicating that TIN may be a more biologically relevant metric for assessing elk forage than AMP. Fall body fat levels are strongly associated with the intake of nutritional resources during the previous summer and fall (Cook 2002, Cook et al. 2004a, 2013), and TIN is more likely to represent cumulative nutritional resources during this period given that it incorporates greenness signals that accrue throughout the growing season, unlike AMP that represents only green up conditions. Elk that were exposed to higher levels of TIN within their home ranges during the summer-fall period had significantly higher body fat levels during the subsequent fall after controlling for lactation (Fig. 13). The importance of TIN to nutritional condition may be further supported by the more uncertain but positive relationship between TIN and winter body fat levels (Fig. 13). This suggests that TIN may represent higher quality habitats on summer range which may be due, in part, to higher forage abundance located in these areas. Forage abundance was positively correlated with TIN, and this relationship was strongest at low elevation sites with high solar radiation and intermediate values of compound topographic index (Fig. 7).

Land managers may be able to improve the nutritional capacity of landscapes and manipulate elk distribution during the summer-fall by implementing forest treatments that increase levels of TIN available on elk summer-fall ranges (Section 5). We found that each type of forest disturbance (wildfire, prescribed burning, thinning, thinning followed by prescribed burning, and clearcutting) created a different response in TIN, indicating that different treatment methods aren't likely to mimic each other and shouldn't be considered as surrogates or replacements (Schwilk et al. 2009, McIver et al. 2013). Our results suggest that treatment activities that include thinning are most likely to result in the greatest long-term (≥ 11 years) increases in TIN (Table 19; Fig. 17). Thinning is predicted to also increase TIN in the short-term (< 10 years), however, there is some uncertainty in this finding. Prescribed burning within 3 years after thinning increases TIN within 10 years; however, our results do not show evidence that the additional effort of prescribed burning after thinning was different from thinning only. Other treatment techniques, however, may be more appropriate in certain areas, depending on management objectives and constraints. It may also be beneficial to use multiple treatments across broad areas to create a temporally and spatially dynamic landscape of varying levels of TIN. Other treatment strategies that may benefit elk habitat by increasing TIN within the first 5 years could include clearcutting, within 11-20 years could include prescribed burning alone, and beyond 20 years could include clearcutting. Evidence for the short term effect of clearcutting and the effect of prescribed burning to increase TIN are weak, but there is strong evidence for the long term effect of clearcutting. These treatment effects also varied by forest vegetation type, with the lowest TIN values occurring generally in PIAL, PIPO, and POPUL, and the highest occurring generally in PSME and TMIX. We suggest that focusing management treatments in forest vegetation types that are common within a region but with the lowest nutritional value. Managers may also consider treating areas identified as important seasonal travel corridors for elk to reduce potential movement to lower elevation forage.

Wildfires were predicted to substantially decrease TIN values across all years post-fire suggesting that elk forage also decreased. These results were contrary to previous research completed in the same study area based on the same ground-based vegetation data used in this study (see Section 3) that found wildfire to generally increase the quality and abundance of elk forage (Proffitt et al. 2017, Proffitt et al. in review). We suggest that the difference in our results may be due to one or more reasons. First, the results may be driven by the inclusion of different burn areas or a greater number of burns that were of higher severity and consequently had limited vegetation regrowth. Second, while there may have been an increase in forage species after fire, it may not have been enough to be detected by the satellites if non-forage species were simultaneously reduced by fire and did not recover. Third, areas with different moisture availabilities or forest types may respond differently to wildfire (e.g., regrowth and duration of green vegetation may be limited on drier upland sites compared to wetter, lower sites) which we did not account for in our analysis. Lastly, strong responses from new growth of trees may reduce the amount of understory vegetation due to shading or reduce the amount of greenness of the understory vegetation detectable by satellites. These uncertainties highlight the need for more detailed research on the response of NDVI to wildfire to better inform management of wildfires for elk forage.

We caution that because we did not perform validations of our models, our results may only be applicable to our study areas and not transferable to other areas. Our two study areas, however, represent climate and vegetation community types that are common across west-central and south-western Montana. Additionally, there was uncertainty in the NDVI-nutrition relationships, and our results indicated that the NDVI metrics play a small role in explaining elk forage relative to other landscape attributes. NDVI is itself a crude measure of vegetation that integrates several, complicating aspects of the vegetation (e.g., different species of varying vegetative forms, vigor, structures, horizontal and vertical densities, reflectance, absorption, and transmissivity; Pettorelli 2013) and may only be capturing portions of the signals related to elk forage. To further clarify relationships between NDVI and nutritional resources for elk, and to make results more transferable across populations of western Montana, more research would be needed that improves study design by matching the scale of elk forage measurements to that measured by NDVI, collecting data from additional populations representing the full diversity of landscapes occupied by elk in western Montana, and performing model validation in new areas. Similarly, more research is needed to determine if the relationships between TIN and fall ingesta-free body fat are consistent across elk populations.

# Section 7 - Literature Cited

Aikens, E. O., M. J. Kauffman, J. A. Merkle, S. P. H. Dwinnell, G. L. Fralick, and K. L. Monteith. 2017. The greenscape shapes surfing of resource waves in a large migratory herbivore. Ecology Letters 20:741–750.

Ares, A., S. D. Berryman, and K. J. Puettmann. 2009. Understory vegetation response to thinning disturbance of varying complexity in coniferous stands. Applied Vegetation Science 12:472–487.

Arnett, J. T., N. C. Coops, L. D. Daniels, and R. W. Falls. 2015. Detecting forest damage after a low-severity fire using remote sensing at multiple scales. International Journal of Applied Earth Observation and Geoinformation 35:239–246.

Arnold, T. W. 2010. Uninformative parameters and model selection using Akaike's Information Criterion. The Journal of Wildlife Management 74:1175–1178.

Barber, J., R. Bush, and D. Berglund. 2011. The Region 1 existing vegetation classification system and its relationship to Region 1 inventory data and map products. Numbered Report 11-10. USDA Forest Service. Pages 1–39. USDA Forest Service Region 1, Missoula, Montana, USA.

Beurs, K. de, and P. Townsend. 2008. Estimating the effect of gypsy moth defoliation using MODIS. Remote Sensing of Environment 112:3983–3990.

Bischof, R., L. E. Loe, E. L. Meisingset, B. Zimmermann, B. Van Moorter, and A. Mysterud. 2012. A migratory northern ungulate in the pursuit of spring: jumping or surfing the green wave? The American Naturalist 180:407–424.

Borowik, T., N. Pettorelli, L. Sönnichsen, and B. Jedrzejewska. 2013. Normalized difference vegetation index (NDVI) as a predictor of forage availability for ungulates in forest and field habitats. European Journal of Wildlife Research 59.

Buma, B. 2012. Evaluating the utility and seasonality of NDVI values for assessing post-disturbance recovery in a subalpine forest. Environmental Monitoring and Assessment 184:3849–3860.

Burcham, M. G., D. W. Edge, and L. C. Marcum. 1999. Elk use of private land refuges. Wildlife Society Bulletin 27:833–839.

Burnham, K. P., and D. R. Anderson. 2002. Model selection and multimodel inference: a practical information-theoretic approach. Second edition. Page 512. Springer-Verlag, Berlin, Germany.

Canon, S. K., P. J. Urness, and N. V. Debyle. 1987. Habitat selection, foraging behavior, and dietary nutrition of elk in burned aspen forest. Journal of Range Management 40:433–438.

Conner, M. M., G. C. White, and D. J. Freddy. 2001. Elk movement in response to early-season hunting in northwest Colorado. The Journal of Wildlife Management 65:926–940.

Cook, J. G. 2002. Nutrition and Food. Pages 259–349 *in* D. E. Toweill and J. W. Thomas, editors. North american elk: Ecology and management. First editions. Smithsonian Institution Press, Washington.

Cook, J. G., R. C. Cook, R. W. Davis, and L. L. Irwin. 2016. Nutritional ecology of elk during summer and autumn in the Pacific Northwest. Wildlife Monographs 195:1–326.

Cook, J. G., B. K. Johnson, R. C. Cook, R. A. Riggs, T. Delcurto, L. D. Bryant, and L. L. Irwin. 2004a. Effects of summer-autumn nutrition and parturition date on reproduction and survival of elk. Wildlife Monographs 155:1–61.

Cook, J. G., L. J. Quinlan, L. L. Irwin, L. D. Bryant, R. A. Riggs, and J. W. Thomas. 1996. Nutrition-growth relations of elk calves during late summer and fall. The Journal of Wildlife Management 60:528.

Cook, R. C., J. G. Cook, and L. D. Mech. 2004b. Nutritional condition of northern Yellowstone elk. Journal of Mammalogy 85:714–722.

Cook, R. C., J. G. Cook, T. R. Stephenson, W. L. Myers, S. M. Mccorquodale, D. J. Vales, L. L. Irwin, P. B. Hall, R. D. Spencer, S. L. Murphie, K. A. Schoenecker, and P. J. Miller. 2010. Revisions of rump fat and body scoring indices for deer, elk, and moose. The Journal of Wildlife Management 74:880–896.

Cook, R. C., J. G. Cook, D. J. Vales, B. K. Johnson, S. M. Mccorquodale, L. A. Shipley, R. A. Riggs, L. L. Irwin, S. L. Murphie, B. L. Murphie, K. A. Schoenecker, F. Geyer, P. B. Hall, R. D. Spencer, D. A. Immell, D. H. Jackson, B. L. Tiller, P. J. Miller, and L. Schmitz. 2013. Regional and seasonal patterns of nutritional condition and reproduction in elk. Wildlife Monographs 184:1–45.

Demarais, S., and P. Krausman. 2000. Ecology and management of large mammals in North America. Page 778. Prentice Hall, Upper Saddle River, N.J.

DeVoe, J. D., R. A. Garrott, J. J. Rotella, S. R. Challender, P. J. White, M. O'Reilly, and C. J. Butler. 2015. Summer range occupancy modeling of non-native mountain goats in the greater Yellowstone area. Ecosphere 6:art217.

Eacker, D. R., M. Hebblewhite, K. M. Proffitt, B. S. Jimenez, M. S. Mitchell, and H. S. Robinson. 2016. Annual elk calf survival in a multiple carnivore system. The Journal of Wildlife Management 80:1345–1359.

Eklundh, L., T. Johansson, and S. Solberg. 2009. Mapping insect defoliation in Scots pine with MODIS time-series data. Remote Sensing of Environment 113:1566–1573.

Evans, S. B., L. D. Mech, P. J. White, and G. A. Sargent. 2006. Survival of adult female elk in Yellowstone following wolf restoration. Journal of Wildlife Management 70:1372–1378.

Franklin, A. B., D. R. Anderson, R. J. Gutiérrez, and K. P. Burnham. 2000. Climate, habitat quality, and fitness in northern spotted owl populations in northwestern California. Ecological Monographs 70:539–590.

Fryxell, J., J. Greever, and A. Sinclair. 1988. Why are migratory ungulates so abundant? The American Naturalist 131:781–798.

Fu, P., and P. Rich. 1999. Design and implementation of the Solar Analyst: an ArcView extension for modeling solar radiation at landscape scales. *in*. San Diego, USA.

Garroutte, E., A. Hansen, and R. Lawrence. 2016. Using NDVI and EVI to map spatiotemporal variation in the biomass and quality of forage for migratory elk in the Greater Yellowstone Ecosystem. Remote Sensing 8:404.

Goetz, S. J., G. J. Fiske, and A. G. Bunn. 2006. Using satellite time-series data sets to analyze fire disturbance and forest recovery across Canada. Remote Sensing of Environment 101:352–365.

Goodin, D. G., and G. M. Henebry. 1997. A technique for monitoring ecological disturbance in tallgrass prairie using seasonal NDVI trajectories and a discriminant function mixture model. Remote Sensing of Environment 61:270–278.

Haggerty, J. H., and W. R. Travis. 2006. Out of administrative control: absentee owners, resident elk and the shifting nature of wildlife management in southwestern Montana. Geoforum 37:816–830.

Hamel, S., M. Garel, M. Festa-Bianchet, J.-M. Gaillard, and S. D. Côté. 2009. Spring Normalized Difference Vegetation Index (NDVI) predicts annual variation in timing of peak faecal crude protein in mountain ungulates. Journal of Applied Ecology 46:582–589.

Hanley, T. A., C. T. Robbins, A. E. Hagerman, and C. McArthur. 1992. Predicting digestible protein and digestible dry matter in tannin-containing forages consumed by ruminants. Ecology 73:537–541.

Hebblewhite, M. 2006. Linking predation risk and forage to ungulate population dynamics. PhD thesis, Dissertation, University of Alberta, Edmonton, Alberta, CA.

Hebblewhite, M., E. H. Merrill, and G. McDermid. 2008. A multi-scale test of the forage maturation hypothesis in a partially migratory ungulate population. Ecological Monographs 78:141–166.

Herfindal, I., B.-E. Saether, E. J. Solberg, R. Andersen, and K. A. Hogda. 2006. Population characteristics predict responses in moose body mass to temporal variation in the environment. Journal of Animal Ecology 75:1110–1118.

Hicke, J. A., G. P. Asner, E. S. Kasischke, N. H. F. French, J. T. Randerson, G. James Collatz, B. J. Stocks, C. J. Tucker, S. O. Los, and C. B. Field. 2003. Postfire response of North American boreal forest net primary productivity analyzed with satellite observations. Global Change Biology 9:1145–1157.

Hobbs, T. J. 1995. The use of NOAA-AVHRR NDVI data to assess herbage production in the arid rangelands of Central Australia. International Journal of Remote Sensing 16:1289–1302.

Jain, T., M. Battaglia, H.-S. Han, R. Graham, C. Keyes, J. Fried, and J. Sandquist. 2012. A comprehensive guide to fuel management practices for dry mixed conifer forests in the northwestern United States. U.S. Department of Agriculture, Forest Service, Rocky Mountain Research Station, Fort Collins, CO, Gen. Tech. Rep. RMRS-GTR-292.

Jourdonnais, C. S., and D. J. Bedunah. 1990. Prescribed fire and cattle grazing on an elk winter range in Montana. Wildlife Society Bulletin 18.

Kasischke, E. S., and N. H. F. French. 1997. Constraints on using AVHRR composite index imagery to study patterns of vegetation cover in boreal forests. International Journal of Remote Sensing 18:2403–2426.

Krebs, J. 1989. Ecological methodology. Harper Collins, New York, New York, USA.

Long, R. A., J. L. Rachlow, J. G. Kie, and M. Vavra. 2008. Fuels reduction in a western coniferous forest: effects on quantity and quality of forage for elk. Rangeland Ecology & Management 61:302–313.

Lowrey, B., R. A. Garrott, H. M. Miyasaki, G. Fralick, and S. R. Dewey. 2017. Seasonal resource selection by introduced mountain goats in the southwest Greater Yellowstone Area. Ecosphere 8:e01769.

Marshal, J. P., V. C. Bleich, P. R. Krausman, M. L. Reed, and N. G. Andrew. (n.d.). Factors affecting habitat use and distribution of desert mule deer in an arid environment. WileyWildlife Society.

Martínez-jauregui, M., A. San Miguel-ayanz, A. Mysterud, C. Rodríguez-vigal, T. Clutton-brock, R. Langvatn, and T. Coulson. 2009. Are local weather, NDVI and NAO consistent determinants of red deer weight across three contrasting European countries? Global Change Biology 15:1727–1738.

McIver, J. D., S. L. Stephens, J. K. Agee, J. Barbour, R. E. J. Boerner, C. B. Edminster, K. L. Erickson, K. L. Farris, C. J. Fettig, C. E. Fiedler, S. Haase, S. C. Hart, J. E. Keeley, E. E. Knapp, J. F. Lehmkuhl, J. J. Moghaddas, W. Otrosina, K. W. Outcalt, D. W. Schwilk, C. N. Skinner, T. A. Waldrop, C. P. Weatherspoon, D. A. Yaussy, A. Youngblood, and S. Zack. 2013. Ecological effects of alternative fuel-reduction treatments: highlights of the National Fire and Fire Surrogate study (FFS). International Journal of Wildland Fire 22:63.

Merkle, J. A., K. L. Monteith, E. O. Aikens, M. M. Hayes, K. R. Hersey, A. D. Middleton, B. A. Oates, H. Sawyer, B. M. Scurlock, and M. J. Kauffman. 2016. Large herbivores surf waves of green-up in spring. Proceedings of the Royal Society B 283.

Moir, W. H. 1966. Influence of ponderosa pine on herbaceous vegetation. Ecology 47:1045–1048.

Monteith, K. L., V. C. Bleich, T. R. Stephenson, B. M. Pierce, M. M. Conner, J. G. Kie, and R. T. Bowyer. 2014. Life-history characteristics of mule deer: effects of nutrition in a variable environment. Wildlife Monographs 186:1–62.

Mueller, T., K. A. Olson, T. K. Fuller, G. B. Schaller, M. G. Murray, and P. Leimgruber. 2008. In search of forage: predicting dynamic habitats of Mongolian gazelles using satellite-based estimates of vegetation productivity. Journal of Applied Ecology 45:649–658.

Mysterud, A., P. Tryjanowski, M. Panek, N. Pettorelli, and N. C. Stenseth. 2007. Inter-specific synchrony of two contrasting ungulates: wild boar (Sus scrofa) and roe deer (Capreolus capreolus). Oecologia 151:232–239.

Mysterud, A., B. K. Vike, E. L. Meisingset, and I. M. Rivrud. 2017. The role of landscape characteristics for forage maturation and nutritional benefits of migration in red deer. Ecology and Evolution.

Naumburg, E., and L. E. DeWald. 1999. Relationships between Pinus ponderosa forest structure, light characteristics, and understory graminoid species presence and abundance. Forest Ecology and Management 124:205–215.

Noyes, J. H., R. G. Sasser, B. K. Johnson, L. D. Bryant, and B. Alexander. 1997. Accuracy of pregnancy detection by serum protein (PSPB) in elk. Wildlife Society Bulletin (1973-2006) 25:695–698.

Olsson, P.-O., J. Lindström, and L. Eklundh. 2016. Near real-time monitoring of insect induced defoliation in subalpine birch forests with MODIS derived NDVI. Remote Sensing of Environment 181:42–53.

Parker, K. L., P. S. Barboza, and M. P. Gillingham. 2009. Nutrition integrates environmental responses of ungulates. Functional Ecology 23:57–69.

Pearson, S. M., M. G. Turner, L. L. Wallace, and W. H. Romme. 1995. Winter habitat use by large ungulates following fire in northern Yellowstone National Park. Ecological Applications 5:744–755.

Peck, V. R., and J. M. Peek. 1991. Elk, Cervus elaphus, habitat use related to prescribed fire, Tuchodi River, British-Columbia. Canadian Field-Naturalist 105:354–362.

Pettorelli, N. 2013. The Normalized Difference Vegegation Index. Page 194. Oxford University Press, Oxford.

Pettorelli, N., J.-M. Gaillard, A. Mysterud, P. Duncan, N. Chr. Stenseth, D. Delorme, G. Van Laere, C. Toïgo, and F. Klein. 2006. Using a proxy of plant productivity (NDVI) to find key periods for animal performance: the case of roe deer. Oikos 112:565–572.

Pettorelli, N., S. J. Ryan, T. Mueller, N. Bunnefeld, B. Jedrzejewska, M. Lima, and K. Kausrud. 2011. The Normalized Difference Vegetation Index (NDVI): Unforeseen successes in animal ecology. Climate Research 46:15–27.

Pettorelli, N., J. O. Vik, A. Mysterud, J.-M. Gaillard, C. J. Tucker, and N. C. Stenseth. 2005. Using the satellite-derived NDVI to assess ecological responses to environmental change. Trends in Ecology & Evolution 20:503–510.

Pilliod, D., E. Bull, J. Hayes, and B. Wales. 2006. Wildfire and invertebrate response to fuel reduction treatments in dry coniferous forests of the western United States: a synthesis. Page 34. U.S. Department of Agriculture, Forest Service, Rocky Mountain Research Station, Fort Collins, CO, Gen. Tech. Rep. RMRS-GTR-173.

PRISM Climate Group. 2016. Oregon State University.

Proffitt, K. M., J. L. Grigg, R. A. Garrott, K. L. Hamlin, J. Cunningham, J. a. Gude, C. Jourdonnais, A. Press, K. M. Proffitt, J. L. Grigg, R. A. Garrott, L. Kenneth, J. Cunningham, J. a. Gude, C. Jourdonnais, K. L. Hamlin, J. Cunningham, J. a. Gude, and C. Jourdonnais. 2010. Changes in elk resource selection and distributions associated with a late-season elk hunt. Journal of Wildlife Management 74:210–218.

Proffitt, K. M., J. A. Gude, K. L. Hamlin, and M. A. Messer. 2013. Effects of hunter access and habitat security on elk habitat selection in landscapes with a public and private land matrix. The Journal of Wildlife Management 77:514–524.

Proffitt, K. M., J. A. Gude, K. L. Hamlin, R. A. Garrott, J. A. Cunningham, and J. L. Grigg. 2011. Elk distribution and spatial overlap with livestock during the brucellosis transmission risk period. Journal of Applied Ecology 48:471–478.

Proffitt, K. M., M. Hebblewhite, W. Peters, N. Hupp, and J. Shamhart. 2016a. Linking landscape-scale differences in forage to ungulate nutritional ecology. Ecological Applications 26:2156–2174.

Proffitt, K. M., R. Mowry, M. S. Lewis, R. Durham, T. Hayes, C. S. Jourdonnais, P. Ramsey, K. Barker, J. D. DeVoe, and M. S. Mitchell. 2017. North Sapphire Elk Research Project. Pages 1–95. Montana Fish, Wildlife; Parks, Helena, Montana, USA.

Proffitt, K. M., S. Thompson, D. Henry, B. Jimenez, and J. A. Gude. 2016b. Hunter access affects elk resource selection in the Missouri breaks, Montana. The Journal of Wildlife Management 80:1167–1176.

R Development Core Team. 2018. R: a language and environment for statistical computing. Vienna, Austria. <http://www.r-project.org>.

Ranglack, D. H., R. Garrott, J. Rotella, K. M. Proffitt, J. Gude, and J. E. Canfield. 2016. Evaluating elk summer resource selection and applications to summer range habitat management. Montana Department of Fish, Wildlife and Parks, Helena, Montana, USA. Page 36.

Ranglack, D. H., K. M. Proffitt, J. E. Canfield, J. A. Gude, J. Rotella, and R. A. Garrott. 2017. Security areas for elk during archery and rifle hunting seasons. The Journal of Wildlife Management.

Rivrud, I. M., M. Heurich, P. Krupczynski, J. Müller, and A. Mysterud. 2016. Green wave tracking by large herbivores: an experimental approach. Ecology 97:3547–3553.

Robbins, C. T., T. A. Hanley, A. E. Hagerman, O. Hjeljord, D. L. Baker, C. C. Schwartz, and W. W. Mautz. 1987a. Role of tannins in defending plants against ruminants: reduction in protein availability. Ecology 68:98–107.

Robbins, C. T., S. Mole, A. E. Hagerman, and T. A. Hanley. 1987b. Role of tannins in defending plants against ruminants: reduction in dry matter digestion? Ecology 68:1606–1615.

Robinson, N., B. Allred, M. Jones, A. Moreno, J. Kimball, D. Naugle, T. Erickson, and A. Richardson. 2017. A dynamic Landsat derived Normalized Difference Vegetation Index (NDVI) product for the conterminous United States. Remote Sensing 9:863.

Romme, W. H., M. S. Boyce, R. Gresswell, E. H. Merrill, G. W. Minshall, C. Whitlock, and M. G. Turner. 2011. Twenty Years After the 1988 Yellowstone Fires: Lessons About Disturbance and Ecosystems. Ecosystems 14:1196–1215.

Ryan, S. J., P. C. Cross, J. A. Winnie, C. Hay, J. Bowers, and W. M. Getz. 2012. The utility of normalized difference vegetation index for predicting African buffalo forage quality. Journal of Wildlife Management 76:1499–1508.

Ryan, S. J., C. U. Knechtel, and W. M. Getz. 2006. Range and habitat selection of African buffalo in South Africa. Journal of Wildlife Management 70:764–776.

Ryan, S. J., C. U. Knechtel, and W. M. Getz. 2007. Ecological cues, gestation length, and birth timing in African buffalo (Syncerus caffer). Behavioral Ecology 18:635–644.

Sachro, L. L., W. L. Strong, and C. C. Gates. 2005. Prescribed burning effects on summer elk forage availability in the subalpine zone, Banff National Park, Canada. Journal of Environmental Management 77:183–193.

Santin-Janin, H., M. Garel, J.-L. Chapuis, and D. Pontier. 2009. Assessing the performance of NDVI as a proxy for plant biomass using non-linear models: a case study on the Kerguelen archipelago. Polar Biology 32:861–871.

Sawyer, H., and M. J. Kauffman. 2011. Stopover ecology of a migratory ungulate. Journal of Animal Ecology 80:1078–1087.

Schwilk, D. W., J. E. Keeley, E. E. Knapp, J. McIver, J. D. Bailey, C. J. Fettig, C. E. Fiedler, R. J. Harrod, J. J. Moghaddas, K. W. Outcalt, C. N. Skinner, S. L. Stephens, T. A. Waldrop, D. A. Yaussy, and A. Youngblood. 2009. The national Fire and Fire Surrogate study: effects of fuel reduction methods on forest vegetation structure and fuels. Ecological Applications 19:285–304.

Sittler, K. L., K. L. Parker, and M. P. Gillingham. 2015. Resource separation by mountain ungulates on a landscape modified by fire. The Journal of Wildlife Management 79:591–604.

Spruce, J. P., S. Sader, R. E. Ryan, J. Smoot, P. Kuper, K. Ross, D. Prados, J. Russell, G. Gasser, R. McKellip, and W. Hargrove. 2011. Assessment of MODIS NDVI time series data products for detecting forest defoliation by gypsy moth outbreaks. Remote Sensing of Environment 115:427–437.

Su, Y., Q. Guo, B. M. Collins, D. L. Fry, T. Hu, and M. Kelly. 2016. Forest fuel treatment detection using multi-temporal airborne lidar data and high-resolution aerial imagery: a case study in the Sierra Nevada Mountains, California. International Journal of Remote Sensing 37:3322–3345.

Thomas, S. C., C. B. Halpern, D. A. Falk, D. A. Liguori, and K. A. Austin. 1999. Plant diversity in managed forests: understory responses to thinning and fertilization. Ecological Applications 9:864–879.

Trimble, M. J., S. M. Ferreira, and R. J. van Aarde. 2009. Drivers of megaherbivore demographic fluctuations: inference from elephants. Journal of Zoology 279:18–26.

Turner, M. G., Y. Wu, L. L. Wallace, W. H. Romme, and A. Brenkert. 1994. Simulating winter interactions among ungulates, vegetation, and fire in northern Yellowstone Park. Ecological Applications 4:472–496.

U.S. Forest Service. 2016. U.S. Forest Service cut and sold reports.

Uresk, D. W., and K. E. Severson. 1989. Understory-overstory relationships in ponderosa pine forests, Black Hills, South Dakota. Journal of Range Management 42:203–208.

Van Dyke, F., and J. A. Darragh. 2007. Response of elk to changes in plant production and nutrition following prescribed burning. The Journal of Wildlife Management 71:23–29.

Van Soest, P. J. 1982. Nutritional ecology of the ruminant. Page 479. Second editions. Cornell University Press, Ithica, New York.

Wessels, K. J., S. D. Prince, N. Zambatis, S. MacFadyen, P. E. Frost, and D. Van Zyl. 2006. Relationship between herbaceous biomass and 1-km 2 Advanced Very High Resolution Radiometer (AVHRR) NDVI in Kruger National Park, South Africa. International Journal of Remote Sensing 27:951–973.

White, P. J., R. A. Garrott, K. L. Hamlin, R. C. Cook, J. G. Cook, and J. A. Cunningham. 2011. Body condition and pregnancy in northern Yellowstone elk: Evidence for predation risk effects? Ecological Applications 21:3–8.

Wiegand, T., J. Naves, M. F. Garbulsky, and N. Fernández. 2008. Animal habitat quality and ecosystem functioning: exploring seasonal patterns using NDVI. Ecological Monographs 78:87–103.

Willms, J., A. Bartuszevige, D. W. Schwilk, and P. L. Kennedy. 2017. The effects of thinning and burning on understory vegetation in North America: A meta-analysis. Forest Ecology and Management 392:184–194.

Wittemyer, G., H. Barner Rasmussen, and I. Douglas-Hamilton. 2007. Breeding phenology in relation to NDVI variability in free-ranging African elephant. Ecography 30:42–50.

# Appendix A - Estimation of Forage Quality

## Estimation of phenological stage-specific digestible energy

In the Bitterroot Valley study area, we estimated variation in phenological stage of plant species to account for the effect of plant phenology on nutritional availability. In 2014-2015, we estimated the dominant phenological stage (emergent, flowering, fruiting, mature seed, or senescent) of each species at each sampling site. The emergent stage included green plant tissues in the newly emergent, flowering and/or fruiting stages, and plants in the emergent stage were assigned an average forage quality value that was the mean of the newly emergent, flowering, and fruiting stages (see below). In 2012-2013, we estimated the phenological stage of each species at a sample of phenology plots that were stratified across major phenological gradients including elevation, aspect (north, south, flat), and canopy coverage (open and closed) and applied these averaged phenological stage-specific forage quality values for each species to plants within all sampling sites. We constrained the phenology data to 15 July-31 August to correspond to the summer-fall nutritional period (Cook et al. 2013) and applied the species-specific phenological classifications to all sampling sites.

For each phenological stage of each forage species, we estimated digestible energy (kcal/g; DE) by collecting at least 5 plant samples in each of 5 phenological stages (newly emergent, flowering, fruiting, mature seed, and senescent). Replicate plant samples were collected from different areas, then combined into one composite sample and dried at 50° C for 48 hours. We estimated dry matter digestibility using sequential detergent fiber analysis (Van Soest (1982); Wildlife Habitat and Nutrition Lab, Washington State University, Pullman, WA, USA) and an equation developed for wild ungulates (Robbins et al. 1987a, 1987b, Hanley et al. 1992). We then converted dry matter digestibility values to DE (Cook et al. 2016). For phenological stages that lacked representative samples, we used literature values from previous studies (Hebblewhite 2006) or averaged by genus (if available) or lifeform. We applied the same phenological stage-specific DE values to all sampling sites in the Bitterroot Valley (see *Comparison of phenological stage-specific forage quality estimates*).

Across sampling sites in the Bitterroot Valley, the average proportion of forb forage species in each respective phenological stage (emergent, flowering, fruiting, mature seed, and senescent) was 0.35, 0.12, 0.14, 0.30, and 0.09, respectively. For graminoid forage species, average proportions were 0.33, 0.04, 0.09, 0.46, and 0.08, respectively. For shrub forage species, average proportions were 0.45, 0.04, 0.38, 0.10, and 0.03, respectively.

We collected an average of 8 plant samples per species per phenological stage from 31 forage species to estimate DE. DE for all forage plants averaged 2.92 ± 0.37 (SD) and varied by species (Table A1) and phenological stage (Table A2).

## Estimation of mean forage quality at sampling sites

We screened each sampling quadrat to include only forage species and rescaled species percent cover to estimate the proportion of each forage species in each phenological stage

such that the total summed to 1.0 (Fig. A1). We used the proportion cover (i.e., availability) and phenological stage-specific DE estimates for each forage species to estimate the mean DE of forage species by calculating a weighted mean DE using rescaled proportion cover as the weight. Last, we averaged the DE estimates across the 5 sampling quadrats, and we refer to this value as the forage quality per sampling site.
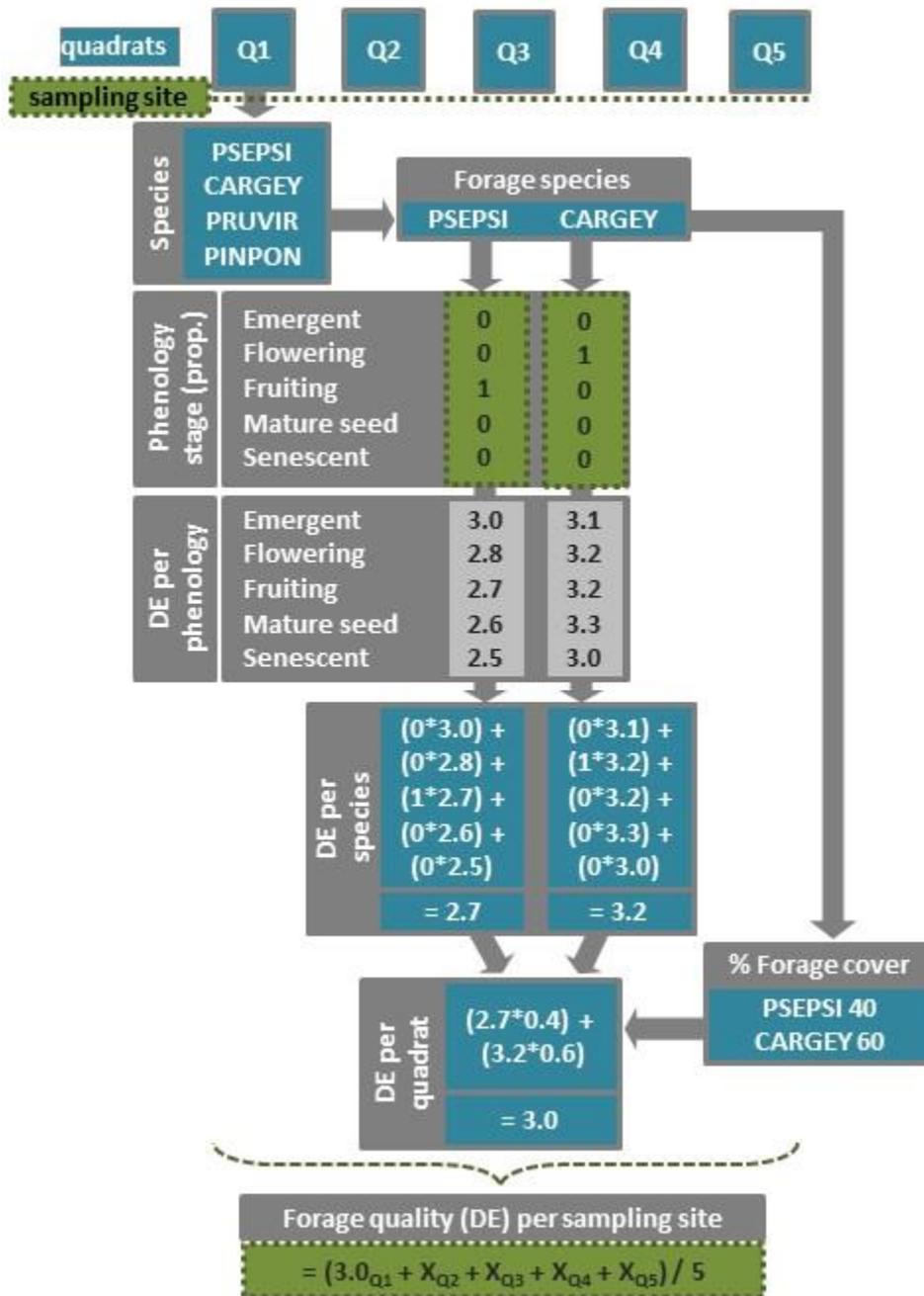


**Figure A1 – Methods for estimating mean forage quality (i.e., digestible energy; kcal/g) at each vegetation sampling site in the Bitterroot Valley in west-central Montana, USA, 2012-2015.**

# Comparison of phenological stage-specific forage quality estimates

To determine if a single mean DE value for each phenological stage of each forage plant species could be applied to all sampling sites across the Bitterroot Valley study area, we tested for differences in phenological stage-specific DE values between plant samples collected from the northern (North Sapphire) and southern (East Fork and West Fork) regions of the study area. We first identified 5 forage species (*Carex geyeri*, *Chamerion angustifolium*, *Lupinus sericeus*, *Xerophyllum tenax*, and *Lupinus* spp.) occurring within the elk diets in at least one of the elk populations. We collected 5 samples in each phenological stage of these species from each study area region. We then tested for differences in DE between study area regions for each species and species-specific phenological stage using the Bonferroni multiple comparison method to perform pair-wise comparisons of the means. We detected a significant difference only for flowering Xerophyllum tenax in the species-phenological stage pair-wise comparison between study area regions (p=0.005), indicating that the mean DE in the southern region was 0.35 kcal/g greater than the northern region (SE=0.1). Based on these results, we concluded there were no substantial differences in forage quality between study area regions, and we applied a single phenological stage-specific mean DE value for each forage species to both study area regions (Table A1).

**Table A1 - Mean digestible energy (DE, kcal/g), standard deviation (SD), and sample size (N) for elk summer-fall forage species in each phenological stage applied to all sampling sites in the Bitterroot Valley study area in south-west Montana, USA, 2011-2015. Missing values replaced from literature.**

| Species | Emergent | | | Flowering | | | Fruiting | | | Mature Seed | | | Senescent | | |
|---|---|---|---|---|---|---|---|---|---|---|---|---|---|---|---|
| | N | DE | SD | N | DE | SD | N | DE | SD | N | DE | SD | N | DE | SD |
| Achillea millefolium | 5 | 3.22 | 0.09 | 5 | 2.79 | 0.19 | 5 | 2.21 | 0.04 | — | — | — | 5 | 1.97 | 0.21 |
| Agropyron cristatum | 5 | 3.15 | 0.07 | 5 | 3.04 | 0.1 | 6 | 2.74 | 0.11 | — | — | — | 5 | 2.73 | 0.08 |
| Astragalus inflexus | 5 | 3.29 | 0.2 | 5 | 3.14 | 0.27 | 3 | 2.94 | 0.19 | — | — | — | 1 | 3 | — |
| Astragalus sp | — | — | — | — | — | — | 2 | 2.99 | 0.09 | — | — | — | 1 | 3.03 | — |
| Balsamorhiza sagittata | 10 | 3.57 | 0.06 | 17 | 3.48 | 0.17 | 6 | 2.97 | 0.14 | 7 | 3.35 | 0.11 | 12 | 2.75 | 0.26 |
| Bromus tectorum | 10 | 3.06 | 0.37 | 8 | 3.1 | 0.26 | 13 | 2.79 | 0.3 | 1 | 2.37 | — | 7 | 2.84 | 0.15 |
| Carex geyeri | 22 | 3.14 | 0.17 | 26 | 3.2 | 0.17 | 21 | 3.24 | 0.07 | 2 | 3.27 | 0.03 | 21 | 3.06 | 0.28 |
| Centaurea stoebe | 18 | 3.22 | 0.22 | 19 | 2.61 | 0.19 | 11 | 2.49 | 0.1 | — | — | — | 9 | 2.3 | 0.18 |
| Chamerion angustifolium | 14 | 3.36 | 0.14 | 18 | 3.03 | 0.1 | 23 | 2.8 | 0.21 | — | — | — | 11 | 2.72 | 0.26 |
| Elymus glaucus | 5 | 3.28 | 0.06 | 5 | 2.93 | 0.1 | 5 | 2.71 | 0.2 | — | — | — | 5 | 2.48 | 0.07 |
| Equisetum | — | — | — | — | — | — | 4 | 3.17 | 0.25 | — | — | — | — | — | — |
| Equisetum arvense | 6 | 3.52 | 0.11 | 5 | 3.19 | 0.08 | 1 | 3.47 | — | — | — | — | 5 | 3.24 | 0.23 |
| Festuca campestris | 5 | 3.28 | 0.03 | 5 | 3.11 | 0.16 | 5 | 2.74 | 0.09 | — | — | — | 6 | 2.79 | 0.2 |
| Festuca idahoensis | 19 | 3.04 | 0.23 | 6 | 3.12 | 0.13 | 15 | 2.75 | 0.18 | 5 | 2.99 | 0.2 | 15 | 2.7 | 0.24 |
| Koeleria macrantha | 4 | 3.3 | 0.08 | 6 | 3.07 | 0.14 | 5 | 2.75 | 0.19 | — | — | — | 5 | 2.61 | 0.14 |
| Lupinus sericeus | 17 | 3.37 | 0.09 | 12 | 3.34 | 0.08 | 4 | 3.18 | 0.15 | 4 | 3.2 | 0.21 | 2 | 2.57 | 0.08 |
| Lupinus sp | 13 | 3.36 | 0.17 | 15 | 3.06 | 0.33 | 19 | 3 | 0.17 | 1 | 3.35 | — | 16 | 2.8 | 0.3 |
| Medicago sativa | 5 | 3.3 | 0.15 | 5 | 3.23 | 0.02 | 5 | 2.89 | 0.23 | — | — | — | 4 | 2.64 | 0.24 |
| Phleum pratense | 5 | 3.27 | 0.13 | 5 | 2.87 | 0.11 | 5 | 2.79 | 0.06 | — | — | — | 5 | 2.8 | 0.12 |
| Pinus contorta | 5 | 2.27 | 0.18 | — | — | — | — | — | — | — | — | — | — | — | — |
| Poa pratensis | 4 | 3.31 | 0.06 | 5 | 2.93 | 0.16 | 5 | 2.66 | 0.15 | — | — | — | 5 | 2.63 | 0.1 |
| Poa secunda | 2 | 3.02 | 0.26 | 5 | 3 | 0.16 | 5 | 2.66 | 0.08 | — | — | — | 5 | 2.84 | 0.17 |
| Poa sp | 6 | 3.18 | 0.08 | — | — | — | 6 | 2.49 | 0.26 | 3 | 2.96 | 0.25 | 5 | 2.63 | 0.28 |
| Pseudoroegneria spicata | 19 | 3.03 | 0.26 | 12 | 2.89 | 0.2 | 21 | 2.73 | 0.11 | 3 | 2.86 | 0.16 | 13 | 2.49 | 0.14 |
| Shepherdia canadensis | 8 | 3.25 | 0.09 | — | — | — | 5 | 3.13 | 0.14 | — | — | — | 2 | 3.07 | 0.15 |
| Stipa comata | 6 | 2.93 | 0.11 | 5 | 2.94 | 0.08 | 5 | 2.79 | 0.06 | — | — | — | 6 | 2.5 | 0.08 |
| Symphoricarpos albus | 11 | 3.23 | 0.18 | 4 | 3.02 | 0.16 | 14 | 2.78 | 0.14 | — | — | — | 3 | 1.9 | 0.63 |
| Triticum aestivum | 5 | 3.39 | 0.05 | 5 | 3.25 | 0.13 | 4 | 3.2 | 0.09 | — | — | — | 5 | 2.94 | 0.28 |
| Verbascum thapsus | 5 | 2.34 | 0.32 | 5 | 2.68 | 0.18 | 6 | 2.08 | 0.18 | — | — | — | 6 | 1.98 | 0.3 |
| Xerophyllum tenax | 20 | 2.18 | 0.17 | 19 | 2.81 | 0.41 | 15 | 2.3 | 0.27 | 2 | 2.06 | 0.28 | 14 | 1.9 | 0.17 |
| Zea mays | 1 | 3.28 | — | 1 | 3.26 | — | 1 | 3.5 | — | — | — | — | 1 | 3.48 | — |

**Table A2 - Mean digestible energy (DE, kcal/g), standard deviation of DE (SD), and sample size (N) of each phenological stage for each lifeform of elk summer-fall forage species in the Bitterroot Valley in south-west Montana, USA, 2011-2015.**

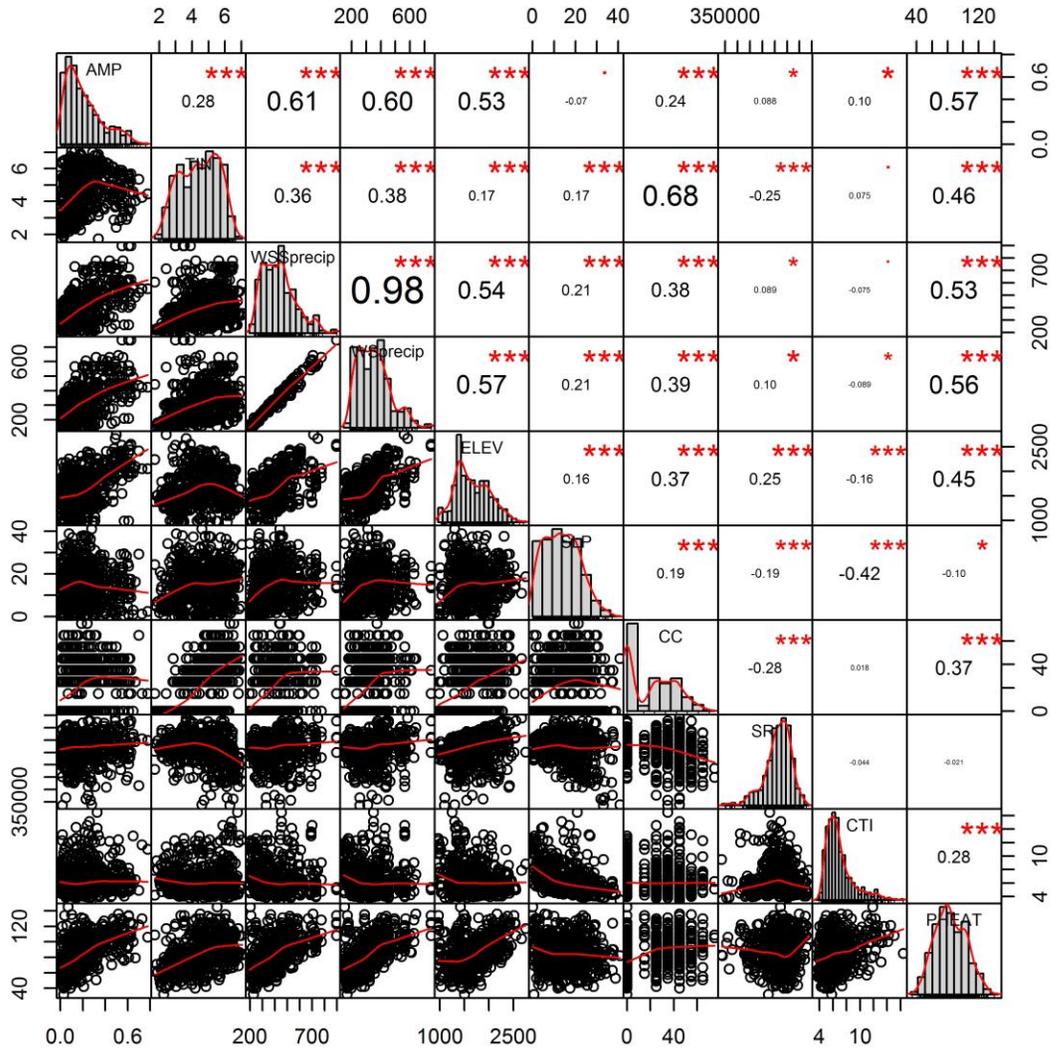| Stage | Forb | | | Graminoid | | | Shrub | | |
|---|---|---|---|---|---|---|---|---|---|
| | N | DE | SD | N | DE | SD | N | DE | SD |
| Emergent | 118 | 3.11 | 0.50 | 118 | 3.13 | 0.23 | 19 | 3.24 | 0.15 |
| Flowering | 125 | 3.02 | 0.37 | 99 | 3.06 | 0.20 | 4 | 3.02 | 0.16 |
| Fruiting | 104 | 2.72 | 0.38 | 122 | 2.84 | 0.27 | 19 | 2.88 | 0.21 |
| Mature seed | 14 | 3.12 | 0.48 | 14 | 2.95 | 0.26 | — | — | — |
| Senescent | 86 | 2.50 | 0.47 | 109 | 2.76 | 0.28 | 5 | 2.37 | 0.79 |

**Figure B1 - Pairwise plots of Pearson correlation coefficients, histograms, and x-y scatter plots of covariates considered in the model suites for evaluating the relationship between elk nutritional resources and NDVI.**
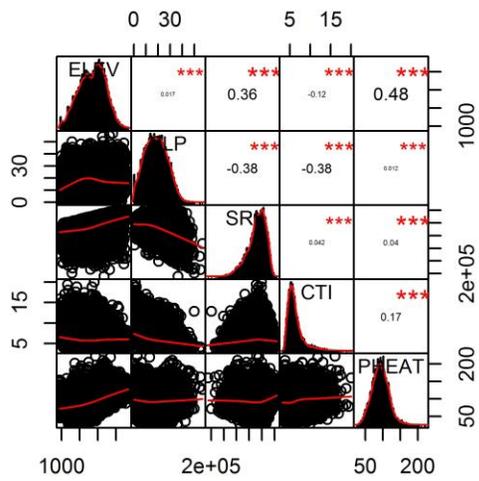
**Figure B2 - Pairwise plots of Pearson correlation coefficients, histograms, and x-y scatter plots of covariates considered in models evaluating the relationship between NDVI and landscape disturbances.**

## Appendix C - Summer-fall Home Range Fidelity of Individual Elk

We compared annual fidelity of summer-fall home ranges by individual female elk by: 1) selecting elk with 2 years of location data that overlapped the summer-fall season (July 1-August 31), 2) calculating summer-fall home ranges of individual elk for each year based on a 95% kernel utilization distribution (using the adehabitatHR package in Program R version 3.4.3; R Development Core Team 2018), and 3) calculating the proportion of area overlap of summer-fall home ranges for each individual. We calculated proportion overlap for 63 elk. The average proportion overlap of summer-fall home ranges was 0.6860095 ± 0.2158755 (SD). 44.4% and 82.5% of elk summer-fall ranges overlapped ≥ 75% and ≥ 50%, respectively, providing relatively strong evidence that elk select for the same summer-fall home ranges each year.